An Approach to Relate Laboratory and Field Moduli of Base Materials

by

Soheil Nazarian, Ph.D., P.E.

Rafael Pezo, Ph.D.

and

Miguel Picornell, Ph.D.

Research Project 0-1336

APPLICATION OF RESILIENT MODULUS TESTS
TO TEXAS BASE MATERIALS

Conducted for

Texas Department of Transportation
in cooperation with
Federal Highway Administration

The Center for Geotechnical and Highway Materials Research
The University of Texas at El Paso
El Paso, TX 79968-0516

Research Report 1336-2F
July 1996

TECHNICAL REPORT STANDARD TITLE PAGE

1. Report No. TX-94 1336-2F	2. Government Accession No.	3. Recipient's Catalog No.
4. Title and Subtitle An Approach to Relate Laboratory and Field Moduli of Base Materials		5. Report Date July, 1996 6. Performing Organization Code
7. Author(s) Nazarian, S., Pezo R., and Picornell P.		8. Performing Organization Report No. Research Report 1336-1
9. Performing Organization Name and Address Center for Geotechnical and Highway Materials Research. The University of Texas at El Paso El Paso, Texas 79968-0516		10. Work Unit No. 11. Contract or Grant No. Study No. 0-1336
12. Sponsoring Agency Name and Address Texas Department of Transportation P.O. Box 5051 Austin, Texas 78763		13. Type of Report and Period Covered Final Report Sept. 1, 1992-Aug 31, 1995 14. Sponsoring Agency Code

15. Supplementary Notes

Research Performed in Cooperation with TxDOT and FHWA
Research Study Title: APPLICATION OF RESILIENT MODULUS TESTS TO TEXAS BASE MATERIALS

16. Abstract

The main objective of this report is to combine the resilient moduli from laboratory testing of base materials with those obtained in the field using nondestructive testing devices.

Laboratory tests were carried out in two stages. First, virgin materials from the quarry compacted to optimum moisture content were tested. In the second stage, similar base materials were retrieved from in-service roads. Specimens were prepared and tested at the corresponding field densities and moisture contents. Nondestructive tests were performed with the Falling Weight Deflectometer (FWD) and the Seismic Pavement Analyzer. It was found that it may be difficult to directly compare moduli from laboratory and field tests. A methodology was proposed that can be used to combine these parameters in pavement design. The proposed methodology should be validated and modified using field tests. Results from accelerated pavement tests should be particularly valuable.

17. Key Words Pavement Design, Modulus, Laboratory Testing, Nondestructive Testing, Flexible Pavements, Resilient Modulus, Seismic Pavement Analyzer	18. Distribution Statement No restrictions. This document is available to the public through the National Technical Information Service, 5285 Port Royal Road, Springfield, Virginia 22161

19. Security Classif. (of this report)	20. Security Classif. (of this page)	21. No. of Pages	22. Price
Unclassified	Unclassified	59	

Form DOT F 1700.7 (8-69)

NOT INTENDED FOR CONSTRUCTION, BIDDING, OR PERMIT PURPOSES

Soheil Nazarian, Ph.D., P.E. (69263)
Rafael Pezo, Ph.D.
Miguel Picornell, Ph.D.

Acknowledgements

The authors would like to give their sincere appreciation to Harold Albers of the TxDOT Materials and Test Division for his ever-present support. Mark McDaniel of TxDOT enthusiastically followed the progress of the project and provided valuable advice. Thanks are also due to the laboratory personnel of the ten districts that provided their assistance during, before, and after field tests, and for putting up with all sorts of demands we imposed on their tight schedules.

The Seismic Pavement Analyzer tests were reduced by Deren Yuan of UTEP. Tom Scullion of Texas Transportation Institute was instrumental in reducing the FWD data. Emad Abdallah did an excellent job of conducting the computer modelling. The laboratory tests were performed by Jaime Rojas and Kelvin Kroeker.

Abstract

Resilient moduli of base materials are important parameters in the new pavement design method adopted by AASHTO and many state agencies. Numerous projects dealing with improvements of MR test protocol have been funded by federal and state agencies. Unfortunately, little effort has been put forth to implement the methods in pavement design.

The main objective of this report is to combine the resilient moduli from laboratory testing with those obtained in the field using nondestructive testing devices. In that manner, one can more effectively incorporate the results in everyday design.

Laboratory tests were carried out in two stages. First, virgin materials from the quarry compacted to optimum moisture content were tested. In the second stage, similar base materials were retrieved from in-service roads. Specimens were prepared and tested at the corresponding field densities and moisture contents. Nondestructive tests were performed with the Falling Weight Deflectometer (FWD) and the Seismic Pavement Analyzer.

Based on the tests of ten different base materials from different parts of Texas, it may be difficult to directly compare moduli from laboratory and field tests. A methodology was proposed that can be used to combine these parameters in pavement design. The proposed methodology should be validated and modified using field tests. Results from accelerated pavement tests should be particularly valuable.

Implementation Statement

All the required equipment has been purchased or manufactured at UTEP and transferred to TxDOT. The testing methodology has been drafted and tested on numerous synthetic and actual base specimens. In our opinion, this test methodology should be immediately implemented on trial basis so that the possible logistical and practical problems with the protocol can be addressed.

Table of Contents

List of Tables

List of Figures

Chapter 1

Introduction

Problem Statement

Successful design of new pavements and accurate prediction of the remaining life of existing roads depend on the proper characterization of the pavement materials. For this reason, the new design methods (e.g., the 1986 AASHTO Pavement design guide) require the use of resilient modulus tests for determining the stiffness parameters and the constitutive behavior of pavement components, such as subgrade, subbase and base.

The characterization of subgrade materials with resilient modulus tests was the subject of Project 1177 carried out at the Center for Transportation Research (CTR) and at The University of Texas at El Paso (UTEP). As a part of that project, CTR developed guidelines for testing primarily cohesive soils (Pezo et al., 1992) and UTEP developed a procedure to test predominantly granular materials (Feliberti et al., 1992). Based on an extensive testing program, these procedures were found to be quite repeatable and easy to perform. Project 1336 (this project) was initiated to characterize base materials.

An ideal mechanistic pavement design process includes the following four steps:

1. determine pavement-related physical constants, such as types of existing materials,
2. test the candidate pavement with a nondestructive testing device to determine its in situ moduli,
3. determine the laboratory properties of each layer, and
4. use an appropriate algorithm to estimate the remaining life of the pavement.

Unfortunately, all these steps have their own limitations, because the type and extent of layers may not be accurately known. The nondestructive test methods do not always yield reliable results. The laboratory results may not be representative because of the specimen size and sample disturbance. The models used to estimate remaining life are usually over-simplified, and depending on their complexity, may not consider factors such as nonlinearity, visco-elasticity or the dynamic nature of the loading. Given these limitations, the state-of-practice should be significantly improved before a truly mechanistic procedure can be implemented.

The main focus of the present study is to compare modulus values obtained nondestructively with those obtained on laboratory specimens. The main questions to be addressed are the following:

1. Do the laboratory and field moduli compare reasonably well?
2. Can these values be combined for a reasonable design value?

Objectives

The primary objective of this report is to incorporate the results from laboratory MR tests with those obtained from nondestructive field tests, so that a realistic approach which can be used in pavement design can be developed. The steps taken to achieve this goal were the following:

1. perform resilient modulus tests on virgin base materials from ten quarries in Texas following the state-of-practice,

2. perform resilient modulus test on materials retrieved from in-service roads, constructed using materials from the same ten quarries.

3. determine moduli from the Falling Weight Deflectometer (FWD) tests on the same ten test sections as in item 2,

4. determine moduli from the Seismic Pavement Analyzer (SPA) tests on the ten test sections,

5. compare the results from the laboratory and the two field tests to determine whether a unique relationship can be developed, and finally

6. determine whether these methodologies can be combined to better predict moduli of base.

Organization

The report contains five chapters. Chapter 2 includes background information and results of a literature search. Chapter 3 contains a detailed explanation of the procedures followed during field work, laboratory tests, nondestructive tests and data reduction. The results from all sites are presented and discussed in Chapter 4. The final chapter consists of a summary, conclusions and future directions. Several appendices are included which contain a detailed description of methodologies including the raw data collected at different sites.

Chapter 2

Background

Moduli of pavement layers are measured in the laboratory or in situ, or are determined from empirical relationships. The resilient modulus (MR) test is the major laboratory test. The state-of-the-art in field testing consists of the Falling Weight Deflectometer (FWD), or the Seismic Pavement Analyzer (SPA) tests. The most widely used empirical relationships are proposed in the latest AASHTO design manual.

Laboratory tests are essential to study the parameters which affect the properties of the material. However, moduli from laboratory tests are normally less than the in situ results by anywhere from ten to several hundred percent. This discrepancy can be due to a variety of reasons such as: sampling disturbance, differences in the state-of-stress between the specimen and in-place pavement material, nonrepresentative specimens, long-term time effects, and inherent errors in the field and laboratory test procedures (Anderson and Woods, 1975).

Field tests are more practical and more desirable because they are rapid to perform, and because they test a large volume of material in its natural state-of-stress. However, the FWD data interpretation may yield non-unique results. The SPA measures stiffness in the linear-elastic range; therefore, a methodology for extrapolating the moduli to higher strain levels should be contemplated.

Empirical relations are sometimes useful in the preliminary stages of design and planning. These methods cannot take into account the site-dependent variation in properties as in situ methods can; therefore, it is neither suitable nor appropriate to use empirical relations to obtain accurate properties of pavement layers for final design of major projects.

This chapter contains a brief description of the methods used in this study, a theoretical discussion of the relationships between different methods, and various attempts by other investigators in the recent past to correlate laboratory and field moduli.

Resilient Modulus Tests

A review of the fundamentals of resilient modulus testing and the state-of-practice in performing these tests are incorporated in Report 1336-1 (Nazarian et al., 1996). A comprehensive literature search on this topic can also be found in Barksdale et al. (1994). For the sake of brevity, that information is not repeated here.

The resilient modulus of subgrade and base materials are typically determined in a repeated load triaxial test. The test is performed by placing a specimen in a cell and applying repeated axial load after subjecting the specimen to all around confining pressure (see Figure 2.1). The recoverable axial deformation and the applied load is measured. The resilient modulus is calculated from

$$M_R = \sigma_d / \epsilon_{ax} \tag{2.1}$$

Parameter σ_d, the axial deviatoric stress, is

$$\sigma_d = P / A_i \tag{2.2}$$

where P is the applied load and A_i is the original cross-sectional area of the specimen. Parameter ϵ_{ax}, the resilient axial strain, is calculated from

$$\epsilon_{ax} = \Delta L / L_i \tag{2.3}$$

where ΔL is recoverable axial deformation along a gage length, L_i. The Poisson's ratio ν is calculated from

$$\nu = - \epsilon_{lat} / \epsilon_{ax} \tag{2.4}$$

Parameter ϵ_{lat}, the lateral strain, is calculated from

$$\epsilon_{lat} = \Delta d / d_i \tag{2.5}$$

where Δd is the recoverable lateral deformation measured at the specimen's mid-height and d_i is the original diameter of the specimen.

The step-by-step procedure for determining resilient moduli of different materials is included in Appendix A. Briefly, the specimen is prepared in a cylindrical split mold in six lifts. A standard Proctor hammer is dropped 25 times on each lift to compact the base materials obtained from the quarry. A modified Proctor hammer is used on the base materials retrieved from the in-service roads. For each of the in-service materials, the number of hammer drops is determined by trial and error so that the field moisture content and density can be simultaneously achieved. The material required for the preparation of the specimen is homogenized at the desired moisture content by adding the required water, thoroughly mixing, and storing for one day.

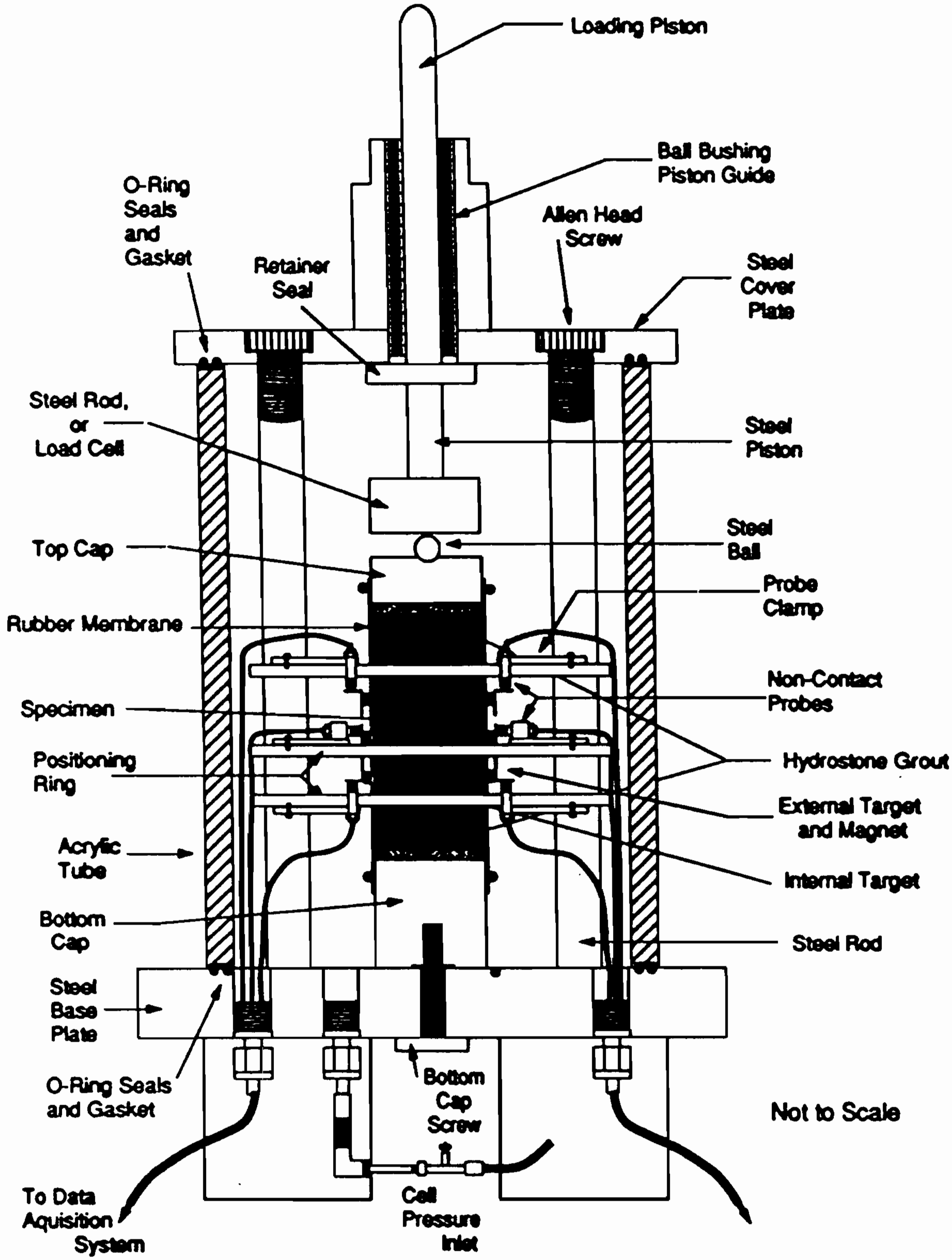

Figure 2.1 - Schematic of Resilient Modulus Test

Table 2.1 - Proposed Testing Sequence for Base Materials

Sequence No.	Confining Pressure	Deviatoric Stress (KPa)	Number of Load Applications
1	35	35	5
2	35	70	5
3	35	105	5
4	70	35	5
5	70	70	5
6	70	105	5
7	70	140	5
8	105	35	5
9	105	70	5
10	105	105	5
11	105	140	5
12	105	210	5

The resilient modulus tests consisted of applying various deviatoric stresses at different confining pressures as shown in Table 2.1. The confining pressure is either applied by subjecting the specimen to vacuum or by compressed air inside the acrylic cell surrounding the specimen. The pressure is monitored by a pressure gage.

A haver-sine loading waveform with a loading duration of 0.1 seconds and rest period of 0.9 seconds is used. The axial deformations are measured along the middle one-third of the specimen with six non-contact proximeter sensors. Two non-contact probes are used to measure lateral deformations so that Poisson's ratios can also be determined. Five cycles of loading are applied at every stage to optimize testing time, and to minimize the degradation of the specimen. From the measured axial and lateral displacements at a particular deviatoric stress and confining pressure, the resilient modulus and Poisson's ratio of the specimen are determined using Equations 2.1 through 2.5.

The constitutive model used to describe the results of the MR tests is

$$M_R = k_1 \, \sigma_d^{k2} \, \sigma_c^{k3}. \tag{2.6}$$

σ_d and σ_c are the deviatoric stress and confining pressure, respectively. Parameters k_1 through k_3 are statistically-determined coefficients.

Falling Weight Deflectometer

The most dominant NDT device for pavements is the Falling Weight Deflectometer (FWD). This device imparts transient impulse forces to the pavement through a circular loading plate, and measures the resulting deflection basin at selected points. The load and measured deflection basins are then used with an inversion algorithm to "backcalculate" the modulus of each layer (Lytton, 1989).

In the analysis of the load-deflection measurements, the pavement is modelled as a multi-layered, linear elastic system. Each layer is characterized by a Young's modulus and a Poisson's ratio. The load is assumed to be static. A computer program is then used to conduct the "deflection-basin fitting." The deflection-basin fitting consists of determining the deflections based on a set of assumed moduli, and of adjusting these modulus values until the differences between the measured and calculated deflections are minimized. In the present study, the program MODULUS was used. As summarized by Uzan (1994), more sophisticated algorithms for basin fitting exists. These algorithms use numerical techniques, (i.e., use boundary element or finite element methods), or model the materials in a more sophisticated manner (i.e., consider their visco-elastic and nonlinear behaviors), or model the loads more appropriately (i.e., dynamically). Such models were not considered for this project, since at the present time none of these programs are routinely used in practice.

Seismic Pavement Analyzer

The Seismic Pavement Analyzer (SPA, patent pending) is an instrument designed and constructed to monitor conditions associated with pavement deterioration. It measures such conditions as voids or loss of support under a rigid pavement, softening of asphalt-concrete pavement layers, and delamination of overlays. A lengthy discussion on the background of the device can be found in Report 1243-1 (Nazarian et al., 1995). The SPA detects these types of pavement conditions by estimating Young's and shear moduli in the pavement, base, and subgrade from wave propagation measurements.

The SPA lowers transducers and sources to the pavement and digitally records surface deformations induced by a large pneumatic hammer which generates low-frequency vibrations, and a small pneumatic hammer which generates high-frequency vibrations (see Figure 2.2).

This transducer frame is mounted on a trailer that can be towed behind a vehicle. The SPA is controlled by an operator at a computer connected to the trailer by a cable. The computer may be run from the cab of the truck towing the SPA or from various locations around the SPA.

All measurements are spot measurements; that is, the device has to be towed and situated at a specific point before measurements can be made. A complete testing cycle at one point, which takes less than one minute, includes situating at the site, lowering the sources and receivers, making measurements, and withdrawing the equipment.

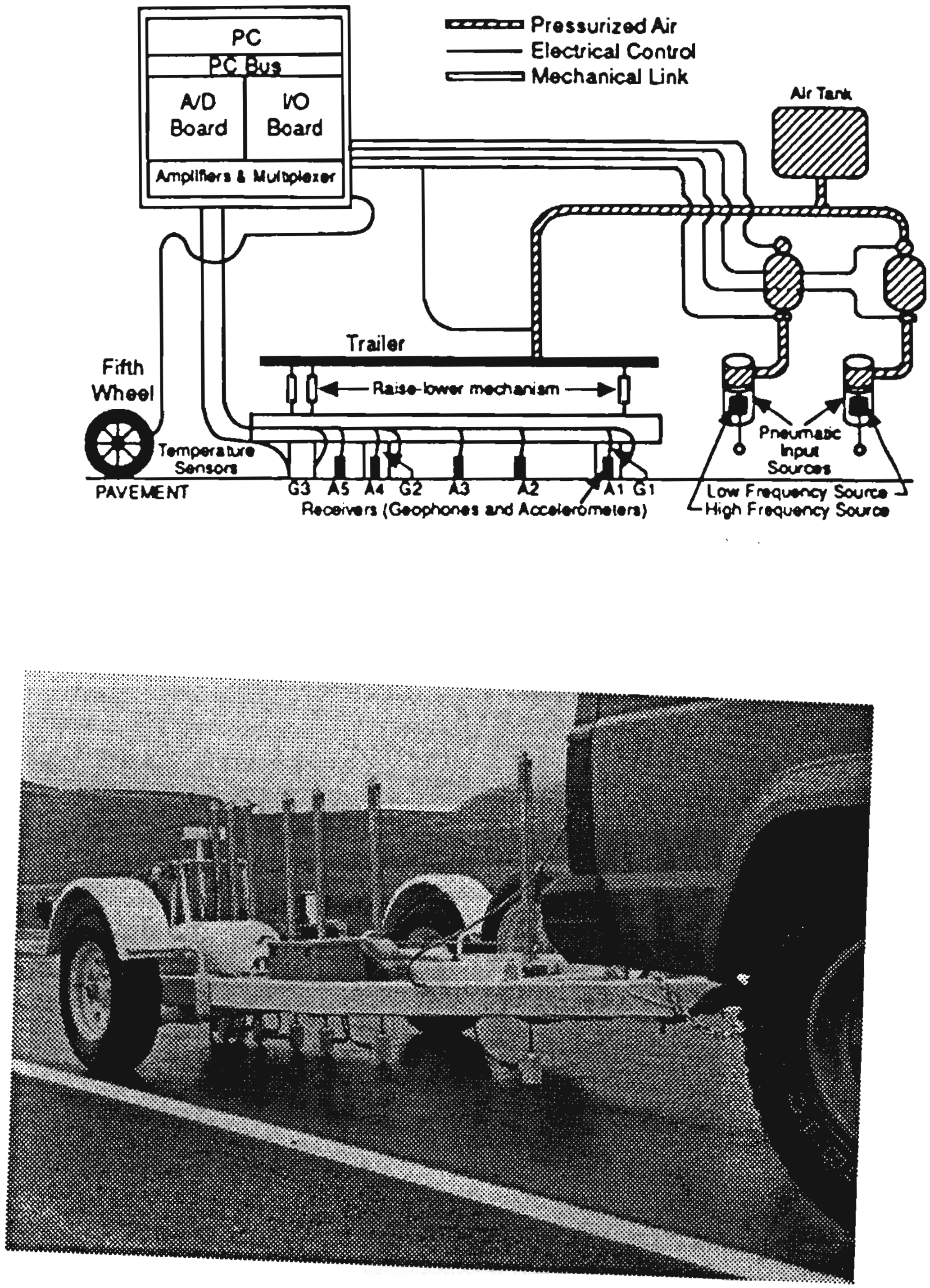

Figure 2.2 - Schematic of Seismic Pavement Analyzer

Five different tests are carried out with the SPA:

1. Spectral Analysis of Surface Waves (SASW),
2. Impulse Response (IR),
3. Ultrasonic Body Wave (UBW),
4. Ultrasonic Surface Wave (USW), and
5. Impact Echo (IE).

The main method used in this study is the SASW method which can nondestructively determine modulus profiles of pavement sections . Figure 2.2 depicts the set-up used for the SASW tests. All accelerometers and geophones are used to record seismic waves as they pass by them. A computer algorithm utilizes the time records to determine automatically a representative dispersion curve which is a variation of seismic velocity with wavelength (Nazarian and Desai, 1993). The last step determines the elastic modulus of different layers, given the dispersion curve. A recently developed automated inversion process (Yuan and Nazarian, 1993) determines the stiffness profile of the pavement section.

Two parameters are obtained with the IR method—the shear modulus of the subgrade and the damping ratio of the system. These two parameters characterize the existence of several distress precursors. In general, the modulus of the subgrade can be used to delineate between good and poor support. The damping ratio can distinguish between the loss of support or weak support (Nazarian etal., 1995).

The ultrasonic-body-wave method can directly measure Young's modulus of the top layer, which is an offshoot of the SASW method. The major distinction between these two methods is that in the ultrasonic-surface-wave method the shear modulus of the top layer can be easily and directly determined without a complex inversion algorithm. The results from these two methods can be combined to readily determine Poisson's ratio of the top layer.

The impact-echo method can effectively locate defects, voids, cracks, and zones of deterioration within concrete.

Determination of Moduli

The behavior of most bases and subgrades under load can be represented by a stress-strain curve similar to the one shown in Figure 2.3. Three significant parameters related to this curve are the following:

1. the initial tangent modulus, or maximum modulus (E_{max}) — the slope of the tangent to the curve passing through the origin,
2. the strength of the material (σ_{max}) — the horizontal line asymptotic to the curve, and
3. the secant modulus (E_1, E_2 or E_3) — the slope of a line connecting the origin to any point of the curve.

The initial tangent modulus is directly affected by the stress state, and the void ratio (density) of the material. The secant modulus is strongly affected by the magnitude of strain applied to the specimen.

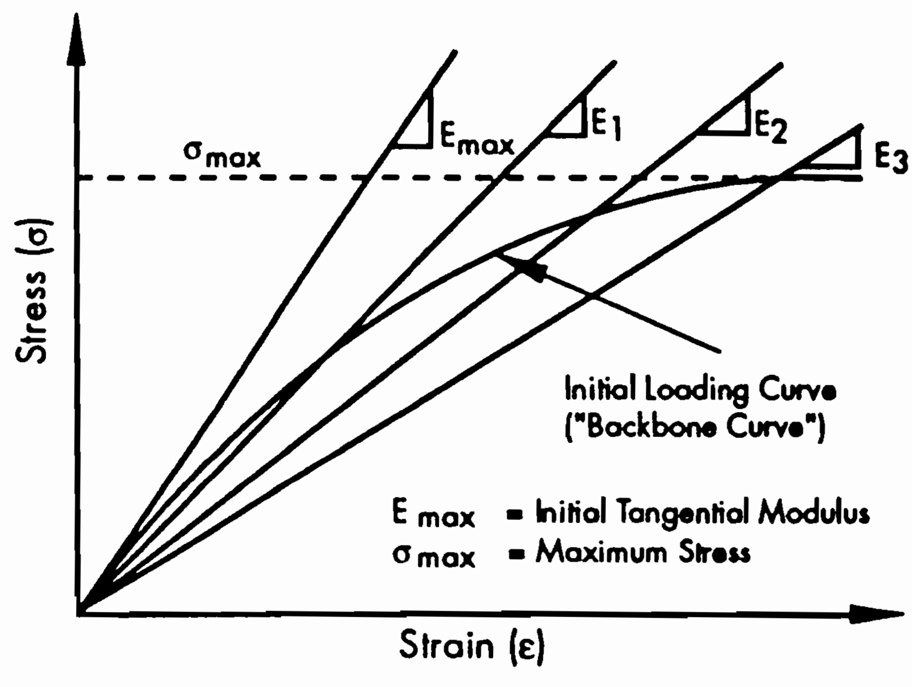

Figure 2.3 - Typical Stress-Strain Curve for a Material

Stokoe et al. (1988) identified four ranges of strain amplitude. The four categories are as follows:

1. small strains, also called elastic strain, where material behaves linearly,
2. medium strains, where nonlinear elastic behavior dominates,
3. large strains, where significant plastic deformation occurs but failure is not reached, and
4. failure strains.

The thresholds are shown in figure 2.4. Also, shown in the figure are two other thresholds which are important for bases and subgrade-the number of cycles of load (denoted as strain repetition threshold) and strain rate of the load applied (strain rate threshold). The strain rate threshold roughly coincides with the limit of the small strains. The strain repetition threshold is located within medium-strain region. As soon as the strain repetition threshold has been exceeded, progressive failure will be imminent.

Figure 2.5 shows a typical variation in secant modulus with strain. For small strains, the modulus is equal to the initial tangent modulus, E_{max}. In the medium-strain levels, a gradual decrease in modulus occurs. In the large strain region, the rate of decrease in modulus with strain significantly increases, until at failure strain the modulus again becomes asymptotic to a constant value.

The resilient modulus tests are typically performed in the medium and large strain regions. It is difficult to routinely perform MR tests at low strains because of the limitations in the loading mechanism. Referring to Figure 2.4, for MR tests at small deviatoric stresses, the moduli measured are not affected by the number of cycles or the strain rate. However, for larger deviatoric stresses, where the strains are in large strain region, the strain rate, as well as, the number of cycles become quite important.

Resilient modulus tests are load-controlled, undrained tests. In addition, resilient modulus tests are carried out in stages; that is the specimen is subjected to numerous levels of confining pressure and deviatoric stress. A major assumption in stage testing of a specimen is that the previous load applications have not altered the properties of the specimen. At high deviatoric stresses (i.e., higher strains), significant build-up of pore pressure and permanent deformation may occur. This phenomenon may adversely affect the constitutive model developed from MR tests. In the protocol proposed in Report 1336-1, the load sequences that may cause the degradation of the specimen are removed to a large extent. On soft materials, the strain levels should be carefully monitored to ensure that the material has not been degraded during tests.

Under the FWD loads, the strains in the base range from small to medium. For weak pavements, the strains may extend into the large region; therefore, the moduli may be affected by the strain rate of the applied load. A typical FWD pulse is about 30 msec long, whereas the specimen during the MR tests is subjected to 100 msec long load pulses. The magnitudes of load-induced stresses and strains under the FWD impact are directly related to the moduli of the different layers in the pavement systems. As such, the moduli determined with the FWD are secant moduli at some unknown strain level. In addition, since the strain levels and stresses decrease with depth (especially for thicker bases), the secant moduli of the top and the bottom of the base layer may differ significantly.

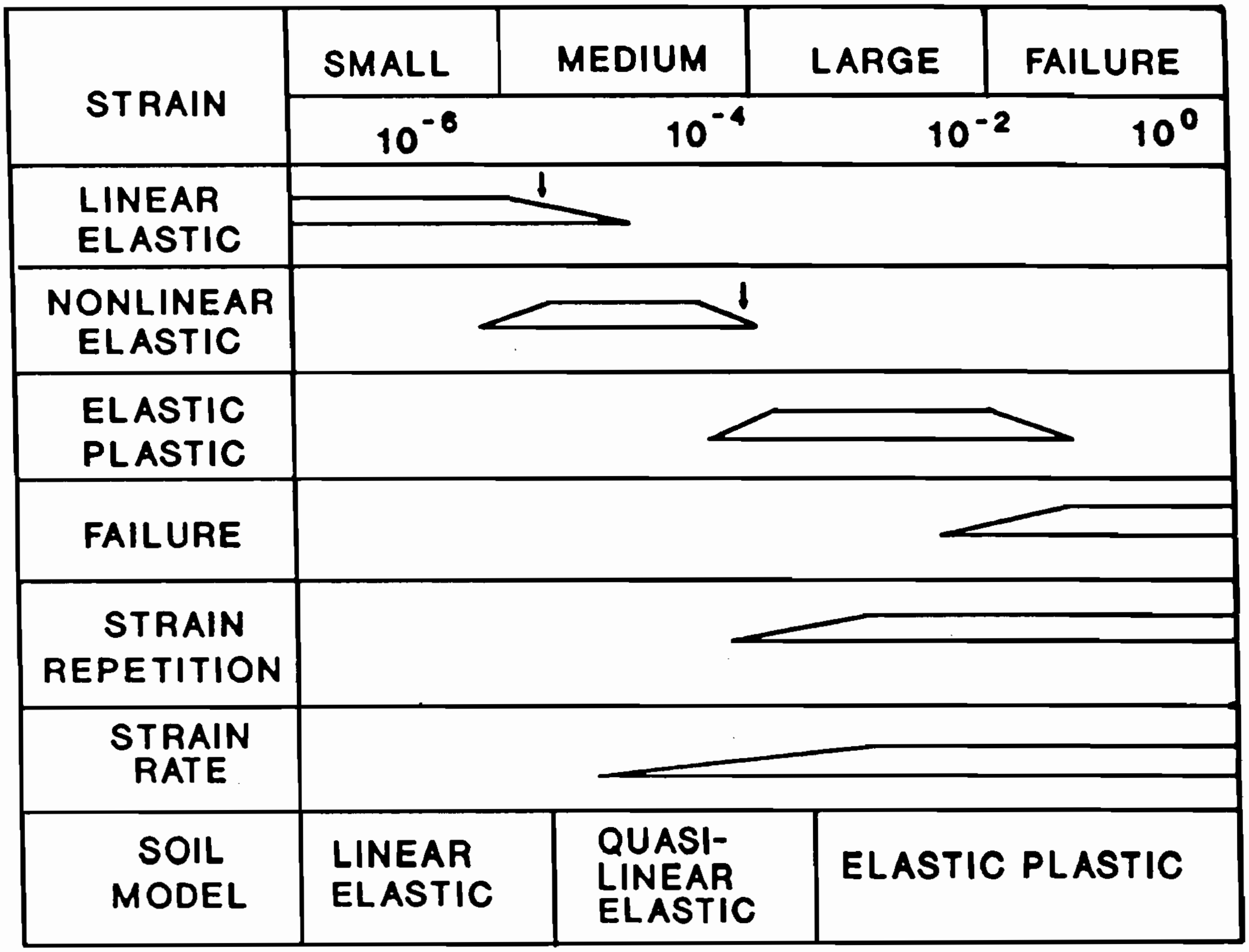

Figure 2.4 - Behavior of Materials at Different Strain Levels

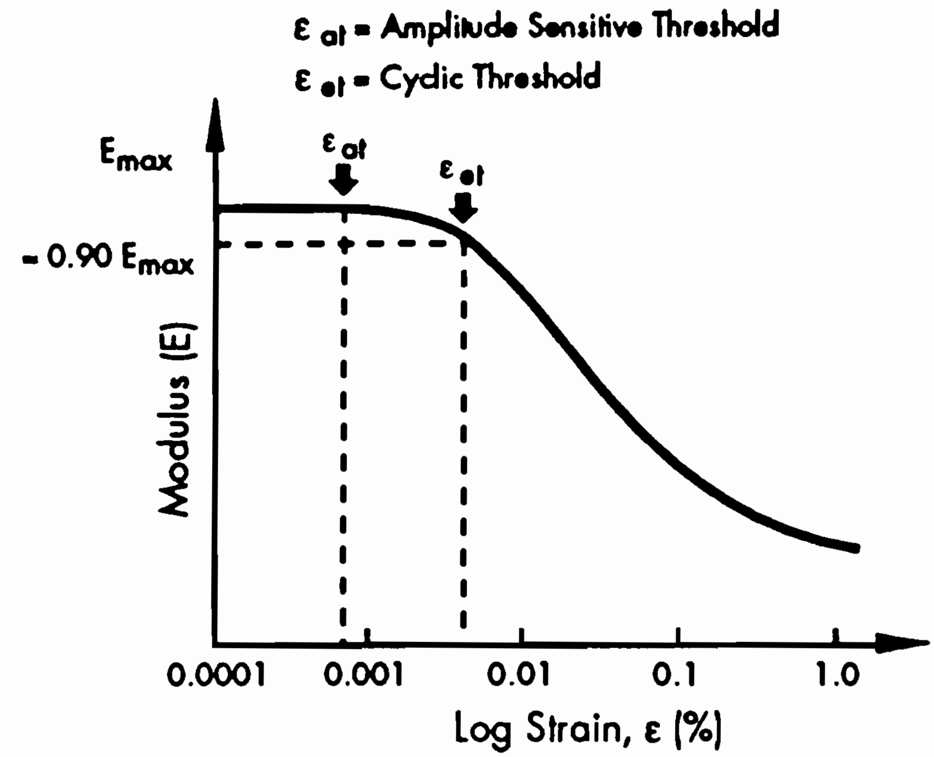

Figure 2.5 - Typical Variation of Secant Modulus of a Granular Material with Strain Level

All moduli measured with the SPA are in the small-strain range; therefore, the modulus reported for a layer is theoretically a fundamental material property. The modulus is independent of the strain level or of other factors that affect the FWD modulus. However, to use SPA moduli in the design, an algorithm is necessary for determining the variation in modulus with strain and the state of stress. Such a model was developed by Nazarian et al. (1987), based on numerous resonant column tests performed on granular materials by Ni (1987).

Figure 2.6 shows the model which considers the effects of the strain level and the octahedral normal stress. The octahedral normal stress is the average of the three principal stresses (i.e., 1/3 of the first stress invariant). Before wheel loads are applied, this stress is equivalent to the confining stress used in the laboratory. Several important points can be deduced from Figure 2.6. First, at a given strain, the material becomes stiffer, as the normal octahedral stress increases. Second, there is a threshold strain level below which the material behaves elastically (i.e., the secant modulus is equal to the initial tangent modulus). Third, an increase in strain above the threshold level results in a reduction in the modulus of the material, and hence, nonlinear behavior.

The report compares moduli measured using three different methods. Each method has advantages and weaknesses as reflected in Table 2.2. Therefore, any comparative study should be carried out with caution.

Table 2.2 - Advantages and Disadvantages of Methods Used to Obtain Moduli

Test Method	Major Advantage(s)	Major Weakness(es)
Resilient Modulus	Valuable for developing constitutive model for a material (i.e., variation in modulus with the state of stress and strain)	i. Very difficult to prepare specimens with the same characteristics of in situ materials ii. Time consuming and expensive to perform
Falling Weight Deflectometer	i. Covers a representative volume of material ii. Imposes loads that approximate wheel loads	i. Accurate determination of moduli of pavement layers may be difficult due to problems with backcalculation ii. The state-of-stress within pavement strongly depends on moduli of different layers, and hence is unknown.
Seismic Pavement Analyzer	i. Covers a representative volume of material ii. Measures a fundamentally-correct parameter (i.e., linear elastic modulus)	State-of-stress during SPA tests differs from the state-of-stress under actual loads

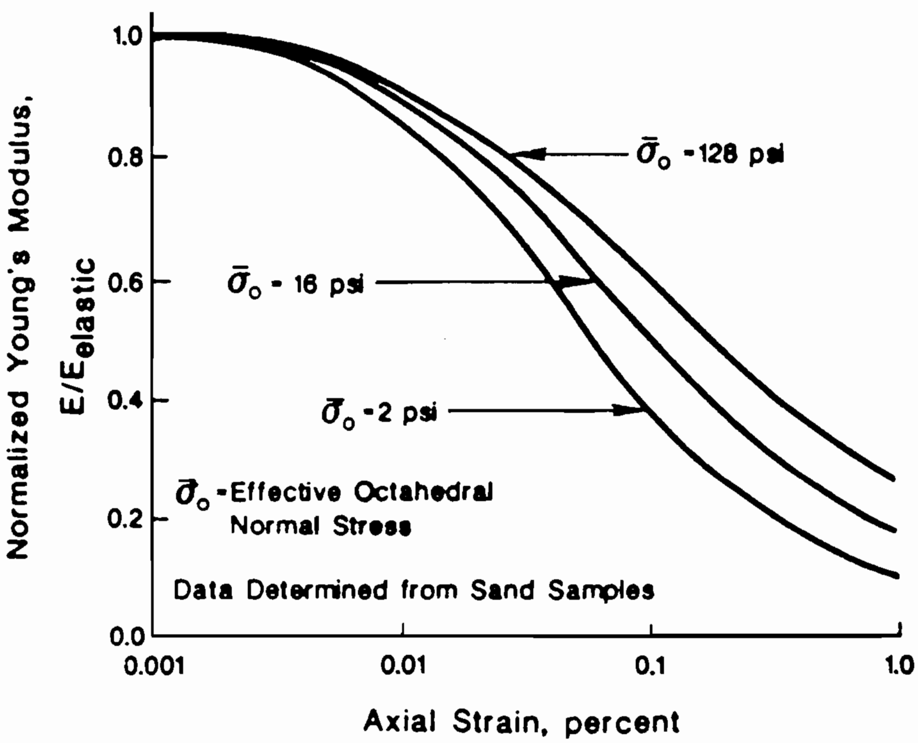

Figure 2.6 - Nonlinear Model for Determining Equivalent-Linear Moduli of a Granular Material

Two approaches can be proposed to determine the modulus of a layer under actual load. The first approach is to employ high-intensity loads in an attempt to evaluate the nonlinear behavior of the pavement. Then, the elastic theory is used to backcalculate the modulus profile. The advantage of this method is that an equivalent nonlinear modulus of the pavement may be determined. These moduli will be adequate to predict the deformation of the surface of the pavement under similar applied load. If these moduli are used to determine stresses and strains within the pavement system, substantial errors may occur since the modulus of that layer is variable because of load-induced nonlinearity. This can be readily done with the FWD device.

As an example, an approximate distribution of modulus with depth and radial distance for a typical flexible pavement is shown in Figure 2.7 (see Nazarian et al., 1987). The y-axis shows the ratio of secant modulus and its corresponding initial tangent modulus. The AC layer and the subgrade at point 5 do not exhibit much nonlinear behavior, since their nonlinear moduli are relatively similar to their linear elastic moduli. However, directly under the load, the modulus of base is substantially less than its linear-elastic modulus, and varies by a factor of about 1.5 from the top to the bottom of the layer. The base behaves in a nonlinear fashion, from the center of the loaded area out to normalized radial distances of 1.5.

The second approach is borrowed from the geotechnical earthquake engineering field as applied to determining the effects of local soil profiles on the amplification of the intensity of earthquakes (National Research Council, 1985). In this method, the linear-elastic moduli of different layers are measured in situ, and laboratory tests are performed on representative specimens to determine the variation in the modulus with the state-of-stress. By incorporating the results from the laboratory and field, the actual nonlinear properties of any material can be determined at any load level. This can be readily done with the SPA and MR tests.

More than 30 years of research and practical experience in the earthquake engineering community have shown that the nonlinear behavior of soil deposits can be more realistically determined using the second approach (Glaser, 1994). However, since this approach has not yet been implemented, its applicability to pavement design should be further studied.

Another very important parameter is the Poisson's ratio of the material. Rodriguez-Gomez et al. (1991) showed that small variation in Poisson's ratio of different layers would significantly affect the backcalculated moduli from FWD. At high load-levels, the dilative nature of the granular materials may yield large Poisson's ratios which may defy the laws of elasticity.

Since measuring the in situ Poisson's ratio was beyond the scope of the project, and since the laboratory tests yield similar Poisson's ratios for each material, this matter is not pursued any further.

Past Investigation

For the last twenty years, many investigators have tried to develop relationships between laboratory and field moduli. This section focuses on work done in the last ten years. Before that time, most

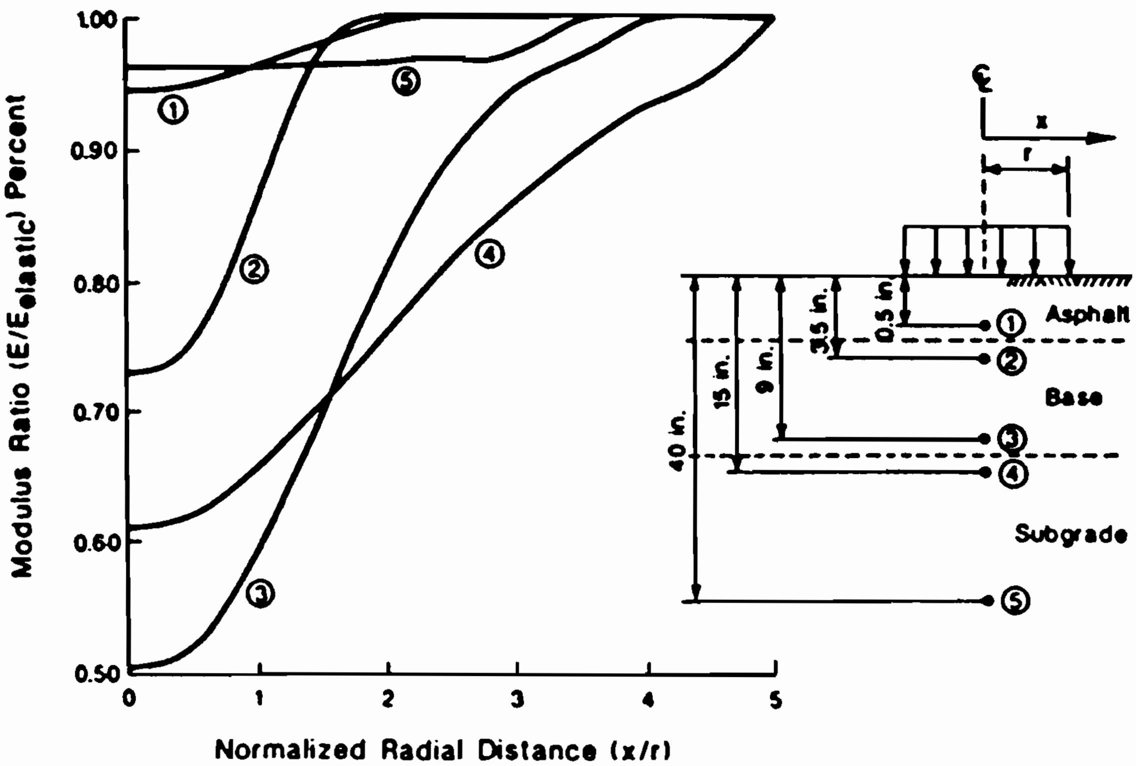

Figure 2.7 - Variation in Modulus with depth and radial distance for a Typical Pavement Under a load of 35 MN.

Table 2.3 - Comparison of Moduli from Different Sources (from Daleiden et al., 1994).

Ratio	Mean	Standard Deviation	Maximum	Minimum
Laboratory/ Backcalculated	0.57	0.67	10.34	0.01
Estimated/ Laboratory	4.65	3.81	58.09	1.10
Estimated/ Backcalculated	2.34	2.94	36.56	0.20

resilient modulus tests were performed following protocols that are not considered acceptable by today's standards. A review of the early development and application of resilient modulus tests can be found in the proceedings of a workshop held in Oregon (Vinson, 1989).

Moduli obtained from the SPA and laboratory tests have never been compared in the literature, since the SPA has just been developed. The only relatively comprehensive comparisons between seismic moduli and those from FWD can be found in Nazarian et al. (1987). Most comparisons are typically carried out between FWD and laboratory moduli. Furthermore, most investigations have been focused on the subgrade and not on the base.

Daleiden et al. (1994) demonstrates the challenges involved in comparing moduli from laboratory, FWD tests, and empirical relationships. They studied the results from more than 700 sections of the long-term-pavement-performance (LTPP) program monitored under the Strategic Highway Research Program (SHRP). Their findings are summarized in Table 2.3. In all cases, the standard deviations are about the same as the corresponding means. This shows that a direct relationship cannot be expected between the laboratory and field data. Based on the explanations provided in the previous section, one should not be surprised by this finding. Daleiden et al. finally reported three regression equations for clays, silts and sands. In these models, the load and deflection of sensor 7, as well as thickness of different layers, specific gravity, degree of saturation and dry density of the material should be input. The coefficients of determination (R^2) for the three models varied between 0.78 and 0.89.

Based on test results on ten pavement sections, Rodhe and Scullion (1990) indicated that without an appropriate analytical procedure, it would be difficult to offer any correlations between base moduli from FWD and laboratory moduli.

Akram et al. (1994) presented results from comprehensive tests on two pavement sections using the FWD, laboratory tests and multi-depth Deflectometer (MDD). The laboratory and FWD data compared relatively well at one site, but rather poorly at the other. Once again, they emphasized the importance of proper analytical modelling in determining reasonable results.

George and Uddin (1994) followed a procedure similar to that of Nazarian et al.(1987). They reported good agreement between FWD moduli and resilient moduli measured with a gyratory shear testing device.

Almeida et al. (1994) described the importance of considering the nonlinear behavior of pavement materials. They also offered a finite element code that can backcalculate the nonlinear moduli of pavement layers.

Stubstad et al. (1994) presented several case studies indicating the importance of considering the stress-sensitivity of pavement materials in any mechanistic approach.

In summary, the general consensus of the experts in the field is that a simple relationship does not exist that can reconcile the results from the laboratory and field tests. To successfully conduct pavement analysis and design, laboratory and field results should be linked through some analytical algorithm.

Chapter 3

Test Methodologies

As indicated before, ten different sites were tested. The test program at each site is described in the following chapter.

Selection of Sites

The detailed procedure followed to select the ten candidate districts is included in Nazarian etal. (1996). Briefly, a questionnaire was mailed to all districts to obtain an inventory of the types and volumes of different bases used throughout the state. Based on the response, base materials from specific quarries in ten districts were requested. At least six specimens from each base material were tested following the procedure detailed in Appendix A. Tests were carried out at near optimum, 2 percent dry of optimum, and 2 percent wet of optimum to determine the variation in modulus with moisture.

The second phase of this study consisted of testing base materials from the same quarries after they were laid down in pavement sections for some time. In this case, the specimens were compacted to the moisture contents and densities measured in the field.

The specific locations of sites were typically suggested by the district laboratory engineers based on a series of requirements suggested to them. The characteristics of the ideal site consisted of the following:

1. a flexible pavement free of excessive cracks,
2. two to three years old,
3. at least 75 mm of asphalt concrete pavement layer (ACP),
4. relatively soft subgrade (no caliche), and
5. bedrock at least 7 m deep.

As discussed in the next chapter, some of these requirements had to be relaxed in a few districts simply because adequate sites could not be found.

Retrieval of Materials

The materials necessary were retrieved from a trench dug in the pavement. The procedure followed consisted of the following steps:

1. A 1-m by 1-m section of asphalt concrete was removed using a concrete saw. The cutting operation was typically carried out with no or little water to minimize changes to the moisture of base.

2. Several specimens of the asphalt concrete were saved for future laboratory tests.

3. At least two moisture and density tests were carried out on top of the exposed base layer using a nuclear-density device.

4. About 300 Kg of the base material were carefully removed and bagged for shipping to the UTEP laboratory.

5. At least six random samples were retrieved so that the in-place moisture content of the base could be verified.

6. The trench was thoroughly cleaned to the top of the subgrade by removing the excess base material from it.

7. If possible, two to four 75-mm thin-walled samplers (shelby tubes) were pushed into the subgrade using a drill rig so that intact subgrade materials could be obtained.

8. The pavement section was then backfilled and repaired.

Nondestructive Testing

Either immediately before, or at the first available period after the trenching operations, FWD and SPA tests were performed at each site. The field NDT testing program at each site normally consisted of performing FWD and SPA tests at eleven locations each about 20 m apart. Five points were located before and after the trench. The eleventh point was in the vicinity of the trench. In this manner, variations in the material properties along the site could be somehow quantified.

Demonstration of Data Reduction Processes

In this section, the results from the site located in the El Paso district are included to clarify the procedures followed. This site was selected because the results were generally representative of most sites.

Index tests. The grain size distribution curves from the materials retrieved from the quarry and the in-place materials are compared in Figure 3.1. Even though, the shapes of the two gradation curves

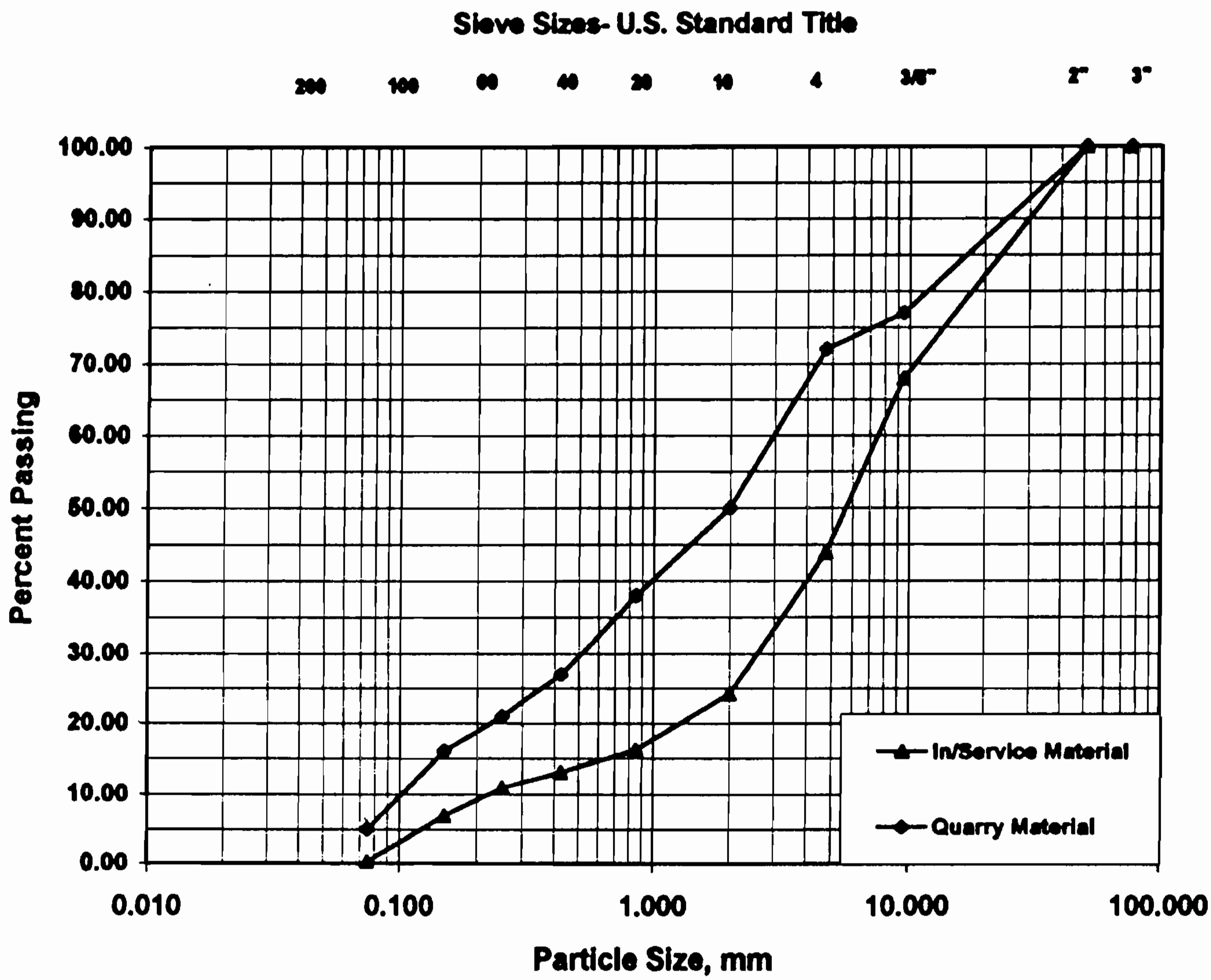

Figure 3.1 - Comparison of Grain Size Distribution of Quarry and In-Service Materials

are similar, the materials from the quarry seem to contain more fine aggregates than the materials from the in-service road.

From the Proctor test the field moisture content was about 3.1 percent, whereas the optimum moisture content was reported as 5.4 percent. The maximum dry density of the quarry material from Proctor tests was about 2290 kg/m^3 while the in-place density was about 2275 kg/m^3 from the quarry. While 25 blows of the standard Proctor hammer was necessary to achieve the maximum density under optimum moisture content, about 27 blows of the modified proctor hammer was necessary to prepare specimens to the water content and density measured in the field. These variations point to the differences between the methods used to evaluate materials in the laboratory and the actual conditions of base layers in the field.

Resilient Modulus Tests. The constants of the constitutive models presented in Equation 2.6 are compared to the specimens prepared from the in-service and quarry materials in Table 3.1. The coefficients of determination for both models are fortunately quite high. Typically, more variability in the results from the in-service materials are seen because of difficulties in preparing specimens with fixed values of moisture content and density.

Table 3.1 - Comparison of Constitutive models for Quarry and In-Service Materials

Material	Constants for Constitutive Model			R^2
	K_1	K_2	K_3	
Quarry	51359	-0.005	0.440	0.999
In-Service	51042	-0.237	0.201	0.972

Some differences and similarities exist between the two models. The values of K_2 related to the deviatoric stress, are negative in both cases. This indicates that the modulus decreases with deviatoric stress (or strain), which is consistent with the fundamental behavior of granular materials. However, the magnitude of K_2 is very small in materials from the quarry and larger for in-service materials. Aside from approximations associated with the curve fitting process, one possible explanation can be given for the differences.

For in-service materials, MR tests were carried out at higher deviatoric stresses and confining pressures. Since the resilient modulus test is a load-controlled test, the strain levels imposed on the in-service specimens are higher than those of the quarry materials. As such, the in-service materials may show higher dependence on strain.

Parameter K_3, which is related to confining pressure, varies between 0.2 and 0.45. These values are considered reasonable for granular materials. The value of 0.2, may be on the lower bonds usually reported.

Dynamic Cone Penetration Tests. At each site, the Dynamic Cone Penetration (DCP) device was also used at one point. The device is an excellent tool for obtaining information with regards to relative stiffness of different layers. However, due to its empirical nature, it is not justifiable to correlate results from DCP to moduli. Figure 3.2 shows a typical variation in penetration with depth for the site. A depth of zero corresponds to the top of the base. The transition from one layer to another was defined rather well. The results from DCP tests at all sites are included in Appendix B.

SPA Tests. The next step consisted of reducing the SPA results. To demonstate the raw data, typical dispersion curves from the points tested are shown in Figure 3.3. Due to problems with the SPA, results from only seven data points are reported.

For longer wavelengths, the dispersion curves are very similar indicating that the modulus of subgrade is similar. However, for Stations 1, 7, and 11, the dispersion curves at high frequencies are different. Similar variabilities are evident in the FWD data.

Table 3.2 shows the variation in modulus and thickness of the pavement at all points. The modulus of the AC layer is relatively constant. The modulus of the base varies by about 30 percent along the 60 m of pavement in the vicinity of the trench, mostly because of higher than average base of station 11. Stations 1 and 7 exhibits thicker than usual base. The coefficient of variation of the subgrade is about 11 percent indicating large variations in the modulus of the subgrade layer. Mean moduli for the AC, base and subgrade are 9 GPa, 708 MPa and 536 MPa, respectively.

FWD Tests. Finally, the variations in deflections with sensor location for the points tested with the FWD are shown in Table 3.3. The mean and coefficient of variation for each sensor are also included in the table. The coefficients of variation vary from 10 percent to 27 percent. The variations correspond 10 percent for sensors farther from the load, and 27 percent for those near the loading pad. These variations are at least quantitatively in line with the moduli obtained with SPA.

Initially, it was intended to select sites based on the uniformity of the deflection basins. However, this was not always possible. Field work at each site had to be coordinated in advance. Unfortunately, several breakdown of NDT devices occurred very close to the time when the field work had to be carried out.

Young's moduli of the three layers at each point are also reported in Table 3.4. On the average, moduli of the AC, base and subgrade are 2.1 GPa, 302 MPa and 157 MPa, respectively. The coefficients of variations are equal to zero for AC (modulus assumed as known), and more than 30 percent for base, indicating large variation in the modulus values.

Comparison of Moduli. The last step of the process consisted of comparing moduli from different methods. A rational approach was devised to perform this task. It should be mentioned that the proposed methodology is rather approximate and should be considered as an initial attempt.

From a laboratory MR test, a constitutive model is obtained. As per Eq. 2.6, the modulus has to be calculated at a given confining pressure and given deviatoric stress. To determine these stresses, the layered-elastic computer program KENLAYER (Huang, 1994) was used. In that program, moduli, thickness and Poisson's ratio of each layer, as well as the applied load, are input. The outputs of the program are the stresses and strains at any requested point. The input load was assumed to be a standard dual-tandem truck load.

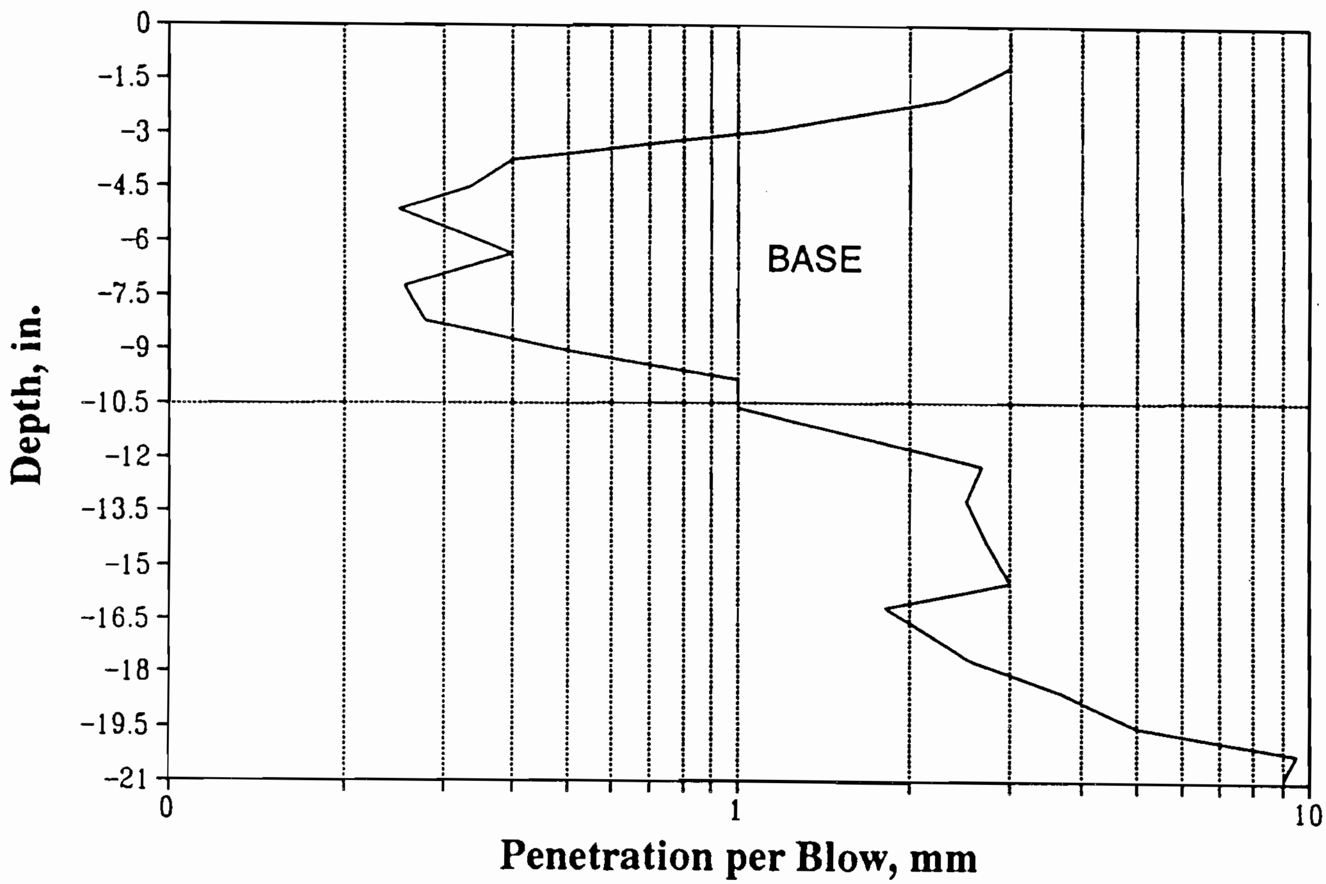

Figure 3.2 - Typical Dynamic Cone Penetration Resistance Results

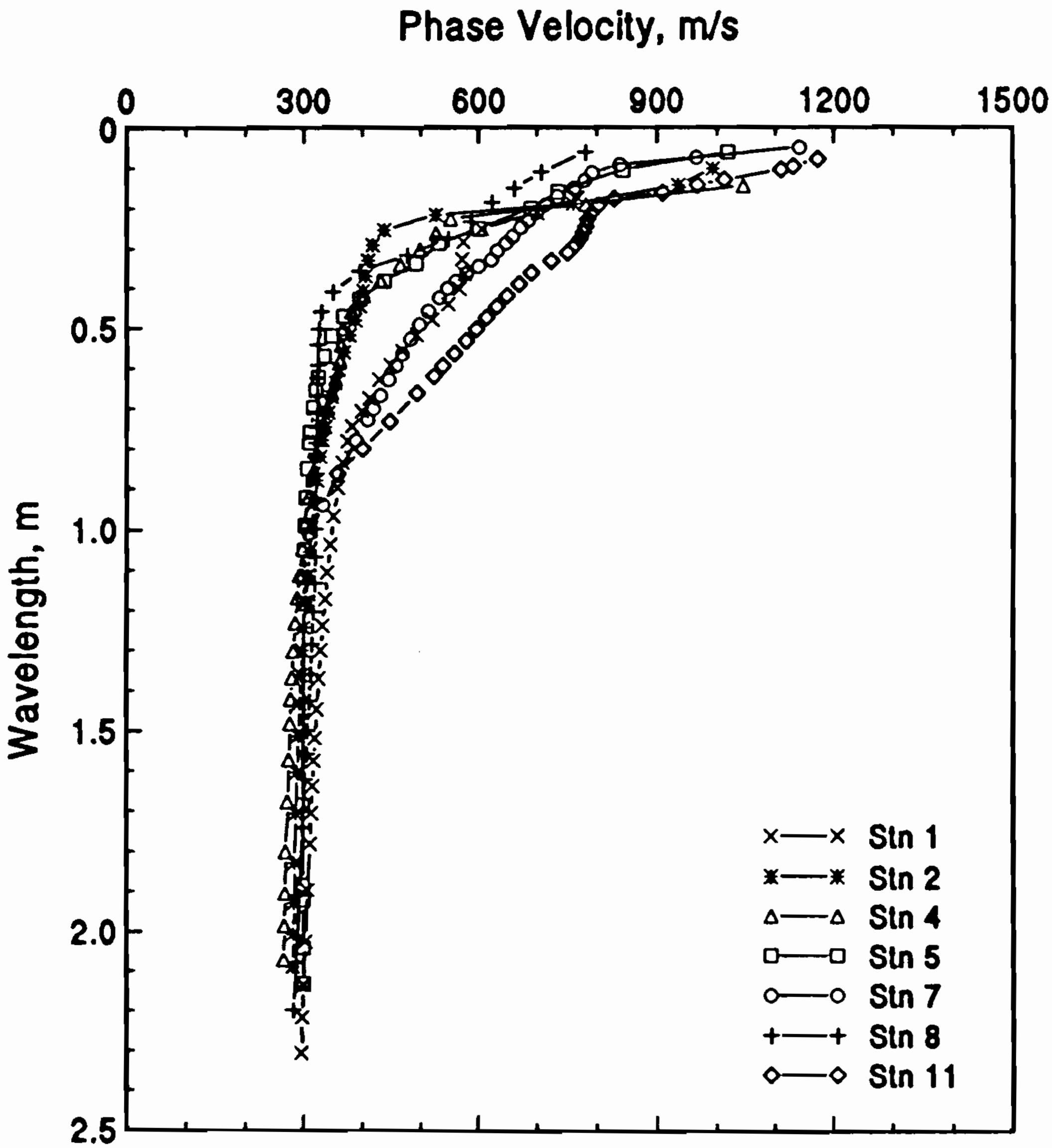

Figure 3.3 - Comparison of Dispersion Curves

Table 3.2 - Variation in Modulus and Thickness from SPA Tests

Station	Modulus , KPa			Thickness, mm	
	AC	Base	Subgrade	AC	Base
1	9753	778	667	66	272
2	9799	647	527	52	256
4	102585	601	524	53	216
5	8231	556	535	59	241
7	8882	571	535	62	290
8	8568	627	489	74	265
11	10398	1176	476	75	202
Mean	9413	708	536	63	249
C.V.,%	9.0	30.9	11.6	14.7	12.6

Table 3.3 - Variations in Deflections with Test Location from FWD

Station	Load, KN	Measured Deflection, micron						
		R1	R2	R3	R4	R5	R6	R7
1	40	349	164	78	52	40	32	23
2	40	447	203	90	59	46	34	24
3	41	278	129	66	48	39	33	24
4	40	358	166	70	48	38	30	22
5	40	289	133	63	43	34	31	21
6	40	380	154	75	52	41	34	23
7	40	491	224	94	64	50	41	28
8	39	419	190	81	54	45	35	26
9	40	411	184	86	57	46	33	22
10	39	504	258	109	65	49	41	29
11	40	350	169	78	52	41	33	22
Mean	40	400	184	80	55	43	34	25
C.V.,%	1.03	23.3	26.8	19.8	15.9	13.5	11.1	10.3

Table 3.4 - Variations in Moduli from FWD with Test Location

Station	Modulus, MPa			Abs. Error/ sensor, percent
	AC	Base	Subgrade	
1	2069	380	166	7.14
2	2069	240	143	7.01
3	2069	474	174	9.47
4	2069	339	179	9.45
5	2069	456	196	9.87
6	2069	247	161	7.43
7	2069	194	130	8.93
8	2069	246	150	9.95
9	2069	266	147	6.33
10	2069	195	120	8.47
11	2069	383	161	8.64
Mean	2069*	302	157	8.20
C.V., %	0.0*	32.5	14.0	17.49

* A default fixed value was assumed because the layer was about 60 mm thick.

To compare the results from SPA and the laboratory tests, the average moduli obtained by the SPA were input to KENLAYER, and the vertical stresses were determined within the base layer at 25-mm intervals directly under a wheel. The vertical stress at each point was assumed to be equal to the deviatoric stress of the laboratory model (i.e. Eq. 2.6). The confining pressure was assumed to be equal to the normal octahedral stress in the layer, and was calculated from

$$\sigma_C = \sigma_{oct} = [(1 + 2k_o)/3]\ \sigma_v \tag{3.1}$$

where:

σ_C = laboratory confining pressure,
σ_{oct} = field octahedral stress,
k_o = coefficient of earth pressure at rest, and
σ_v = vertical stress.

Parameter k_o is related to the angle of internal friction (ϕ), and the overconsolidation ratio (OCR) through (Mayne and Kulhawy, 1982)

$$k_o = (1\text{-}\sin\phi)\ OCR^{\sin\phi}. \tag{3.2}$$

Since the base layer is heavily compacted, a k_o value of unity was assumed.

Using these deviatoric and confining stresses, moduli from tests using quarry and in-service materials were determined at 25-mm intervals. In that manner, a determination of the variation in modulus with depth could be made.

Table 3.5 shows the variations in vertical stress and modulus with depth for the example site for models developed from quarry and in-place materials. The variations shown in the table are rather representative of most sites studied here. In most cases, the variation in modulus with depth was about 10 percent; therefore, the average modulus was used for comparison purposes.

The base modulus from the SPA was also adjusted to consider the reduction in modulus due to load-induced nonlinearity. The reduction in modulus was determined using the model presented in Figure 2.6, along with the octahedral stress and the strain calculated from KENLAYER. The SPA modulus was then multiplied by the reduction factor to determine the "modified modulus."

Table 3.5 also contains the variation in strain and modified SPA modulus for the example site. Once again, the variations, which are rather typical for most sites studied here, were rather small. The average modified SPA moduli were used for comparing moduli.

The procedure outlined above yields approximate results, because a linear-elastic computer algorithm was used to determine the nonlinear stress and strain parameters of the soil. To study the level of approximation associated with this assumption, the problem was also approached from another direction. KENLAYER would allow the user to introduce a nonlinear constitutive model for each layer. The constitutive model incorporated in the program is in the form of

$$M_R = m_1\ \theta^{m2} \tag{3.3}$$

where θ is the bulk stress (i.e. three times the octahedral stress). However, the models developed from laboratory tests in this study were in the form of

$$M_R = k_1\ \sigma_d^{k2}\ \sigma_c^{k3}. \tag{3.4}$$

Since a coefficient of earth pressure at rest of unity was assumed for the base material, it can be shown that

$$m_2 = k_2 + k_3. \tag{3.5}$$

By substituting Equation 3.4 in Equation 3.3, the value of m_1 was obtained by trial and error from

$$m_1 = [k_1\ \sigma_d^{k2}\ \sigma_c^{k3}]\ /\ \theta^{m2}. \tag{3.6}$$

The stresses in the equation correspond to the middle of the base layer. In this manner, a model for the base was obtained, which models the nonlinear behavior of the base in an approximate fashion.

Table 3.5 - Comparison of Moduli Obtained from Laboratory and SPA Using a Linear-Elastic Algorithm

Depth from Top of Base, mm	Vertical Stress, KPa	Laboratory Modulus, MPa		Vertical Strain, μstrain	Modified SPA Modulus, MPa
		Quarry	In-Service		
25	188	501	442	239.2	574
50	162	470	424	211.7	585
75	141	442	426	187.4	594
100	123	416	428	166.9	603
125	109	395	430	148.8	612
150	99	378	432	139.1	617
175	90	363	433	131.0	621
200	82	350	434	124.6	624
Mean	124	414	429	169.0	604
Std. Dev.	37	53	5	24.4	18

With this model, KENLAYER was again executed to obtain the relevant stresses and strains at the middle of 50-mm sublayers within the base. Following the approach discussed above, the laboratory moduli and reduction factors for SPA moduli were again obtained. For the sake of clarity, the moduli obtained in this manner will be called "nonlinear" moduli, hereafter. These values are only approximate equivalent-linear values, since the constitutive model and the approach followed in KENLAYER are both rather approximate.

Table 3.6 shows variations in moduli obtained following this approach. Once again, the variations in modulus with depth within the base layer are typically within 10 percent of the average modulus; therefore, the average value was used as the representative of the base modulus. Similar trends were observed for the quarry and in-service materials.

Finally, the same approaches were followed using the FWD moduli. Representative results from the "linear" and "nonlinear" models obtained in that manner are shown in Tables 3.7 and 3.8. Trends similar to those obtained from models developed based on the SPA results (i.e. Tables 3.5 and 3.6) are observed. The FWD moduli are not modified for load-induced nonlinear behavior. One of the major assumptions in this test methodology is that this matter has already been taken into account.

The variations in the laboratory moduli with depth from the "linear" and "nonlinear" models using the SPA and FWD results are included in Figure 3.4. As indicated before, the linear and nonlinear moduli are quite close; therefore, at least for the approximate model used here, the nonlinear effects are small.

Table 3.6 - Comparison of Moduli Obtained from Laboratory and SPA Using a Nonlinear Algorithm

Depth from Top of Base, mm	Vertical Stress, KPa	Laboratory Modulus, MPa		Vertical Strain, µstrain	Modified SPA Modulus, MPa
		Quarry	In-Service		
25	188	491	422	239.3	574
75	141	434	426	186.3	595
125	109	393	430	147.0	613
175	90	365	433	129.1	622
Mean	132	421	428	175.4	601
Std. Dev.	43	55	5	27.8	21

Table 3.7 - Comparison of Moduli Obtained from Laboratory and FWD Using a Linear-Elastic Algorithm

Depth from Top of Base, mm	Vertical Stress, KPa	Laboratory Modulus, MPa	
		Quarry	In-Service
25	236	554	418
50	203	518	420
75	175	486	423
100	153	458	425
125	134	433	427
150	119	410	429
175	107	393	430
200	97	375	432
Mean	153	453	425
Std. Dev.	49	63	5

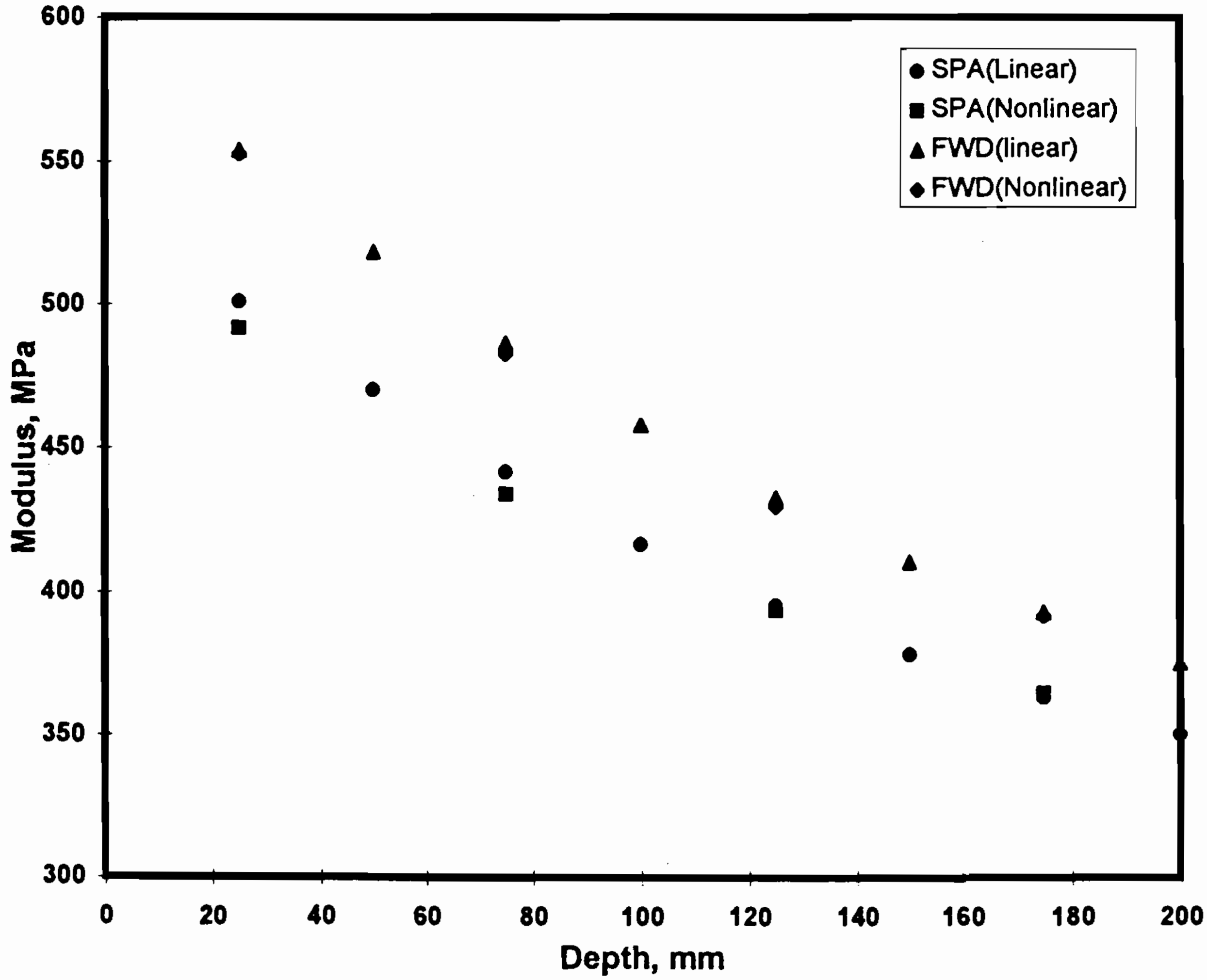

Figure 3.4 - Comparison of Linear and nonlinear moduli from Example Site

Table 3.8 - Comparison of Moduli Obtained from Laboratory and FWD Using a Nonlinear Algorithm

Depth from Top of Base, mm	Vertical Stress, KPa	Laboratory Modulus, MPa	
		Quarry	In-Service
25	236	552	418
75	175	483	423
125	134	430	427
175	107	391	430
Mean	163	464	424
Std. Dev.	56	70	5

For each of the four sets of data, the modulus increases slightly with depth. From Equation 2.6, modulus increases as the confining pressure increases or as the deviatoric stress decreases. Depending on the values of the exponents for these two parameters (i.e. k_2 or k_3), the modulus may increase or decrease with depth. Both trends have been observed in this research.

Finally, the representative moduli from different methods are compared in Table 3.9. The average moduli from the laboratory tests on quarry and in-service materials are quite close for this site, and are about 441 MPa (when the FWD moduli was used to calculate the state of stress) and 423 MPa (when the SPA moduli were used to calculate the state of stress). Typically, the results from the two laboratory methods are not close. In addition, these moduli are relatively independent of the linear or nonlinear models used in KENLAYER. This trend was applicable to most soils tested.

The FWD modulus for the base layer was on the average 302 MPa, which is about 40 percent less than the laboratory moduli. On the other hand, the average base modulus from SPA was about 600 MPa — twice the FWD modulus and about 40 percent greater than the laboratory moduli. These types of variation in moduli from different methods are typical.

Table 3.9 - Summary of Representative Moduli from Different Methods

Device	Model	Laboratory Modulus, MPa		Field Modulus, MPa	
		Quarry	In-Service	SPA	FWD
FWD	Linear	453	425	--	302
	Nonlinear	464	424	--	302
SPA	Linear	414	429	604	--
	Nonlinear	421	428	601	--

Chapter 4

Presentation of Results

Location of Sites

As indicated before, ten sites in ten different districts were tested. The location and type of materials at each site are included in Table 4.1. Base materials include limestone for five sites, caliche for two sites, iron-ore for two others, and sand and gravel for one site.

The results from nondestructive tests at some sites are not available. The FWD test results are missing for Childress and San Angelo. Tests were arranged for San Angelo several times, but due to unforeseen equipment breakdown, tests could not be performed. Tests were carried out at the Childress site, but the data disk was corrupt and could not be retrieved. In addition, quarry materials from the Lufkin district were not tested in the laboratory because the materials were not received at UTEP.

Index Properties

The gradation curves for different materials are summarized in Table 4.2. The materials from in-service test pits are typically different from those obtained from the quarry. It seems that the fine contents of the quarry materials are higher in almost all districts. The sand contents are also higher for the quarry materials.

Table 4.3 reflects the Atterberg limits. In some cases, the Atterberg limit tests could not be performed because of a lack of fine contents in the in-service materials. In most cases, the liquid limits and plasticity indices of the quarry and in-service materials are in agreement. However, in several cases, substantial differences can be detected. Based on the gradation and Atterberg limits, most materials are well-graded gravel (GW) or well-graded sands (SW), according to the unified soil classification system.

Table 4.1 - Locations of Sites Tested

Material Type	District	Location	Layer Thickness, mm		
			AC	Base	Subbase
Limestone	Brownwood	FM 45	25	279	
	El Paso	US 62	76	203	229
	Paris	FM 2820	13	254	
	San Angelo	US 67	51	305	
	San Antonio	Loop 1604	64	267	
Caliche	Corpus Christi	SH 44	114	254	203
	Odessa	FM 1788	38	203	
Iron-Ore	Lufkin	SH 7	102	356	
	Tyler	SH 110	76	279	
Sand and Gravel	Childress	US 287	51	229	381

Table 4.2 - Gradations of Materials Tested

Material Type	District	Gradation (percent passing)					
		In-Service Materials			Quarry Materials		
		#4	#40	#200	#4	#40	#200
Limestone	Brownwood	44	8	0	30	14	6
	El Paso	44	13	0	48	21	7
	Paris	38	15	1	50	34	6
	San Angelo	59	12	1	43	15	4
	San Antonio	33	6	0	51	26	5
Caliche	Corpus Christi	46	19	2	38	27	4
	Odessa	51	18	1	60	32	8
Iron-Ore	Lufkin	42	19	1	--	--	--
	Tyler	46	22	1	69	32	4
Sand and Gravel	Childress	51	20	0	60	32	7

Table 4.3 - Atterberg Limits of Materials Tested

Material Type	District	Water Content, percent			
		In-Service Materials		Quarry Materials	
		LL	PI	LL	PI
Limestone	Brownwood	21.0	7.4	16.6	3.4
	El Paso	24.3	8.7	24.0	8.0
	Paris	NP	NP	21.2	3.4
	San Angelo	15.5	2.9	14.6	2.1
	San Antonio	NP	NP	23.5	9.8
Caliche	Corpus Christi	34.5	7.5	33.0	10.0
	Odessa	24.0	6.9	NP	NP
Iron-Ore	Lufkin	17.3	0.4	NP	NP
	Tyler	18.8	1.7	27.0	6.9
Sand & Gravel	Childress	14.6	2.2	28.7	8.9

Table 4.4 -Dry Densities and Moisture Contents of Materials Tested

Material Type	District	Dry Density, Kg/m^3		Moisture Content, %	
		Field/No. of Blows* (Measured)	Maximum (Proctor)	Field (Measured)	Optimum (Proctor)
Limestone	Brownwood	2179 / 40	2330	5.8	3.8
	El Paso	2275 / 27	2290	3.1	5.4
	Paris	1922 / 20	2040	10.3	7.9
	San Angelo	2323 / 60	2290	8.5	6.5
	San Antonio	2243 / 30	2390	7.5	7.5
Caliche	Corpus Christi	1714 / 17	1660	19.0	17.8
	Odessa	2147 / 65	2100	6.3	4.3
Iron-Ore	Lufkin	2003 / 30	--	8.5	--
	Tyler	2163 / 15	2290	10.5	7.8
Sand & Gravel	Childress	2275 / 35	2160	3.2	5.5

* No. of Blows corresponds to number of blows per 50-mm lift of material using a modified Proctor hammer

In Table 4.4, the field moisture content and density of each base are compared with the respective optimum water content and maximum dry density measured with the Proctor compaction tests on quarry materials. The field moisture contents typically differ by about 2 percent from the optimum values. In some cases, the field moisture contents are higher, and in some other instances are lower than the corresponding optimum moisture contents. The San Antonio site is the only one where the optimum and measured moisture contents are similar.

As reflected in Table 4.4, the actual field densities are fairly close to the maximum densities obtained from the Proctor tests, with a maximum difference of about ten percent and a typical difference of about 3 percent. The number of blows required to prepare the specimens which simultaneously simulate both the moisture contents and densities measured in the field, are also included in the table. The numbers, which are established based on trial and error, are indications of the levels of effort needed to compact the specimens. The number of blows vary anywhere from 15 and 17 as a low for Corpus Christi and Tyler, to 60 and 65 as a high for San Angelo and Odessa.

Resilient Modulus Tests

The constitutive models for the resilient modulus tests performed on the quarry and in-service materials are included in Table 4.5. The raw data for specimens prepared from in-service materials are included in Appendix C. The results from quarry materials are reported in Nazarian et al. (1996), and are not repeated herein for the sake of brevity. In general, the coefficients of determination were above 0.9 indicating that the models are representative of the collected data.

The results from the quarry materials are more repeatable as compared to the in-service materials, because of the ease in the specimen preparation. As indicated before, quarry materials were prepared by adding appropriate amounts of water to the materials and by following the standard compaction procedure. For the in-service materials, both the moisture content and the density had to be close to target values. These targets could only be met by trial and error.

Some differences are evident between the models developed for the quarry and in-service materials. The primary differences are in the values of k_2 (the exponent of the term corresponding to deviatoric stress in Equation 2.6). For the quarry materials, the parameters k_2 are typically small; whereas for the in-service materials these values are much larger. One reason for these differences can be that higher confining pressures and deviatoric stresses are used during testing in-servece materials. The second reason is that the in-service materials are coarser due to changes in gradation.

Differences in the values of k_3 (exponent of the confining pressure term in Equation 2.6) can also be detected. These changes are less significant than those for the k_2 term. In most cases, k_3's from the in-service materials are lower to compensate for larger values measured for k_2's.

The value of k_1 for each material is the indication of its overall stiffness, and vary accordingly. To properly utilize these parameters, representative deviatoric stresses and confining pressures should be determined. Also the use of such models implies that the load-induced nonlinear moduli are to be considered. These models are rather complicated for linear-elastic analysis.

Table 4.5 - Constitutive Models from Resilient Modulus Tests on Quarry and In-Service Materials

Material Type	District	Specimen	Quarry k_1	Quarry k_2	Quarry k_3	Quarry R^2	In-Service k_1	In-Service k_2	In-Service k_3	In-Service R^2
Lime-stone	Brown-wood	1	12548	0.022	0.711	0.999	55414	-0.151	0.621	0.996
		2	12548	0.20	0.710	0.999	101047	-0.120	0.505	0.999
		Average	12548	0.021	0.711		74865	-0.135	0.563	
	El Paso	1	58047	-0.010	0.420	0.999	493433	-0.137	0.069	0.153
		2	44670	0.000	0.460	0.999	231880	-0.284	0.490	0.989
		Average	51359	-0.005	0.440		510420	-0.237	0.201	
	Paris	1	67205	-0.010	0.330	0.996	34281	-0.314	0.541	0.921
		2	39312	-0.010	0.430	0.999	547171	-0.537	0.157	0.982
		Average	53259	-0.010	0.380		123530	-0.303	0.260	
	San Angelo	1	77417	0.000	0.340	0.996	43649	-0.232	0.420	0.918
		2	51330	-0.010	0.470	0.998	140778	-0.750	0.667	0.991
		Average	64374	-0.005	0.405		80832	-0.444	0.568	
	San Antonio	1	67845	-0.010	0.400	0.999	21648	-0.143	0.586	0.697
		2	59695	-0.010	0.430	0.999	417813	-0.710	0.118	0.957
		Average	63770	-0.010	0.415		171307	-0.265	0.313	

Table 4.5 (cont.) - Constitutive Models from Resilient Modulus Tests on Quarry and In-Service Materials

Material Type	District	Specimen	Quarry				In-Service			
			k_1	k_2	k_3	R^2	k_1	k_2	k_3	R^2
Caliche	Corpus Christi	1	155258	-0.040	0.020	0.999	71383	-0.247	0.404	0.974
		2	149874	-0.030	0.030	0.999	91757	-0.294	0.435	0.998
		Average	152566	-0.035	0.025		79525	-0.265	0.417	
	Odessa	1	231694	-0.040	0.000	0.999	803144	-0.419	0.304	0.992
		2	230308	-0.040	0.000	0.999	544826	-0.204	0.037	0.994
		Average	231001	-0.040	0.000		652401	-0.301	0.163	
Iron-Ore	Lufkin	1					34154	-0.278	0.830	0.997
		2					492594	-0.632	0.476	0.992
		Average					170976	-0.494	0.601	
	Tyler	1	128396	-0.030	0.080	0.999	736757	-0.291	0.087	0.954
		2	129040	-0.020	0.070	0.999	819690	-0.693	0.309	0.992
		Average	128718	-0.025	0.075		735141	-0.388	0.131	
Sand & Gravel	Childress	1	39348	0.020	0.340	0.967	331837	-0.365	0.507	0.983
		2	42748	0.010	0.350	0.946	100953	-0.550	0.478	0.985
		Average	41048	0.015	0.345		161949	-0.300	0.459	

Seismic Pavement Analyzer Tests

The variation in modulus and thickness of each pavement layer along with their coefficients of variation are included in Table 4.6. The idealized dispersion curves from all points tested at each site are included in Appendix D. The detailed modulus profile for each point can be found in Appendix E. In some cases, less than 11 points are reported because of problems with the prototype SPA.

In general, the moduli of the AC layers are measured with small variability. The coefficients of variation range from 4 to 16 percent. The moduli vary from 7 to 14 GPa, which are typical of seismic moduli measured for AC layers. These values are larger than reported by other devices, since they are representative of the linear-elastic, high frequency moduli of the layers.

The base moduli vary significantly between the ten sites. The softest bases are from the Lufkin and Brownwood districts with respective moduli of about 500 MPa. The stiffest base can be found in the Odessa and San Antonio districts with moduli of about 1900 MPa.

Large variabilities are associated with the measured base moduli at several sites. The coefficients of variation vary from about 10 to 50 percent with an average of about 25 to 30 percent. Same levels of variability are observed from the FWD data. The trends in the coefficients of variation are quite consistent between the FWD and the SPA results. The coefficients of variation from the two methods increase and decrease at the same rate.

Subgrade moduli also seem to be quite variable. The stiffest subgrade has a modulus of about 970 MPa which is from San Antonio, and the softest subgrade is from Brownwood with a modulus of about 300 MPa. Once again, large variations in modulus can be observed at several sites. The coefficients of variation vary from about 10 to more than 40 percent. As shown in Table 4.7, such large variations are recorded with the FWD.

Falling Weight Deflectometer Tests

The results from the FWD tests are summarized in Table 4.7. Detailed results can be found in Appendix F. In general, the deflection basin fitting was carried out with mixed success as judged by the average error per sensor. For two sites, San Antonio and Tyler, the average differences between the measured and calculated deflections are more than 20 percent.

The modulus of AC was assumed to be constant for five sites. In general, the moduli of AC vary from 2 GPa to 3.3 GPa, about three times less than those measured by the SPA. For the three sites where the moduli were estimated, the coefficients of variation for the AC moduli are about 15 to 30 percent.

The base moduli largely vary between different sites. The softest base is located in the Lufkin district with a modulus of about 174 MPa, and the stiffest one is in San Antonio with a modulus of about 2000 MPa. Based on the SPA data, these two sites also contain the softest and stiffest base materials. The coefficients of variation in the base moduli at different sites are rather high and vary from 24 to 80 percent.

Table 4.6 - Modulus Profiles from SASW Tests

Material Type	District	AC Modulus, MPa	AC Thickness, mm	Base Modulus, MPa	Base Thickness, mm	Subgrade Modulus, MPa
Lime-stone	Brown-wood	10435 (6.2%)*	15 (29.9%)	555 (25.1%)	275 (8.81)	305 (19.5%)
	El Paso	9413 (9.0%)	63 (14.7%)	708 (31%)	249 (12.6%)	536 (11.6%)
	Paris	8707 (7.1%)	24 (12.3%)	658 (33.4%)	256 (6.9%)	263 (20.4%)
	San Angelo	12619 (9.4%)	59 (17.7%)	772 (49.7%)	173 (17.4%)	304 (42.9%)
	San Antonio	14575 (7.4%)	65 (6.5%)	1876 (29.3%)	256 (6.4%)	971 (36.1%)
Caliche	Corpus Christi	12608 (4.7%)	90 (11.5%)	924 (18.2%)	214 (16.6%)	694 (10.0%)
	Odessa	11323 (8.0%)	38 (9.5%)	1992 (23.2%)	166 (17.5%)	544 (23.6%)
Iron-Ore	Lufkin	10038 (7.6%)	83 (6.7%)	446 (11.0%)	260 (15.9%)	349 (19.0%)
	Tyler	132487 (5.4%)	65 (6.8%)	1424 (11.4%)	250 (11.2%)	601 (5.4%)
Sand & Gravel	Childress	13624 (14.9%)	61.4 (11.5%)	680 (35.5%)	198 (12.4%)	335 (43.1%)

* Numbers in parentheses correspond to coefficients of variation.

Table 4.7 - Modulus Profiles from FWD Tests

Material Type	District	AC Modulus, MPa	Base Modulus, MPa	Subgrade Modulus, MPa	Avg. Error/ Sensor, percent
Limestone	Brownwood	2069 (--**)	507 (25.5%)	139 (15.0%)	5.32
	El Paso	2069 (--**)	300 (36.5%)	155 (16.7%)	8.2
	Paris	2482 (--**)	385 (56.9%)	81 (18.4%)	6.35
	San Antonio	2489 (--**)	2104 (28.4%)	103 (43.4%)	22.42
Caliche	Corpus Christi	2131 (27.0%)	430 (81.1%)	72 (19.8%)	2.9
	Odessa	2482 (--**)	914 (19.3%)	247 (12.7%)	7.15
Iron-Ore	Lufkin	3310 (30.0%)	174 (34.5%)	88 (23.9%)	3.18
	Tyler	3096 (16.0%)	372 (24.1%)	134 (22.8%)	21.47

* Numbers in parentheses correspond to coefficients of variation.

** Assumed to be a fixed value, and was not backcalculated.

The subgrade moduli vary significantly. The smallest and largest moduli are 72 MPa (in the Corpus Christi district) and 247 MPa (in the Odessa district), respectively. The coefficients of variation for different districts are smaller and vary from 12 percent (for the Odessa district) to 43 percent (for the San Antonio district). These are more or less similar to those obtained from the SPA moduli.

Comparison of Laboratory Moduli

The process involved in determining moduli from constitutive models is described in Chapter 3. Basically, representative deviatoric stresses and confining pressures are determined using the program KENLAYER. These two stresses, along with the appropriate constants obtained from Table 4.5, are then input in Equation 2.8 to obtain moduli.

Table 4.8 shows representative base moduli for the quarry and in-service materials using the linear and nonlinear models. For compatibility, for each condition two sets of moduli are reported, one entitled SPA and the other FWD. As indicated before, to compare laboratory and FWD moduli, the in situ stresses were obtained by inputting moduli from FWD tests in KENLAYER. Similarly, to compare SPA and laboratory moduli, in situ moduli from SPA were input in KENLAYER.

Table 4.8 - Representative Laboratory Moduli under Standard Tandem Axles Using FWD and SPA Moduli

Material Type	District	Modulus, MPa							
		Quarry				In-Service			
		Linear Model		Nonlinear Model		Linear Model		Nonlinear Model	
		FWD	SPA	FWD	SPA	FWD	SPA	FWD	SPA
Limestone	Brownwood	607	591	635	630	722	710	750	742
	El Paso	458	418	469	425	425	428	424	427
	Paris	393	399	385	409	97	97	97	97
	San Angelo	--[1]	444	--[1]	454	--[1]	147	--[1]	149
	San Antonio	492	472	511	478	218	217	220	218
Caliche	Corpus Christi	146	146	146	146	163	156	163	157
	Odessa	186	187	186	186	312	315	307	310
Iron-Ore	Lufkin	--[2]	--[2]	--[2]	--[2]	269	270	297	296
	Tyler	163	163	164	164	221	221	213	213
Sand & Gravel	Childress	--[1]	243	--[1]	252	--[1]	354	--[1]	361

[1] modulus is not calculated because FWD results were not available.
[2] modulus is not calculated because quarry material was not available.

Figure 4.1 compares the linear and nonlinear moduli of each method. Based on results from both the FWD and SPA, using a nonlinear model does not appreciably affect the average moduli. In almost all cases, the base layers did not experience appreciable load-induced nonlinear behavior. This seems to be true for models developed from MR tests on specimens from quarry and in-service materials. One of the reasons for this may be that the lowest strain levels subjected to the specimen with the MR tests may not be in the linear elastic range as defined in Figures 2.4 and 2.5.

Since the nonlinear procedure used in KENLAYER is approximate, it may also be desirable to verify this conclusion by using a finite element code. More sophisticated analysis was not done here because it was outside the scope of the work. The goal of this project is immediate implementation; therefore, the focus of work has been on methodologies that can be readily and routinely applied.

Since Proctor tests are used to determine the density of base materials, it is important to determine how well the moduli from quarry and in-service materials compare. To achieve this goal, the results from resilient modulus tests on quarry and in-service materials from each district are compared in Figures 4.2 and 4.3.

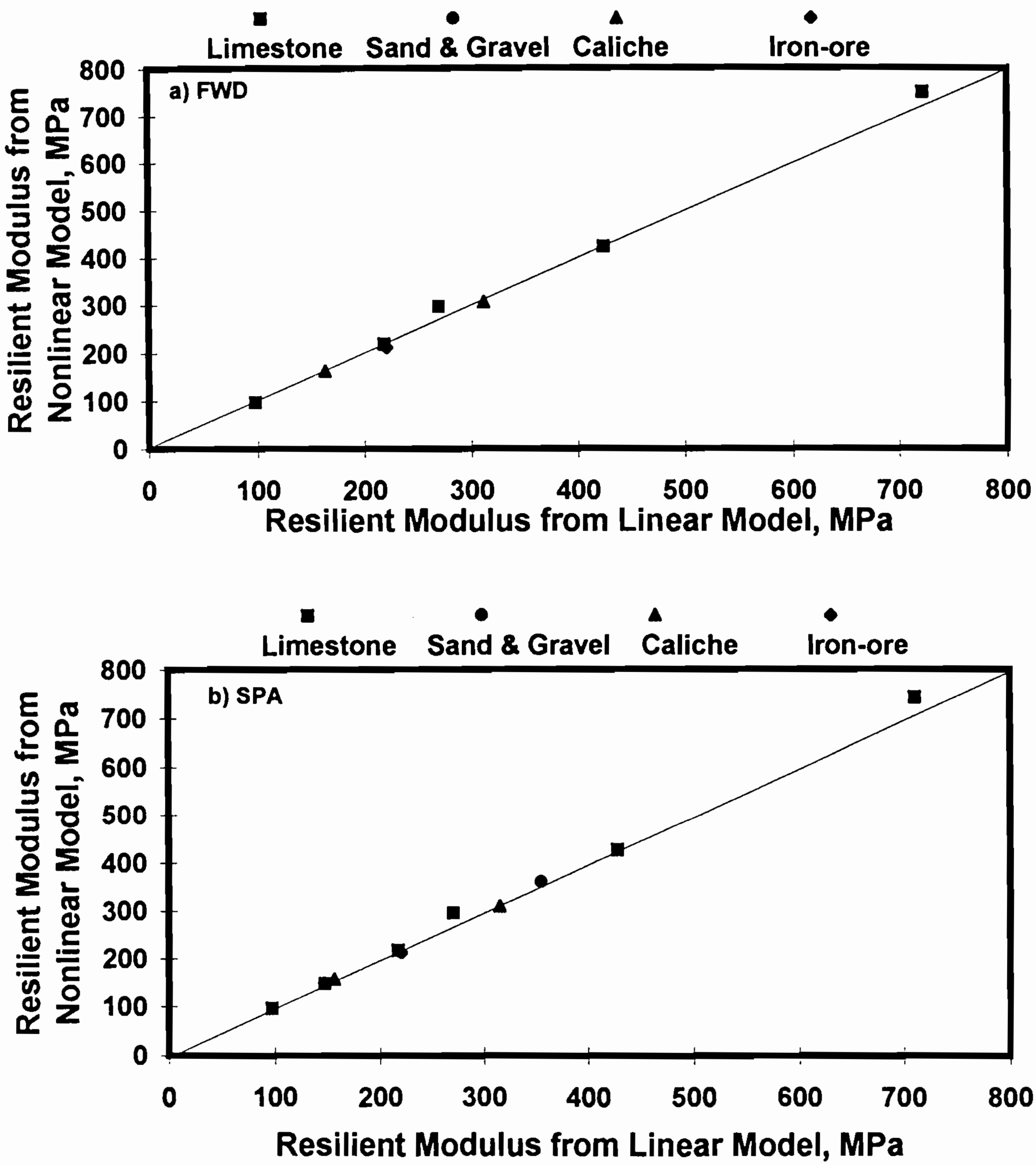

Figure 4.1 - Comparison of Representative Laboratory Moduli from Linear and Nonlinear Models

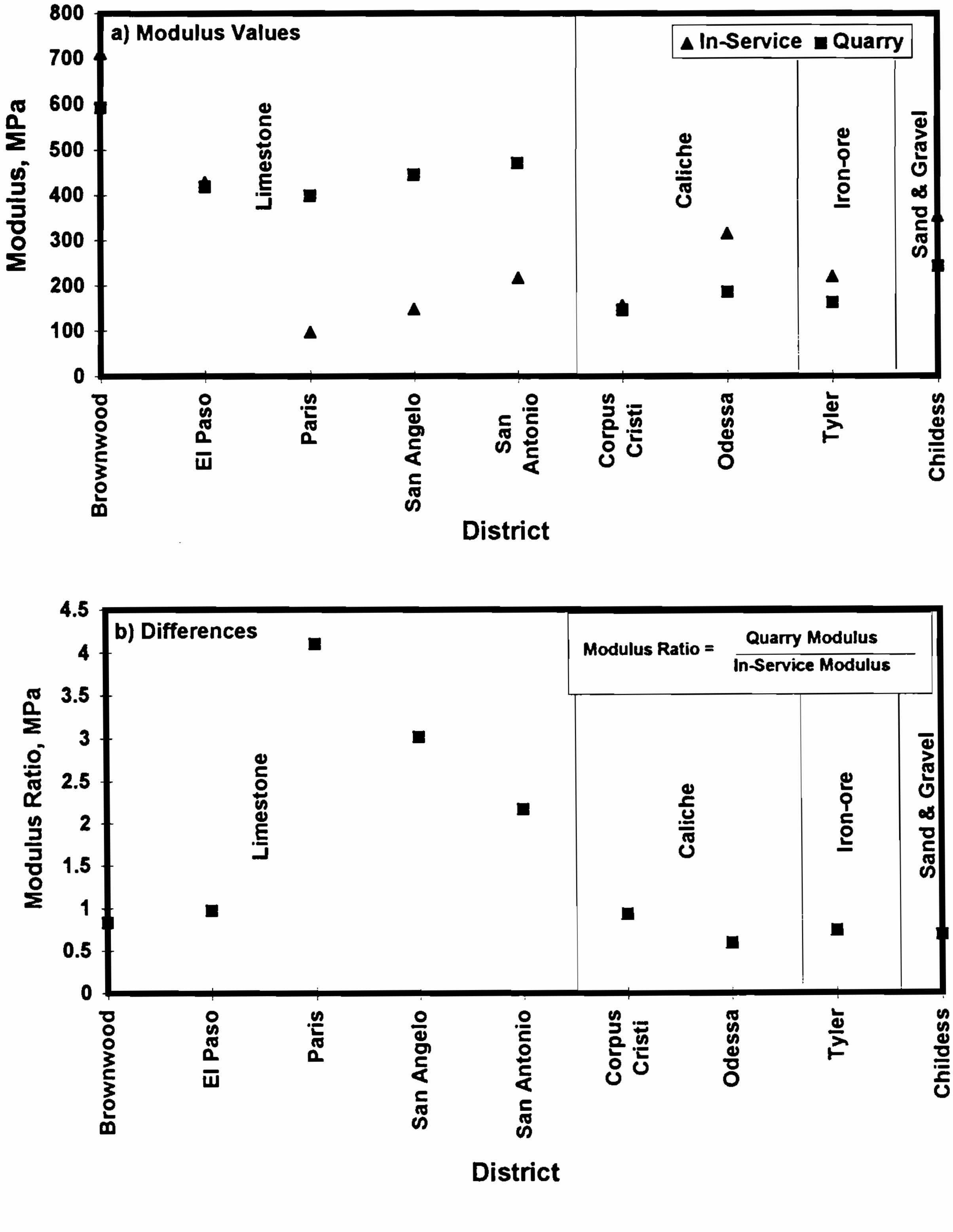

Figure 4.2 - Comparison of Laboratory Moduli from In-Service and Quarry Materials Using SPA Moduli to Determine In Site State of Stress

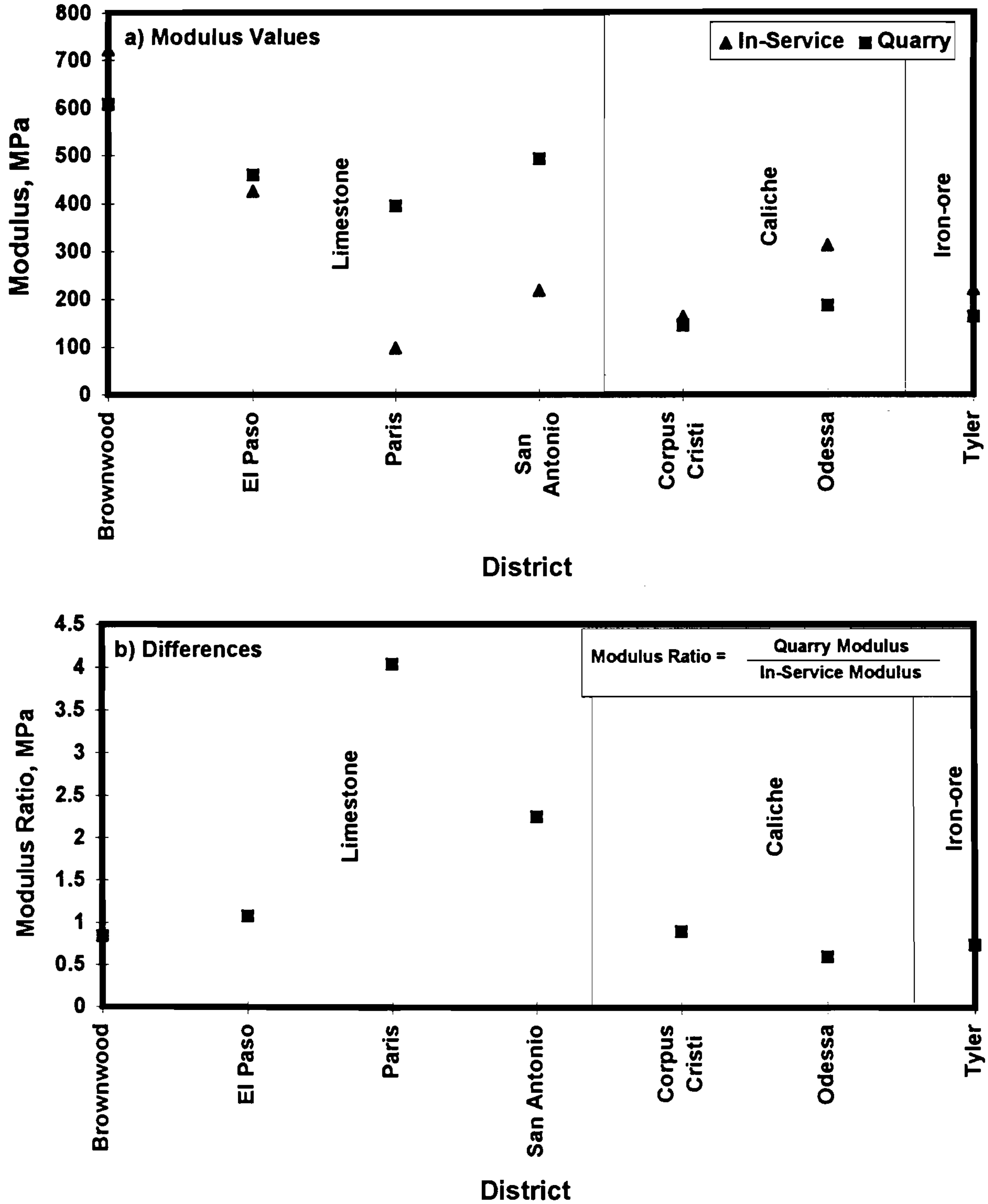

Figure 4.3 - Comparison of Laboratory Moduli from In-Service and Quarry Materials Using FWD Moduli to Determine In Site State of Stress

In Figure 4.2 the laboratory moduli obtained using the state of stress from SPA results are compared. For three districts (San Angelo, San Antonio and Paris), the moduli obtained from quarry materials are significantly higher than those obtained from in-service materials. All these three materials are classified as limestone base. For materials from these three districts, it seems that a large degradation in stiffness occurs. For Brownwood base materials, the in-service modulus is somewhat greater than the quarry modulus, but for the El Paso base materials, the two moduli are similar.

An attempt was made to describe the modulus degradation of the limestones. The differences in moduli from quarry and in-service materials could not be described by differences in the gradation. No statistical correlation could be found between the two parameters. The differences in Atterberg limits were similarly not correlated to the differences in moduli. As indicated before, the densities of the in-service materials were fairly close to maximum dry densities; therefore, it may be concluded that some field related phenomenon has contributed to the degradation of moduli of limestones. The variation in moduli of these base materials with time should be monitored to determine the probable causes of the degradation of these limestone bases.

The two caliche materials behave somewhat differently. For the Corpus Christi materials, the two laboratory moduli are quite close; whereas, for the Odessa caliche, the in-service modulus is about 50 percent higher. For the other two districts (i.e., Childress and Tyler), the in-service moduli are greater than the quarry moduli by 20 to 30 percent.

As shown in Figure 4.3, the same trends are observed when the FWD moduli are used to determine the state of stress. In general, the representative laboratory moduli are not much different when the SPA or FWD is used as the NDT device. In addition, the differences between moduli from laboratory tests on quarry and in-service materials exhibit the same trends.

Such large variations in moduli along a 200 m section of road is rather disturbing. Some of the variabilities in the results reported are due to shortcomings in the data collection and reduction associated with each NDT method. However, it seems that most of the variabilities are site-related. The FWD and SPA tests are based on fundamentally different philosophies and are performed and reduced by two separate groups. It is interesting that in almost all sites, both methods consistently exhibit similar levels of variability in data as judged by the coefficients of variation. This needs to be investigated thoroughly, to determine the following:

1. whether these variabilities are related to construction practices,
2. whether these variabilities are related to time-related physical-chemical changes in the properties with time, and
3. how to account for the test-related variabilities.

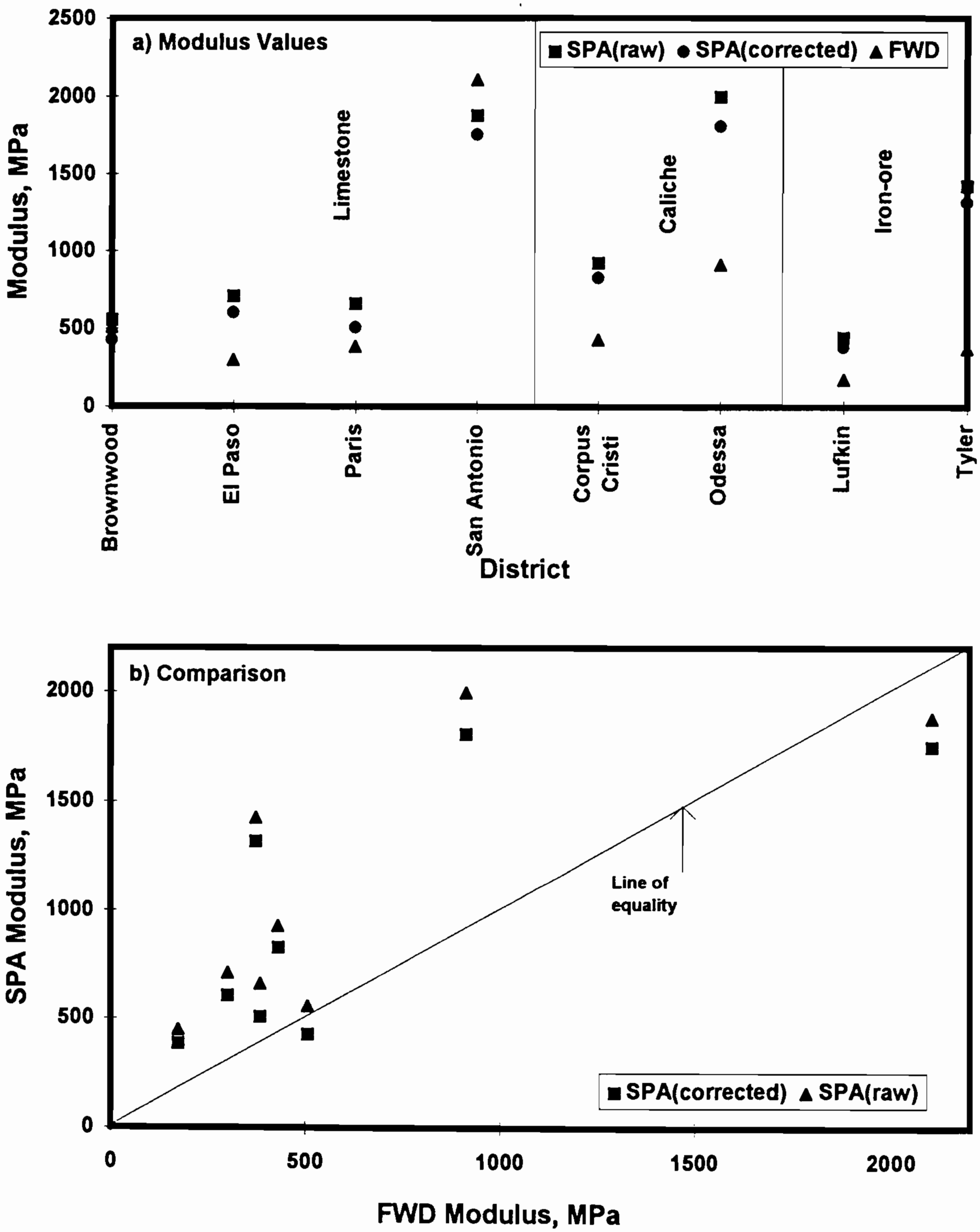

Figure 4.4 - Comparison of In Situ Moduli from FWD and SPA Corrected for State of Stress Under a Standard Dual-Tandem Load

Comparison of Field Moduli

Two NDT devices were used in this study — the FWD device that measures the equivalent-linear modulus, and the SPA that measures the linear elastic modulus of the base layer. The variations in moduli from the two devices for different districts are shown in Figure 4.4. Two sets of moduli are shown for the SPA. The first one marked "raw" is the modulus directly obtained from the SPA.

The second set marked "corrected" refers to results obtained by using the nonlinear model described in Chapter 2, (see Figure 2.6) which determines the equivalent linear modulus of the SPA under a standard dual-tandem axle load. The two sets of SPA moduli do not drastically differ. Once again, for most sections, the load-induced nonlinearities are small.

Moduli obtained from the SPA are typically greater than those of the FWD. Ignoring the results from the San Antonio district, the best fit curves through the raw and corrected data exhibit a slope of 2.1 and 1.9 for the raw and corrected SPA moduli, respectively. By dividing these two quantities by one another, the correction factor for load-induced nonlinearity under a standard dual-tandem axle load is about 10 percent.

A more appropriate way of comparing the SPA and FWD moduli is to determine the load-induced nonlinear moduli under the FWD loading pattern. These results are shown in Figure 4.5. Some scatter in the data is apparent. The moduli are within 70 percent of each other, in all but one case, and the majority of cases vary by 30 percent. Such a comparison is quite encouraging, given the fact that the model used to determine the correction factors is quite approximate, and the software utilized is not the most appropriate one. In the future this deserves further pursuit.

Another important conclusion may be drawn from Figures 4.4 and 4.5. It is of utmost importance to determine the moduli under the stress regimes anticipated for a given road. This means that the moduli from the SPA should be incorporated with the proper constitutive model to determine the representative modulus for the layer. On the other hand, the load should be adjusted for the FWD tests, so that the stresses are not much different from those experienced under the design loads.

Moduli from laboratory tests using the in-service materials are compared with the moduli reported by the SPA in Figure 4.6. Except for the base materials from the Brownwood district, the laboratory moduli are smaller than those measured in the field. The percentage differences are anywhere between 30 to 90 percent. As indicated before, many years of research in the geotechnical engineering field has established this trend. Even under the most sophisticated sampling techniques for obtaining intact and undisturbed specimens, the laboratory moduli are smaller. The fact that the specimens had to be reconstructed from bag samples, further affects the magnitude of the differences.

The largest differences between the laboratory and SPA moduli are associated with the caliches and the limestones. These two materials are prone to have high concentration of carbonates which with time acts as a cementing agent, causing an increase the in situ modulus of the base. This condition cannot be readily and conveniently reproduced in the laboratory.

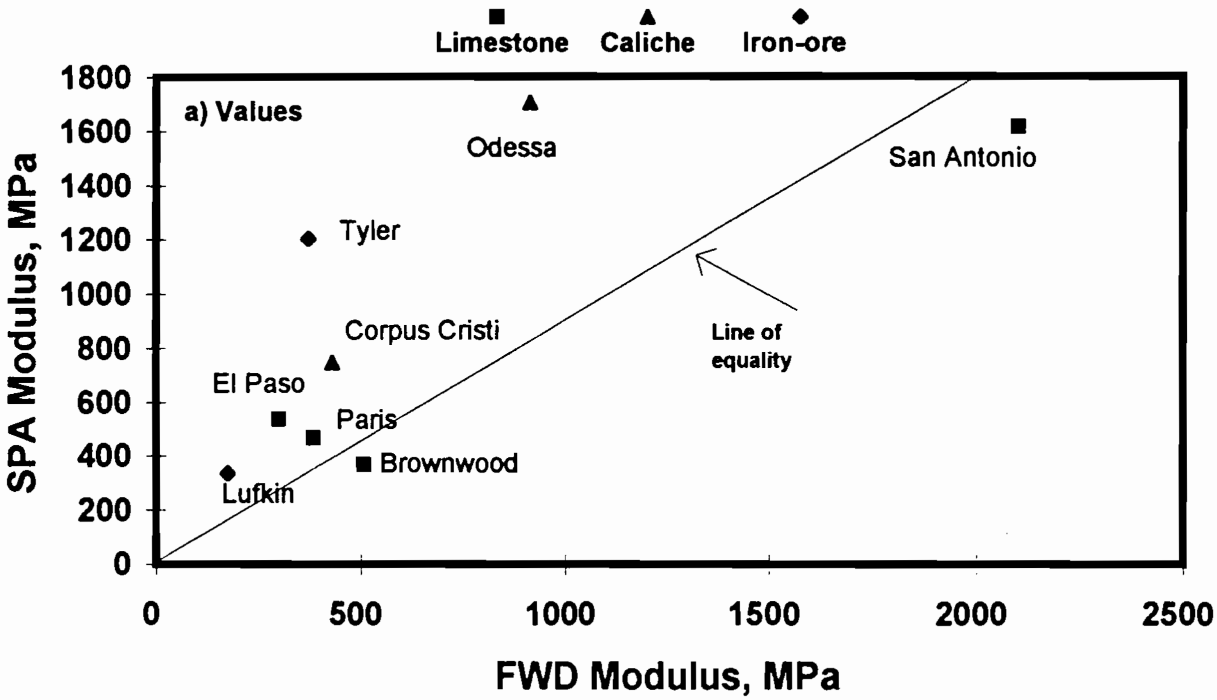

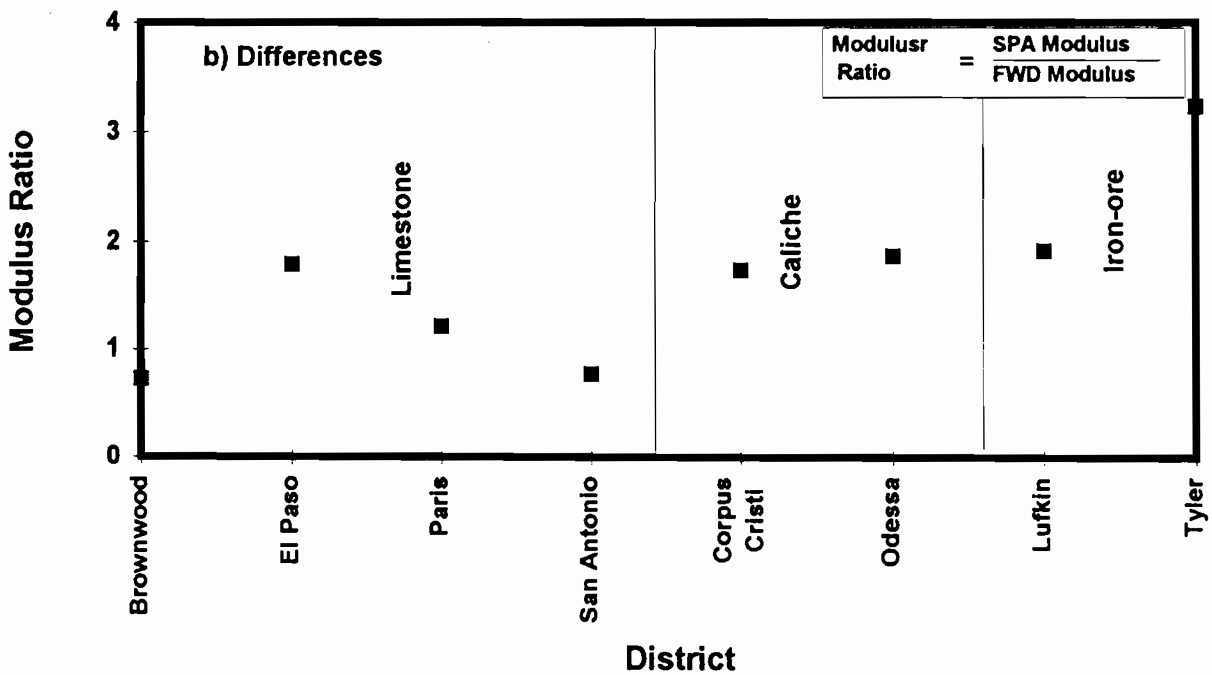

Figure 4.5 - Comparison of In Situ Moduli from FWD and SPA Corrected for State of Stress under a 40 KN FWD Load.

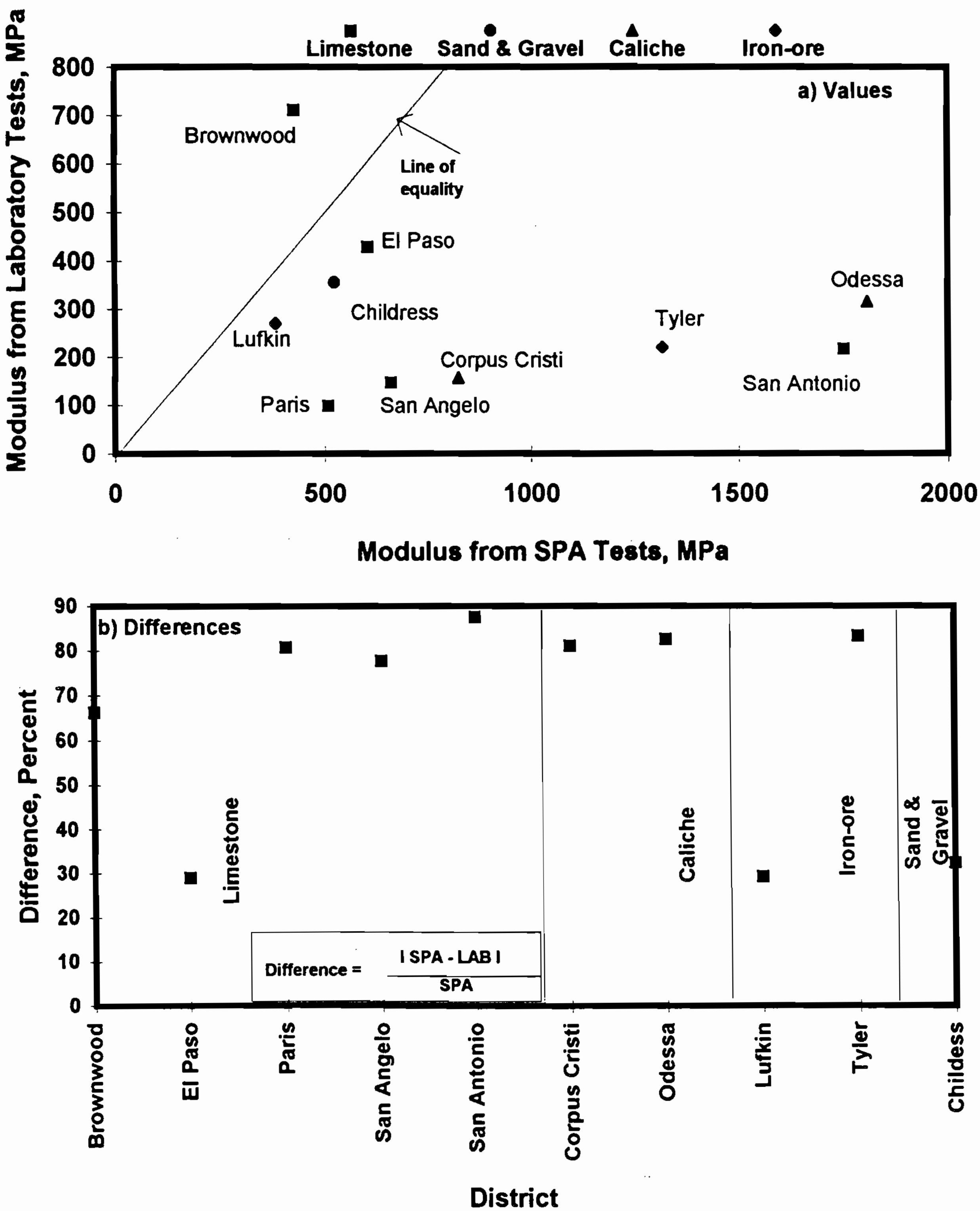

Figure 4.6 - Comparison of In Situ Moduli from SPA and Laboratory Tests of In-Service Materials for Loads under a Standard Dual-tandem Truck Load.

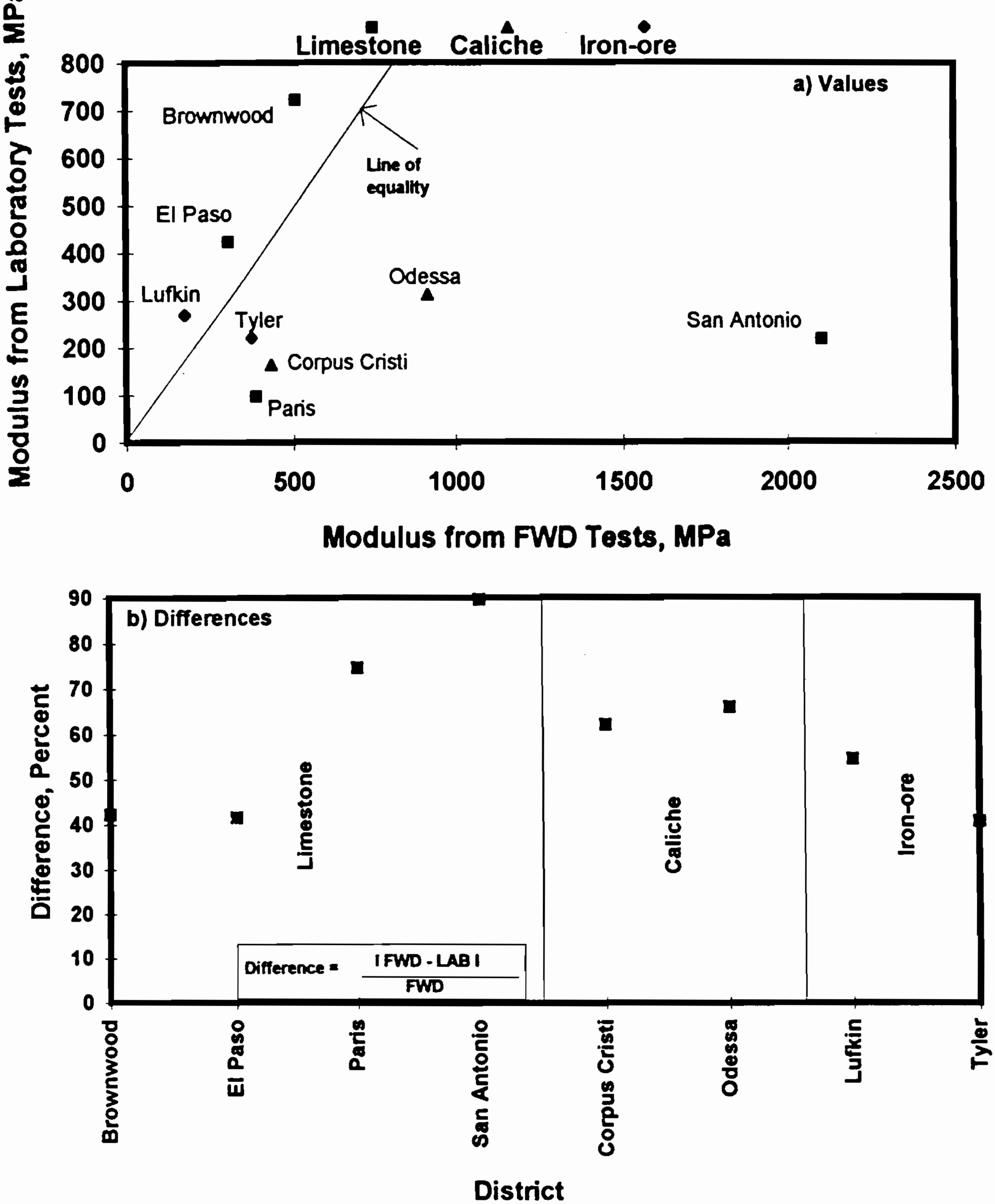

Figure 4.7 - Comparison of In Situ Moduli from FWD and Laboratory Tests of In-Service Materials for Loads under a Standard Dual-Tandem Truck Load.

The moduli of the base from FWD and laboratory are compared in Figure 4.7. Practically speaking, the same trends observed for the moduli from SPA in Figure 4.6 also apply in Figure 4.7. The differences between the laboratory and FWD moduli are in the range of 40 to 90 percent. When compared to SPA, moduli from FWD are slightly closer to those obtained from laboratory tests. However, the differences are still quite large.

In summary, the laboratory and field results provide different results. As indicated in Chapter 2, they should be used in a complementary fashion in the design and analysis.

Chapter 5

Summary and Conclusions

The primary objective of this report is to incorporate the results from laboratory MR tests with those obtained from nondestructive field tests so that a realistic approach which can be used in pavement design can be developed. To achieve this objective several steps were taken.

Laboratory resilient modulus tests were performed on virgin base materials from ten quarries in Texas following the state-of-practice. Resilient modulus tests were also conducted on materials from the same quarries, which were retrieved from test pits dug from in-service roads. The Falling Weight Deflectometer (FWD) tests were performed on the ten test sections. An alternative NDT test was carried out with the Seismic Pavement Analyzer (SPA). To compare the results from laboratory and field tests, a rational methodology was proposed. The results from the two sets of laboratory moduli, and the two field tests were then compared.

The following broad conclusions can be drawn:

1. Laboratory tests are essential to study the parameters that affect the properties of the material.

2. Virgin and in-service base materials retrieved from the same quarry do not exhibit similar properties. The gradation curves and Atterberg limits of the two materials somewhat vary. The in situ moisture content also vary by about 2 percent from the optimum moisture content, while the in situ densities are more or less similar to the maximum dry density.

3. Moduli from laboratory tests performed on specimens of virgin base materials compacted to maximum densities do not favorably compare with moduli obtained from specimens using in-service base materials from the same quarries compacted to the field densities and moisture contents.

4. Significant degradation in the stiffness of the retrieved in-service base materials was observed. This was especially critical for some of the limestone materials. The variations in modulus, as well as the physical-chemical properties of these bases with time should be carried out to determine the timing and possible causes of such degradation.

5. The FWD and SPA moduli exhibit the same trends. The base moduli from the SPA are typically 70 percent higher than those from the FWD.

6. Large variabilities in the moduli of the base layers were observed. The variabilities are most probably site related, since large coefficients of variation were measured independently by both NDT methods.

7. Unique relationship between moduli from laboratory and field tests could not be developed. The laboratory moduli are normally less than the in situ values by anywhere from ten to several hundred percent. This can be due to sampling disturbance, specimens nonrepresentative of field conditions, and long term time effects. Both SPA and FWD provide similar trends.

8. An approach to combine the field and laboratory results is proposed. The method has been proven to be effective in the area of geotechnical earthquake engineering field, but not tested in the pavement engineering area.

9. The verification of the methodology should be carried out in conjunction with MLS or other pavement monitoring procedures.

References

1. Akram T., Scullion T. and Smith R.E. (1994), "Comparing Laboratory and Backcalculated Layer Moduli on Instrumented Pavement Sections," STP 1198, ASTM, Philadelphia, PA, pp. 170-201.

2. de Almeida J.R., Brown S.F. and Thom N.H. (1994), "A Pavement Evaluation Procedure Incorporating Material Nonlinearity," STP 1198, ASTM, Philadelphia, PA, pp. 218-232.

3. Anderson D.G. and Woods R.D. (1975), "Comparison of Field and Laboratory Shear Modulus," proceedings, In Situ Measurement of Soil Properties, ASCE, Vol I, Rayleigh, NC, pp. 69-92.

4. Barksdale R.D., Alba J., Khosla P.N., Kim R., Lambe P.C. and Rahman M.S. (1994), "Laboratory Determination of Resilient Modulus for Flexible Pavement Design," Interim Report Project 1-28, Federal Highway Administration, Washington, DC.

5. Daleiden J.F., Killingsworth B.M., Simpson A.L. and Zamora R.A. (1994), "Analysis of Procedures for establishing In Situ Subgrade Moduli," Transportation Research Record 1462, TRB, Washington, DC, pp. 102-107.

6. Feliberti M.L., Nazarian S. and Thejaraj S. (1992), "A Critical Evaluation of Parameters Affecting Resilient Modulus of Subgrade Soils," Research Report 1177-2, Center for Geotechnical and Highway Materials Research, The University of Texas at El paso, El Paso, TX.

7. George K.P. and Uddin W (1994), "In Situ and Laboratory Characterization of Nonlinear Pavement Layer Moduli," STP 1198, ASTM, Philadelphia, PA, pp. 203-217.

8. Glaser S. (1993), "Estimating In Situ Liquefaction Potential and Permanent Ground Displacements due to Liquefaction for the Siting of Lifelines," Report NISTIR 5150, National Institute of Standards and Technology, Gaithersburg, MD.

9. Huang Y.H. (1994), Pavement Analysis and Design, Prentice Hall, Inc., Englewood Cliffs, NJ, 805 p.

10. Lytton R.L.(1989), "Backcalculation of Layer Moduli — State of the Art," STP 1026, ASTM, Philadelphia, PA, pp. 7-38.

11. Mayne P.W.and Kulhawy F.H. (1982), "K_o-OCR Relationships in Soil," Journal of Geotechnical Engineeering, Vol. 108, No. GT6, ASCE, New York, NY, pp. 851-872.

12. National Research Council (1985), "Liquefaction of Soils During Earthquakes," National Academy Press, washington, DC.

13. Nazarian S., Stokoe K.H. and Briggs R.C. (1987), "Nondestructively DelineatingChanges in Modulus Profiles of Secondary Roads," Transportation Research Record 1136, TRB, Washington, DC, pp. 96-107.

14. Nazarian S. and Desai M. (1993), "Automated Surface Wave Testing: Field Testing," Journal of Geotechnical Engineeering, Vol. 119, No. GT7, ASCE, New York, NY, pp. 1049-1012.

15. Nazarian S., Yuan D. and Baker M.R. (1995), "Rapid determination of Pavement Moduli with Spectral-Analysis-of-Surface-Waves Method," Research Report 1243-1F, Center for Geotechnical and Highway Materials Research, The University of Texas at El Paso, El Paso, TX, 76 p..

16. Nazarian S., Pezo R.F. and Picornell M. (1996), "Testing Methodology for Resilient Modulus of Base Materials," Research Report 1336-1, Center for Geotechnical and Highway Materials Research, The University of Texas at El Paso, El Paso, TX.

17. Ni S.H. (1987), "Evaluation of Dynamic Soil Properties under Three-Dimensional States of Stress Using Resonant Column Equipment," Ph.D. Dissertation, The University of Texas, Austin, TX.

18. Pezo R.F., Claros G.J. Hudson W.R. and Stokoe K.H. (1992), "Development of a Reliable Resilient Modulus Test for Subgrade and Non-Granular Subbase Materials for Use in Routine Pavement Design," Research Report 1177-4F, Center for Transportation Research, The University of Texas, Austin, TX.

19. Rodhe G.T. and Scullion T. (1990), "MODULUS 4.0: Expansion and Validation of the MODULUS Backcalculation System," Research Report 1123-3, Texas Transportation Institute, Texas A&M University, College Station, TX.

20. Rodriguez-Gomez J. , Ferregut C. and Nazarian S. (1991), "Impact of Variability in Thickness of Pavement Layers on Backcalculated Moduli from Nondestructive Testing Devices," Proceedings, Road and Airport Pavement Response Monitoring Systems, ASCE, New York, pp. 261-275.

21. Stokoe K.H., Nazarian S., Rix G.J., Sanchez-Salinero I., Shue J.C. and Mok Y.J. (1988), "In Situ Seismic Testing of Hard-to-Sample Soils by Surface Wave Method," Geotechnical Special Publication No. 20, ASCE, New York, NY, pp. 264-278.

22. Stubstad R.N., Mahoney J.P. and Coetzee N.F. (1994), "Effect of Material Stress Sensitivity on Backcalculated Moduli and Pavement Evaluation," STP 1198, ASTM, Philadelphia, PA, pp. 233-247.

23. Uzan J. (1994), "Advanced Backcalculation Techniques," STP 1198, ASTM, Philadelphia, PA, pp. 3-37.

24. Vinson T.S. (1989), "Fundamentals of Resilient Modulus Resting," Workshop on Resilient Modulus Testing, Oregon State University, Corvallis, OR.

25. Yuan D. and Nazarian S. (1993) "Automated Surface Wave Testing: Inversion Technique," Journal of Geotechnical Engineeering, Vol. 119, No. GT7, ASCE, New York, NY, pp. 1027-1042.

Appendix A

Resilient Modulus Test Procedures

DRAFT
STANDARD METHOD OF RESILIENT MODULUS TEST FOR UNBOUND GRANULAR BASE/SUBBASE MATERIALS

SCOPE

This test method provides a means for determining the Resilient Modulus, M_R, and Poisson's ratio, nu, of cylindrical specimens of granular base/subbase materials under conditions that represent a reasonable simulation of the physical conditions beneath flexible pavements subjected to moving wheel loads. The method provides for the measurement of recovered axial and lateral strains of specimens subjected to repetitive loadings. This test method is a modification of the standard method AASHTO T 294-92.

The properties determined with these procedures can be used in the available linear-elastic and non-linear elastic layered theories to calculate the physical response of pavement structures subjected to traffic loading. They can also be used in the design of pavements following the 1986- AASHTO Guide.

APPLICABLE DOCUMENTS:

- Test Method Tex-101-E, Preparation of Soil and Flexible Base Materials for Testing.
- Test Method Tex-103-E, Determination of Moisture Content in Soil Material.
- Test Method Tex-110-E, Determination of Particle Size Analysis of Soils.
- Test Method Tex-113-E, Laboratory Compaction Characteristics and Moisture-Density Relationship of Base and Cohesionless Sand
- Test Method Tex-117-E, Triaxial Compression Tests for Disturbed Soils and Base Materials.
- Test Method Tex-118-E, Triaxial Compression Test for Undisturbed Soils.

SUMMARY OF THE TEST METHOD

Repeated axial deviatoric forces of fixed magnitude, duration and frequency are applied to an appropriately prepared cylindrical specimen that is subjected to static confining pressures. During the load applications, the resilient axial and lateral deformations are measured to calculate the dynamic stiffness properties of the specimen, namely Resilient Modulus and Poisson's Ratio.

SIGNIFICANCE AND USE

The Resilient Modulus test provides a basic constitutive relationship between stress and strain of the pavement materials and a means of characterizing them under a variety of environmental and load conditions that simulate pavements subjected to moving wheel loads.

BASIC DEFINITIONS

1 P_{max} is the maximum applied axial load to the specimen consisting of the seating load and cyclic load (effect due to confining pressure is not included).

2 P_S is the seating load applied to the specimen to maintain a positive contact between the loading ram and the specimen top cap.

3 P_{cyclic} is the repetitive axial load (cyclic load) applied to the specimen.

4 σ_{max} is the axial stress applied to the specimen that consists of the seating load (P_S) and the cyclic load (P_{cyclic}) over the cross sectional area of the specimen. The confining stress is not included.

5 σ_S is the axial seating or contact stress; that is, the seating load over the cross sectional area of the specimen. It should be maintained at very small values.

6 σ_3 is the total radial stress; that is, the confining pressure in the triaxial chamber.

7 $\sigma_d = \sigma_{max} - \sigma_S$ is the deviatoric axial stress; that is, the maximum repetitive applied axial stress. It is also referred to as the cyclic axial stress.

8 Gage Length is the distance between the top and bottom transducers used to monitor the axial deformations. A gage length equal to one-third of the specimen length shall be used for all testing.

9 ε_a is the resilient axial strain induced by σ_d. This is defined as the resilient (recovered) axial deformation over the gage length.

10 ε_l is the resilient lateral strain also induced by σ_d. This is defined as the resilient (recovered) lateral or radial deformation measured at the mid-section of the specimen over its radius.

11 $M_R = \sigma_d/\varepsilon_a$ is the secant resilient modulus.

12 nu = $-\varepsilon_l/\varepsilon_a$ is the Poisson's ratio.

13 Load duration is the time interval during which the specimen is subjected to a deviatoric stress. A load duration of 0.1 second shall be used.

14 Cycle duration is the time interval between two consecutive applications of deviatoric stress. A cycle duration of 1 second shall be used.

15 Loading wave form is the haversine load pulse in which test specimens are loaded to simulate traffic loading in the laboratory.

APPARATUS

1 Triaxial Pressure Chamber: The pressure chamber is used to contain the test specimen and the confining fluid during the test (air is used as the chamber fluid). A triaxial chamber suitable for the use in resilience testing of granular materials is shown in Figure 1. The chamber is similar to most standard triaxial cells, except that it is somewhat larger to facilitate the internally mounted transducers.

2 Loading Device: the external loading device must possess a stiffness of at least 1,500 kN/mm. This property is actually estimated by placing a jack (or using the hydraulic actuator) between the two platens of the machine, applying several static loads and measuring it displacement.

The loading device shall be capable of providing varying repeated loads in fixed cycles of load and release. A closed-loop electro-hydraulic system is required for this operation. A havesine loading waveform consisting of a load duration of 0.10 seconds and a cycle duration of 1 second, as shown in Figure 2, should be applied to the specimen.

3 Load and Specimen Response Measuring Equipment:

a The axial load measuring device should be an electronic load cell that can either be placed inside the triaxial chamber, between the specimen top cap and the loading piston, or outside of it, that is between the actuator piston and the piston of the triaxial chamber.

The magnitude of friction between the piston and the top plate of the chamber will determine the need for one, or the other approach. Under the different conditions of confining pressure, up to 10 N of frictional force can be tolerated. A load cell of 25 kN in capacity and having an accuracy of $\pm$5 N is recommended for the testing of the specimens of 150-mm in diameter.

b Test chamber pressures shall be monitored with conventional pressure gages, manometers, or pressure transducers having a capacity of 350 kPa and an accuracy of at least 0.5 kPa. The device used to monitor pressure should be regularly checked and periodically calibrated to ensure its proper performance.

c The deformation measuring devices consists of nine internal non-contant probes attached to aluminun rings that are fixed onto the columns inside the triaxial chamber, and one linear variable differential transformer (LVDT) installed on top of the testing frame. Six probes shall be used to monitor the axial deformation, whereas, three shall be used for monitoring the lateral deformations of the specimen. The external LVDT shall be used to monitor the movement of the hydraulic actuator.

The non-contact probes shall be installed 120 degrees apart of each other and should face their corresponding steel targets. The non-contact probes will have a linearity of output and with a maximum range of $\pm$2.0 mm. As such, a prudent gap between the non-contact probes and the targets shall be left in order to ensure that the probes will never go out of range during the entire test. A sketch of their installation is shown in Figure 1.

d Each one of the non-contact probes shall be wired, so that each transducer can be read and the results reviewed independently. Measured displacements shall be averaged for estimating the stiffness properties of the test specimen. They should be regularly checked and periodically calibrated to ensure their proper performance.

e The external LVDT shall be installed in the actuator to monitor its travel. The LVDT will have a linerity of $\pm$0.25 percent of full range output, a repeatability of $\pm$1 percent of full range, a minimum sensitivity of 2 mv/v (AC) or 5 mv/v (DC) and a maximum range of $\pm$25 mm.

f To minimize errors, the entire system should be calibrated periodically. The use of synthetic specimens of known properties is recommended to assess the accuracy and repeatability of the measurements.

g Suitable signal excitation, conditioning and recording equipment are required for simultaneous recording of axial load, air pressure and deformations. The signal shall be clean and free of noise (use shielded cables that are properly grounded).

Filtering the output signal during or after acquisition is discouraged. If filter is used, it should have a frequency greater that 30 Hz. A supplemental study should be made to insure that correct peak readings are obtained from the filtered data compared to the unfiltered data.

h A data acquisition board mounted inside a personal computer having computational and control capabilities should be used. A minimum sampling rate of 200 records per channel per second is recommended. However, a supplemental study is suggested to establish the optimum number of data points to be used for each specific data acquisition system.

4. Specimen Preparation Equipment: A variety of equipment is required to prepare test specimens that are representative of field conditions. Typical equipment includes:

   a Split molds may be used to prepare specimens of 150-mm in diameter and 300 mm in length. For compaction, an automatic tamper (as specified in Tex-113-E) can be used-provided that the area of the rammer's striking face represents no more than 30 percent of the specimen area.

   b Miscellaneous: Other required equipment includes calipers, micrometer gauge, steel rule, rubber membranes 0.25-mm to 0.79-mm thick, rubber O-rings, a membrane expander, scales, moisture content cans, a water-bubble level, and hydrostone cement.

PREPARATION OF TEST SPECIMENS

1 Specimen Size: Specimen length-diameter ratio should not be less than two and not higher than three. Traditionally, minimum specimen diameter is defined as five times it nominal size[1]. As such, for granular base materials with nominal sizes as high as 30 mm, minimum diameter should be 150 mm and minimum specimen length is 300 mm.

2 Test specimen: all the specimens shall be prepared in the laboratory according toTex-101-E. Material shall be first collected according to Tex-400-A.

   a The water content and dry density of the compacted specimens shall not vary more than ± 0.5 percent and ± 2 percent from the specified water content and dry density for the base course, respectively.

   b For evaluation purposes, laboratory compacted specimens shall be prepared at *in situ* water content and at the *in situ* dry density. The compacting effort specified in Test Methods Tex-113-E can be used for compaction, as long as the specimens prepared are full representation of *in situ* conditions. To determine the *in situ* water content and *in situ* density of the base course, Test Method Tex-115-E or AASHTO T-238 and T-239 (nuclear method) can be used.

   c For design purposes, laboratory compacted specimens shall be prepared at the optimum moisture content and the maximum dry density determined as per Tex-113-E as determined by the pavement engineer.

---

1 Nominal size is the particle size of the material corresponding to the 95 percent passing size.

d At least two replicate specimens that represent the desired conditions shall be prepared for testing. Nevertheless, if the pavement engineer feels it is necessary, replicate specimens can be more than two. Specimens can also be prepared at different water contents from the optimum and/or *in situ* water content. This may be required by the pavement engineer who aims at evaluating the variation of these stiffness properties of the pavement materials at the different seasonal conditions.

3 Compaction Method: Tex-113-E is the method of compaction recommended. Nevertheless, the plasticity index of the soil should be first determined in order to select the compacting effort (CE).

a After properly assembling the split mold, a bottom cap shall be placed in position before placing the material into the mold. In addition, a hydrostone paste shall be spread on top of the bottom cap to obtain a thickness no greater than 3 mm. to ensure a strong and uniform contact with the specimen.

b To compact the total volume of the soil (V), six layers are recommended to obtain a more uniform specimen, as well as, to facilitate the placement of the targets. the surface of each layer should be scarified before placing the next layer. Knowing the weight of the hammer (W) and the height of drop (H), the number of blows (N) per layer can be determined as follows:

$$N = \frac{CE \cdot V}{6 \cdot W \cdot H} \tag{1}$$

c Three sets of three steel targets shall be inserted into the specimen during compaction. One set of targets shall be inserted after compacting the second layer, one set after the third layer and one set after the fourth layer of the specimen. Each target shall be inserted at the edge of the specimen and radially spaced 120 degrees apart.

d After specimen compaction has been completed, the compaction water content of the remaining material should be verified. The specimen shall be carefully removed from the mold. If the compacted specimen does not have the desired length, the surface shall be trimmed and flatted.

e Hydrostone paste shall be uniformly spread on top of the specimen in order to obtain a thickness no greater that 3 mm of paste. Then, the excess paste shall be squeezed out by pressing the top cap on top of the specimen. The levelness and alignment of the top cap shall be checked and corrected if necessary, by using a water bubble level and by softly tamping the top cap. Any excess hydrostone paste shall be removed from the specimen.

f The hydrostone paste consists of potable water and hydrostone cement mixed in a 0.40 ratio. Once the water is mixed with the hydrostone cement, the hydration of the paste begins, and its consistency is rapidly obtained. A minimum of 120 minutes (counting from the moment water is added to the hydrostone cement) is recommended as a curing time; this ensures that the grout will be strong enough to withstand the M_R test without risking the accuracy and reliability of the measurements.

g The specimen shall be removed from the mold. The sides of the end caps shall be cleaned, and a film of vacuum grease shall be applied at their sides to facilitate the adherence of the membranes with the end caps.

h A rubber membrane shall be placed in position into the membrane expander. A low vacuum pressure shall be applied to ensure contact between the membrane and the expander. Disconnect the vacuum and unfold the membrane to fully embrace the specimen and its end caps. Then, seal the membranes with O-rings.

i Determine the weight, length and diameter of the specimen, and compute the wet and dry densities of the specimen. The weight of the end caps, O-rings, membrane and hydrostone paste should have been determined prior to specimen preparation.

PLACEMENT OF THE SPECIMEN INTO THE TRIAXIAL CHAMBER & FINAL ASSEMBLY

1 The specimen with the end caps shall be carefully placed and properly aligned into the triaxial chamber. The bottom cap of the specimen shall be connected to the base plate of the triaxial chamber through the bottom cap screw. The O-rings and gaskets shall be properly placed in avoid any leakage.

2 The internal targets should be located by carefully presenting the magnets. One magnet will be assigned to each target (a total of nine). The magnets should be 12 mm in diameter. Bonded rare earth magnets are easier to machine. A pull load rate of 10 N is required to ensure strong contacts with the targets and to eliminate any possibility of slippage during the test.

3 The external targets shall be placed on top of the magnets as shown in Figure 1 and shall be carefully adjusted to leave a prudent gap between them and the non-contact probes.

4 Guided by the steel rods, the three positioning rings shall be fixed at the proper working level; that is, nearby one-third of the length from the top, mid-length and one-third of the length from the bottom of the specimen. The positioning rings allow the non-contacts probes to be close to their corresponding measuring levels and to the targets.

5 The non-contact probes shall be firmly screwed and secured to the probe clamps, whereas the probe clamps shall be firmly secured to the positioning rings. At this stage, it is generally necessary to re-adjust the location of the external targets to ensure that the non-contact probes will not run out of working range during the test.

6 A steel ball shall be placed on top of the top cap so that the axial loadings can be transferred uniformly and concentrically to the specimen. The tub shall then be carefully fit over the base, after applying vacuum grease at the circumferential groove of the base plate of the triaxial chamber ,where the acrylic tube will rest on.

7 The wires of the transducer shall be untangled and fit inside the chamber, so that they do not affect the measurements. After applying vacuum grease a the circumferential groove of the cover plate of the triaxial chamber, the top plate should be placed on the steel rods and acrylic tube and shall be securely tightened with the head screws.

8 The loading piston of the triaxial chamber shall then be released from its secured position, so that the steel rod (or an internal load cell attached to it) contact the steel ball. The piston of the actuator shall then be lowered and attached to the loading piston of the triaxial chamber. Proper alignment of the piston of the actuator with the loading piston of the triaxial chamber is very crucial; as such, the entire assembly (triaxial chamber) may need to be moved sideways, so that perfect alignment can be achieved. Once aligned, the entire testing assembly shall be tightly secured to the testing frame.

9 The triaxial chamber shall then be slid into position under the axial loading device. The loading device shall be lowered and coupled to the piston of the triaxial chamber. Then, a seating pressure of no more than 7 kPa shall be applied to the specimen.

TESTING PROCEDURE

The procedure described in this section is used for undisturbed and laboratory compacted specimens and requires a minimum of 30 minutes of testing time. At least two replicate specimens should be tested as representative of each one of the field conditions to be simulated in the laboratory.

1 A confining pressure of 35 kPa shall be applied to the test specimen. The material shall be stabilized to such confinement for at least 5 minutes.

2 Five repetitions of each one of the following deviatoric stresses shall be applied: 35 kPa, 70 kPa and 105 kPa. During the application of each deviatoric stress the actual applied compressional force and the induced resilient axial deformation of the 5 cycles shall be recorded and averaged. The actual confining pressure, the actual applied deviatoric stress, the induced resilient axial and lateral strains, and the calculated resilient modulus and Poisson's ratio shall be reported on a form similar to one shown in Figure 3. Other

parameters - including the seating stress and the cumulative permanent deformations - can also be reported.

3 The confining pressure shall be increased to 70 kPa following the process mentioned in item 1. Deviatoric stresses described in item 2 shall be applied; furthermore, an additional deviatoric stress of 140 kPa shall be applied.

4 The confining pressure shall then be increased to 105 kPa following the process mentioned in item 1. Deviatoric stresses described in item 2 shall be applied; furthermore, additional deviatoric stresses of 140 kPa and 210 kPa shall then be applied.

5 Generally, if the resilient axial and lateral strains fall below the 0.01 percent (minimum reliable strain estimate) that particular result shall be excluded in further analysis. If the total axial strain is greater than 1 percent, the M_R test shall be stopped.

6 Upon completion of the M_R test, the confining pressure shall be reduced to zero and a load at a rate of 0.5 mm per minute shall be applied to drive the specimen to failure. During this test, the applied axial stress and axial and lateral strains shall be recorded in order to calculate the static Young's Modulus and Poisson's ratio. The triaxial chamber shall then be disassembled.

7 The membranes shall be removed from the specimen. A piece from the core of the specimen shall be used to determine its water content after testing to compare this value with the initial water content.

REPORT

The M_R testing report consists of three parts: (1) the basic information of the test specimen; (2) the testing results and plots of the variations of the moduli and Poisson's ratio; and (3) an analysis of results Figure 3 illustrates a typical M_R testing report.

1 Data sheets shall include the basic information of the material, (e.g., its origin, and Atterberg limits) as well as, information related to the specimen (e.g., its age at the time of testing, its dimensions, its water content, and its dry density). In addition, the following test results should be included: the confining pressures, the seating pressures, the deviatoric stresses, the resilient axial and lateral strains, the permanent deformations, and the calculated resilient moduli and Poisson's ratio of each specimen at each one of the stress states of the test.

2 Four plots are recommended. Two arithmetic plots showing the variation of the resilient modulus and Poisson's ratio with deviatoric stress for a given confining pressure, and two semi-logarithm plots showing the variation of the resilient modulus and Poisson's ratio with logarithm of the resilient axial strain for a given confining pressure.

3 The analysis of results consists of developing a linear regression equation to predict the resilient modulus and Poisson's ratio of the material, and suggesting one M_R and Poisson's ratio value for design. Use all the results obtained from the testing of the replicate specimens in the statistical analysis.

a A regression model accompanied by both its coefficient of determination, R^2, and the standard error of the estimate, SEE, should have the following form:

$$Ln(\varepsilon_a) = a + b \cdot \ln(\sigma_d) + c \cdot \ln(\sigma_3),$$

$$\varepsilon_a = e^{a} * \sigma_d^{b} * \sigma_3^{c} \tag{2}$$

By definition:

$$M_R = \sigma_d / \varepsilon_a$$

Thus, The modulus can be expressed in two similar equations, in terms of either the deviator stress or the axial strain:

$$M_R = e^{-a} * \sigma_d^{(1-b)} * \sigma_3^{-c},$$

$$M_R = K_1 * \sigma_d^{K2} * \sigma_3^{K3} \tag{3}$$

$$M_R = N_1 * \varepsilon_a^{N2} * \sigma_3^{N3}$$

$$M_R = e^{-a/b} * \sigma_d^{(1-b)/b} * \sigma_3^{-c/b}, \tag{4}$$

b The Poisson's ratio to be reported will simply consist of obtaining the average of all the Poisson's ratio values obtained from the testing of the replicate specimens.

c Based on either stress or strain criteria, the pavement engineer can estimate a unique resilient modulus value for use as an input in the AASHTO pavement design guide.

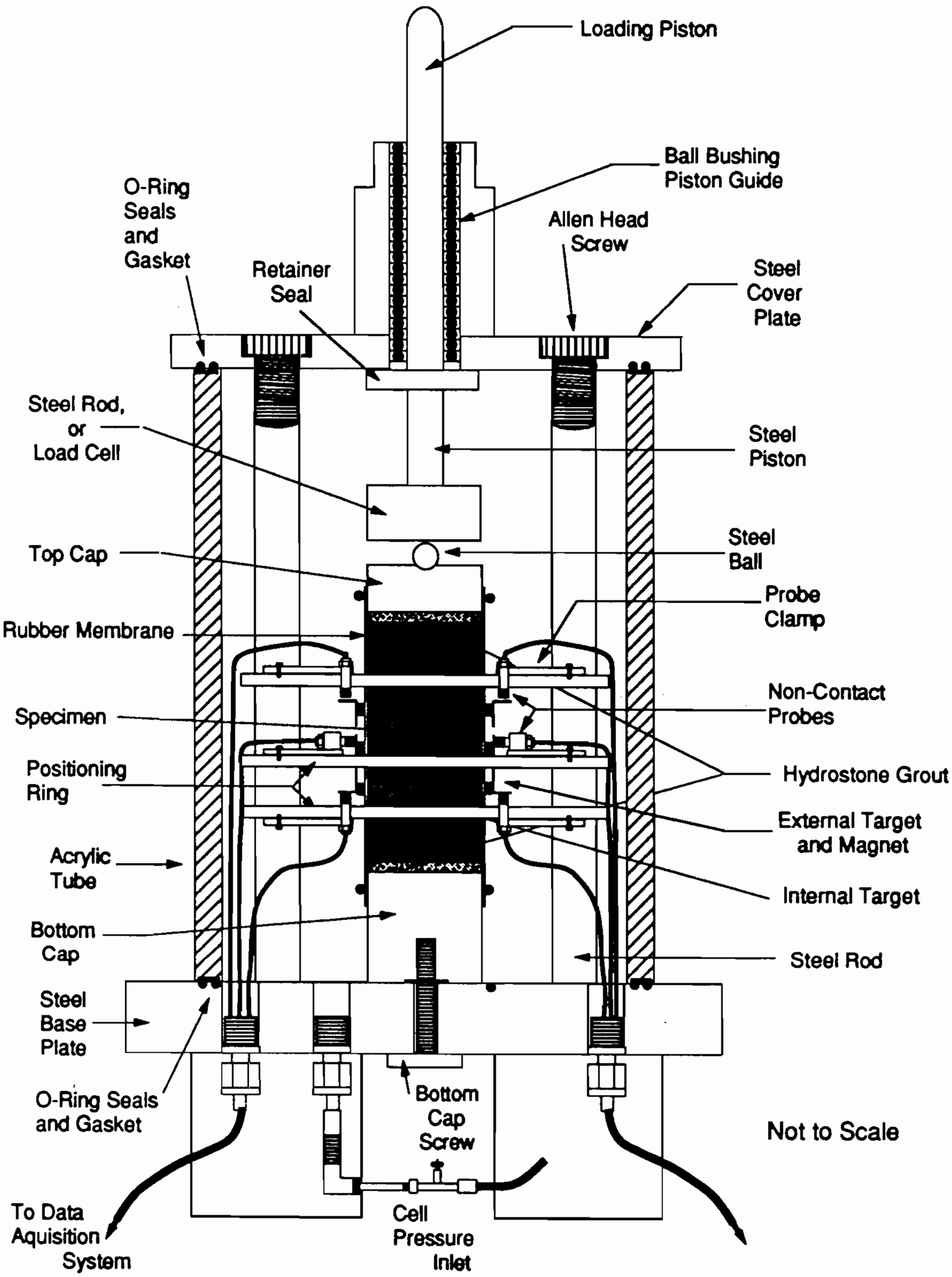

Figure 1. Triaxial Chamber

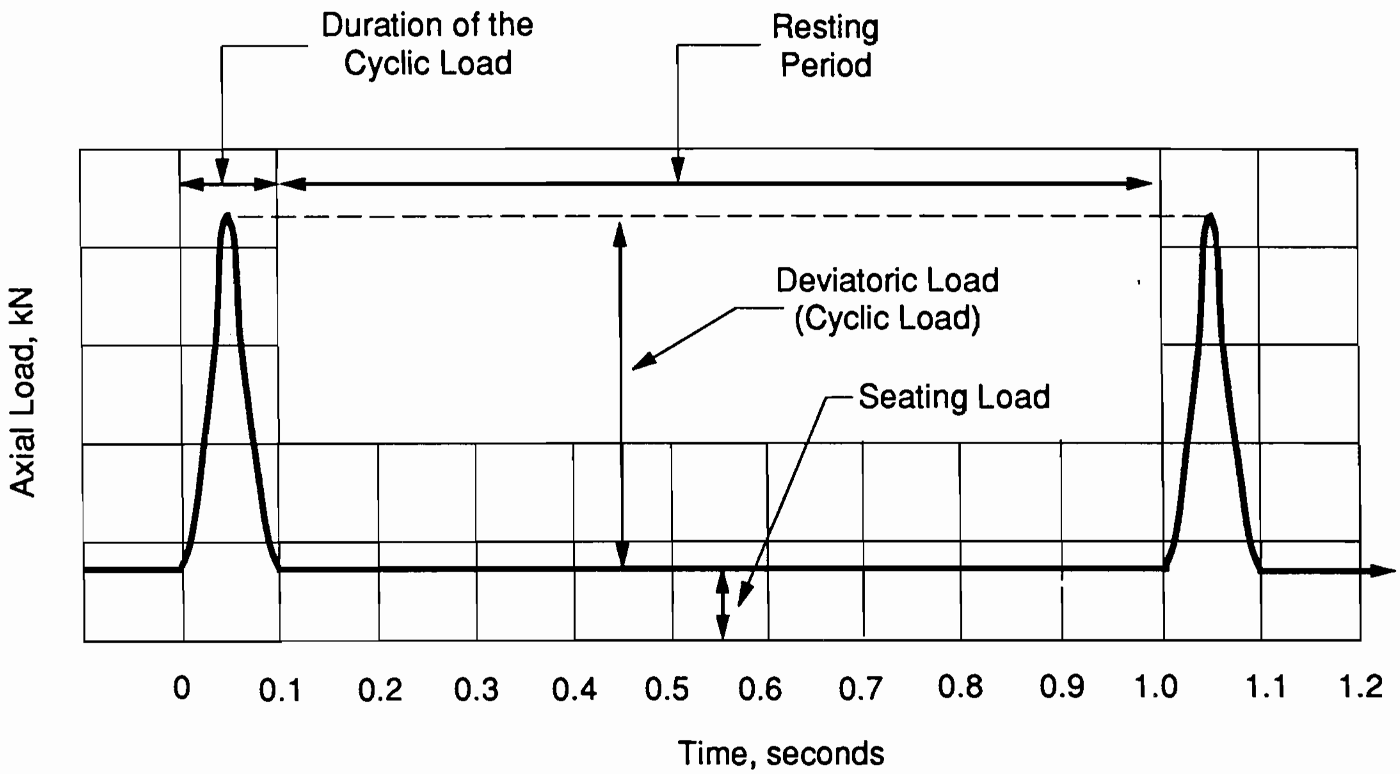

Figure 2. Definition of the Loading Rate, Wave Form and Terms

```
Example.out                RESILIENT MODULUS (MR) TEST RESULTS

SPECIMEN IDENTIFICATION = 1  -  Limestone - Grade 4
DESCRIPTION    =  SAN ANGELO DISTRICT - Tom Green County - R.W. McKinney Alexander Pit
ROAD SOURCE    =  US67 - Frontage Road - Section 1582 - Outside Lane - 150-mm depth
PLASTIC LIMIT =    3.40 percent
LIQUID LIMI   =   16.60 percent
MOISTURE CONTENT  =   3.80 percent
DRY DENSITY       =  23.30 kN/cm3
SPECIMEN HEIGHT   =  308.750  mm
SPECIMEN DIAMETER =  151.250  mm
GAGE LENGTH       =  100.600  mm
```

CONFINING (kPa)	SEATING (kPa)	DEVIATORIC. (kPa)	AXIAL DEF (mm)	LAT. DEF. (mm)	LAT. STR (mm/mm)	AXIAL STR. (mm/mm)	POISSON RATIO	RES. MODULUS (MPa)
34.6	6.95	37.81	0.016700	0.004390	0.000058	0.000166	0.35	227
34.8	5.78	61.10	0.027270	0.007100	0.000094	0.000270	0.35	226
35.4	5.67	83.24	0.036560	0.009300	0.000123	0.000362	0.34	230
69.7	5.49	36.19	0.011310	0.002880	0.000038	0.000112	0.34	322
69.4	5.32	60.86	0.018980	0.004840	0.000064	0.000188	0.34	323
69.9	5.91	84.97	0.026860	0.006660	0.000088	0.000266	0.33	319
70.8	5.87	104.63	0.032920	0.008170	0.000108	0.000326	0.33	321
102.6	5.76	40.06	0.010500	0.002650	0.000035	0.000104	0.33	387
102.9	5.62	61.72	0.016060	0.003930	0.000052	0.000159	0.33	389
103.1	5.44	83.48	0.021920	0.005600	0.000074	0.000217	0.34	385
103.4	7.14	102.15	0.026560	0.006660	0.000088	0.000263	0.33	388
104.2	7.03	188.33	0.049490	0.012250	0.000162	0.000490	0.32	384

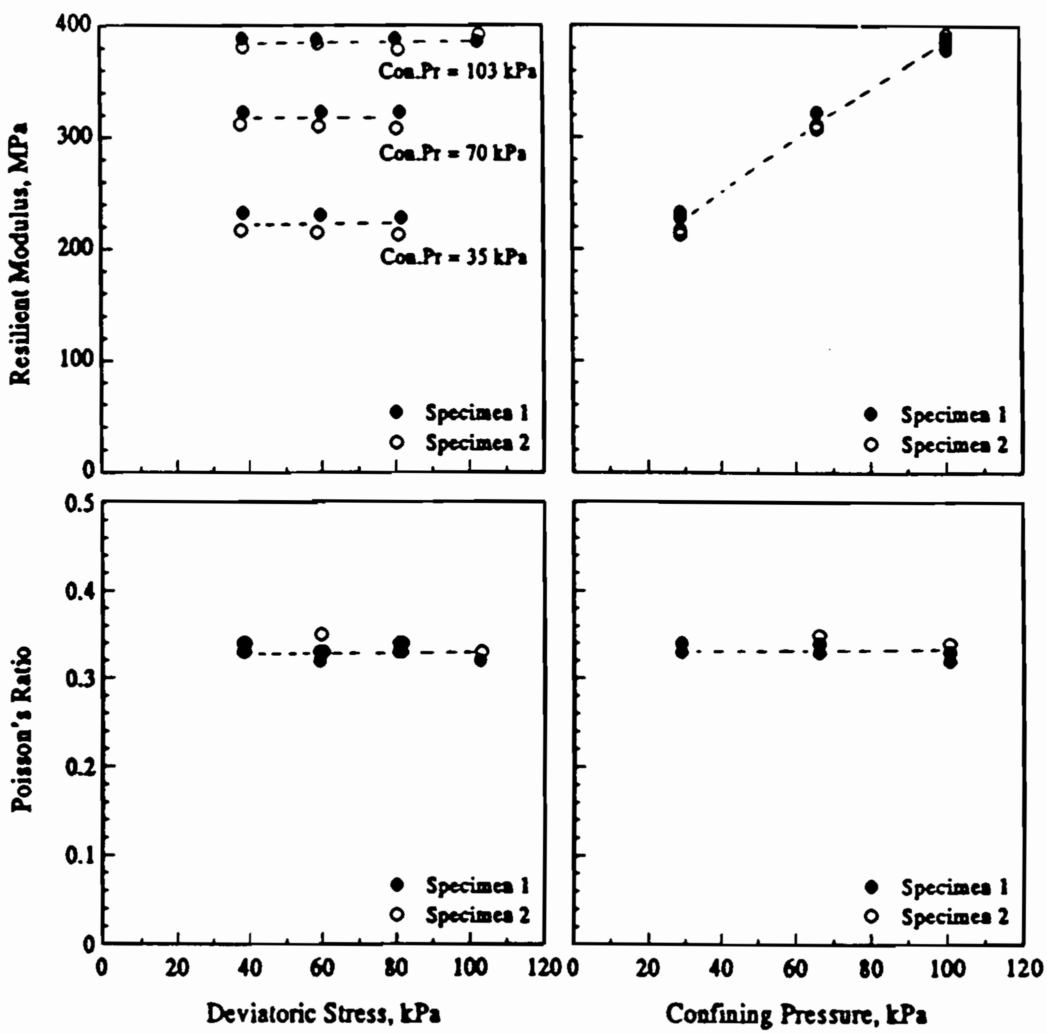

Figure 3. Testing report

Appendix B

Results from Dynamic Cone Penetration Tests

DCP DATA SHEET

Project: Brownwood
Location: FM 45 EB

Date: 7 Nov. 94
Soil Type(s): 0.5" Surface Treatment
11" Flexible Base

No. of Blows	Accumulative Penetration mm	Penetration per Blow Set mm	Penetration Per Blow mm	Hamme Blow Factor	DCP Index	CBR %	Depth in
0	0	-	-	-	-	-	0
14	29	29	2.1	1	2.1	129	-1.1
15	46	17	1.1	1	1.1	254	-1.8
10	66	20	2.0	1	2.0	134	-2.6
10	76	10	1.0	1	1.0	292	-3.0
20	100	24	1.2	1	1.2	238	-3.9
30	126	26	0.9	1	0.9	343	-5.0
40	161	35	0.9	1	0.9	339	-6.3
50	185	24	0.5	1	0.5	664	-7.3
40	213	28	0.7	1	0.7	435	-8.4
30	245	32	1.1	1	1.1	272	-9.6
20	272	27	1.4	1	1.4	209	-10.7
10	295	23	2.3	1	2.3	115	-11.6
5	315	20	4.0	1	4.0	62	-12.4
5	324	9	1.8	1	1.8	151	-12.8

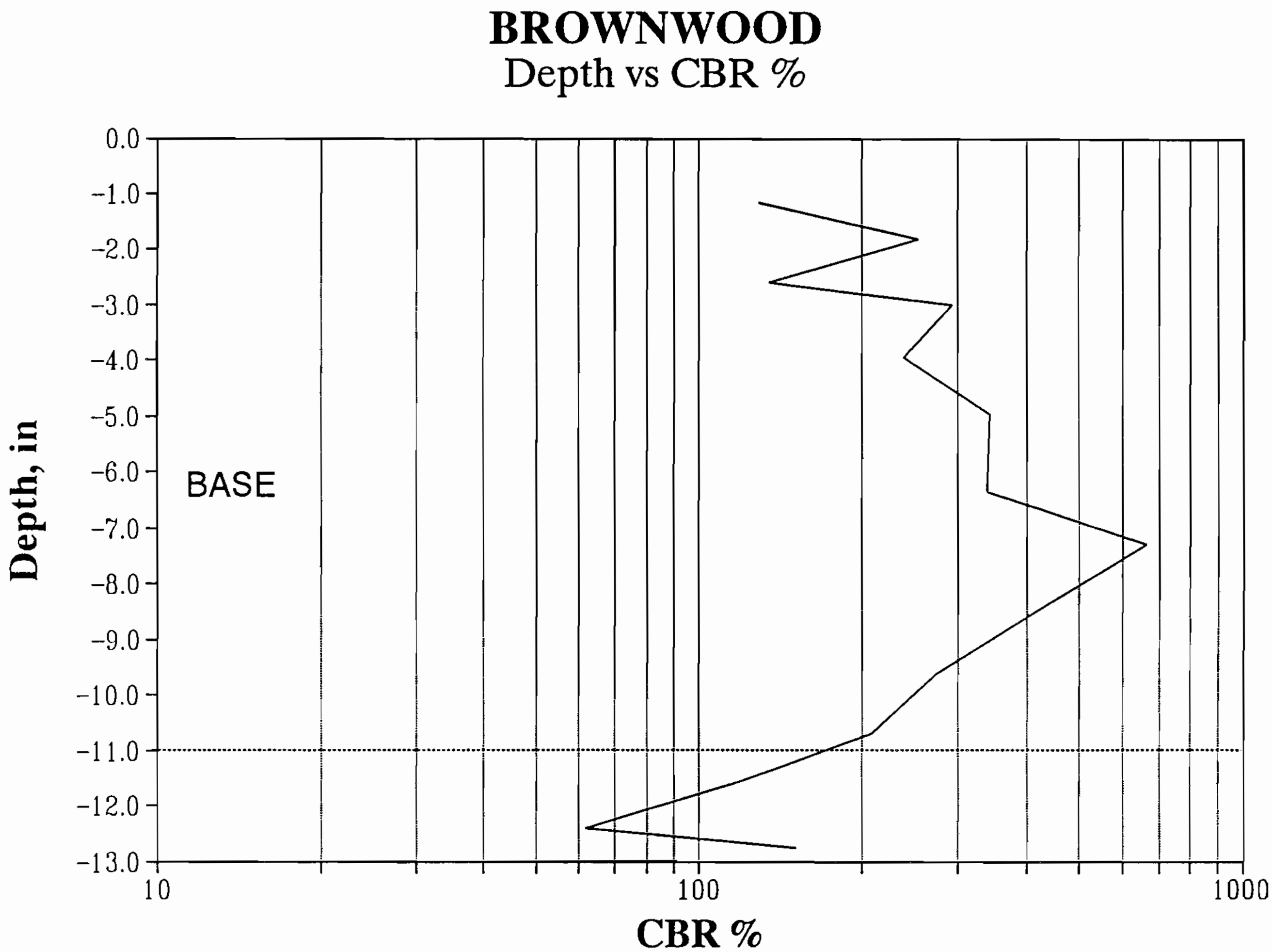
BROWNWOOD
Depth vs CBR %
0.0
-1.0
-2.0
-3.0
-4.0
-5.0
-6.0
-7.0
-8.0
-9.0
-10.0
-11.0
-12.0
-13.0
Depth, in
BASE
10
100
1000
CBR %

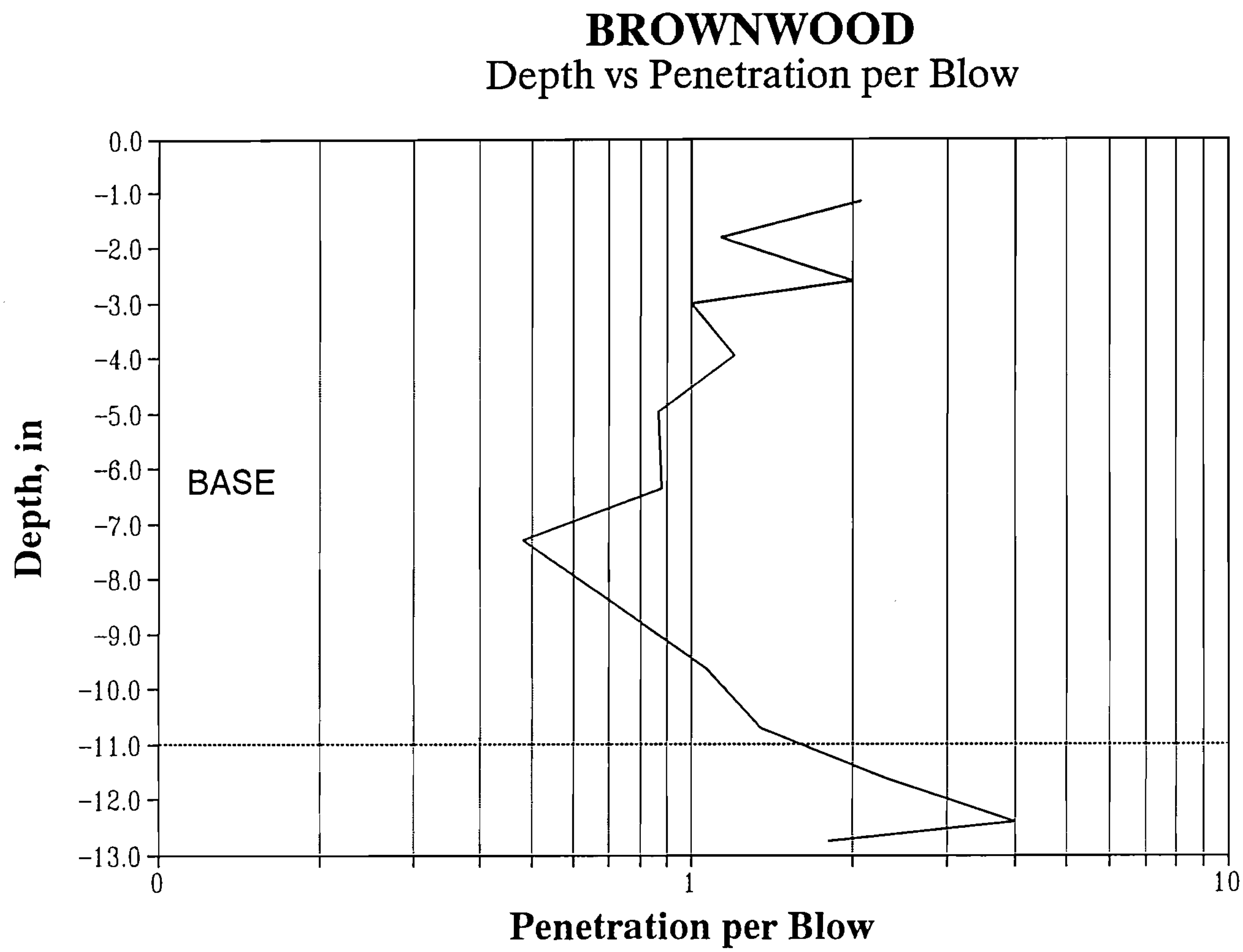
BROWNWOOD
Depth vs Penetration per Blow
0.0
-1.0
-2.0
-3.0
-4.0
-5.0
-6.0
-7.0
-8.0
-9.0
-10.0
-11.0
-12.0
-13.0
Depth, in
BASE
0
1
10
Penetration per Blow

DCP DATA SHEET 1/2

Project: Childress
Location: US 287 NB-CS: 0043-01

Date: 10 Nov. 94
Soil Type(s): 2" AC
9" Sand Gravel Base
15" Salvage

No. of Blows	Accumulative Penetration mm	Penetration per Blow Set mm	Penetration Per Blow mm	Hammer Blow Factor	DCP Index	CBR %	Depth in
0	0	-	-	-	-	-	0
10	52	52	5.2	1	5.2	46	-2.0
10	85	33	3.3	1	3.3	77	-3.3
10	109	24	2.4	1	2.4	110	-4.3
10	129	20	2.0	1	2.0	134	-5.1
20	155	26	1.3	1	1.3	218	-6.1
20	190	35	1.8	1	1.8	156	-7.5
20	225	35	1.8	1	1.8	156	-8.9
20	255	30	1.5	1	1.5	185	-10.0
10	268	13	1.3	1	1.3	218	-10.6
20	290	22	1.1	1	1.1	262	-11.4
20	310	20	1.0	1	1.0	292	-12.2
20	335	25	1.3	1	1.3	227	-13.2
20	359	24	1.2	1	1.2	238	-14.1
20	380	21	1.1	1	1.1	276	-15.0
15	395	15	1.0	1	1.0	292	-15.6
15	415	20	1.3	1	1.3	212	-16.3
15	440	25	1.7	1	1.7	165	-17.3
15	480	40	2.7	1	2.7	97	-18.9
15	540	60	4.0	1	4.0	62	-21.3
5	625	85	17.0	1	17.0	12	-24.6
1	685	60	60.0	1	60.0	3	-27.0
1	745	60	60.0	1	60.0	3	-29.3

DCP DATA SHEET 2/2

Project: Childress
Location: US 287 NB-CS: 0043-01

Date: 10 Nov. 94
Soil Type(s): 2" AC
9" Sand Gravel Base
15" Subbase

No. of Blows	Accumulative Penetration mm	Penetration per Blow Set mm	Penetration Per Blow mm	Hammer Blow Factor	DCP Index	CBR %	Depth in
0	0	-	-	-	-	-	0
10	61	61	6.1	1	6.1	39	-2.4
10	95	34	3.4	1	3.4	74	-3.7
10	125	30	3.0	1	3.0	85	-4.9
10	145	20	2.0	1	2.0	134	-5.7
10	170	25	2.5	1	2.5	105	-6.7
30	225	55	1.8	1	1.8	148	-8.9
30	275	50	1.7	1	1.7	165	-10.8
30	315	40	1.3	1	1.3	212	-12.4
30	344	29	1.0	1	1.0	303	-13.5
30	370	26	0.9	1	0.9	343	-14.6
30	405	35	1.2	1	1.2	246	-15.9
15	427	22	1.5	1	1.5	190	-16.8
10	445	18	1.8	1	1.8	151	-17.5
10	465	20	2.0	1	2.0	134	-18.3
10	494	29	2.9	1	2.9	89	-19.4
5	505	11	2.2	1	2.2	121	-19.9
5	523	18	3.6	1	3.6	70	-20.6
3	534	11	3.7	1	3.7	68	-21.0
5	560	26	5.2	1	5.2	46	-22.0
3	590	30	10.0	1	10.0	22	-23.2
1	610	20	20.0	1	20.0	10	-24.0
1	635	25	25.0	1	25.0	8	-25.0
1	670	35	35.0	1	35.0	5	-26.4

CHILDRESS
Depth vs CBR %

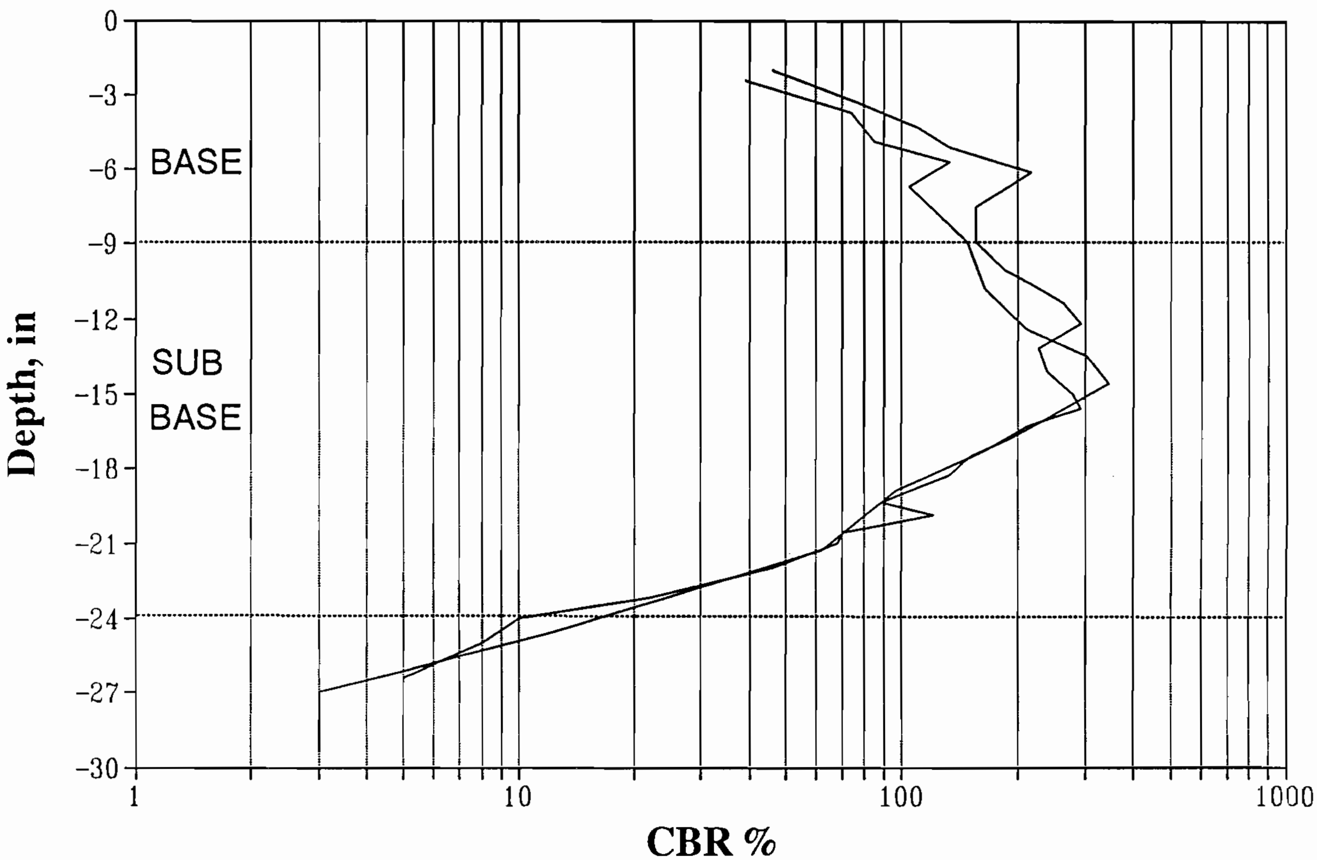

CHILDRESS

Depth vs Penetration per Blow

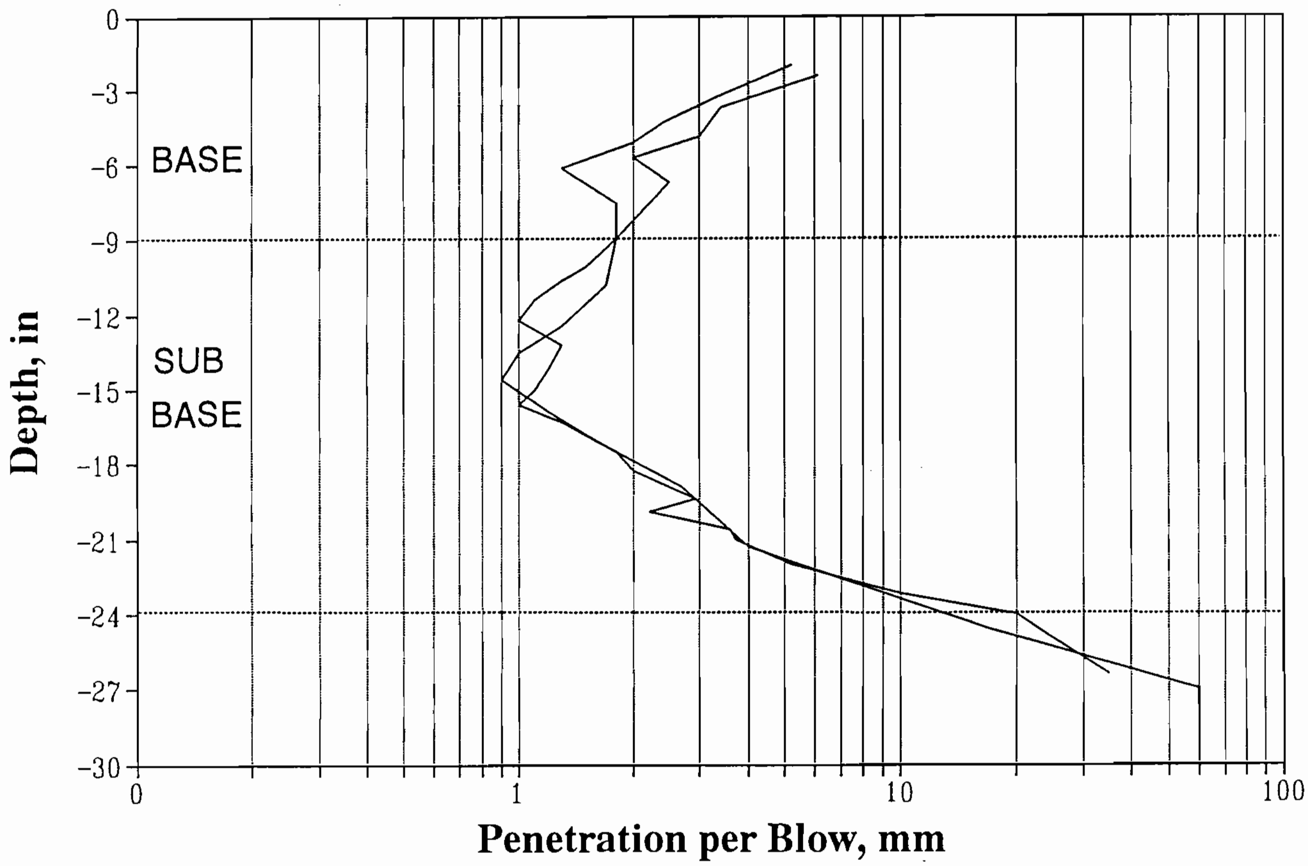

DCP DATA SHEET 1/2

Project: Corpus Christi
Location: SH44 Business EB
CS: 0373-05-023

Date: 6 April 95
Soil Type(s): 4.5" AC
10" Base (1.5% Lime)
8" Subbase-Salvage (4% Lime)

No. of Blows	Accumulative Penetration mm	Penetration per Blow Set mm	Penetration Per Blow mm	Hammer Blow Factor	DCP Index	CBR %	Depth in
0	0	-	-	-	-	-	0
7	92	92	13.1	1	13.1	16	-3.6
10	122	30	3.0	1	3.0	85	-4.8
15	152	30	2.0	1	2.0	134	-6.0
15	172	20	1.3	1	1.3	212	-6.8
15	192	20	1.3	1	1.3	212	-7.6
15	225	33	2.2	1	2.2	121	-8.9
20	262	37	1.9	1	1.9	147	-10.3
9	307	45	5.0	1	5.0	48	-12.1
5	345	38	7.6	1	7.6	30	-13.6
10	413	68	6.8	1	6.8	34	-16.3
5	452	39	7.8	1	7.8	29	-17.8
3	480	28	9.3	1	9.3	24	-18.9

DCP DATA SHEET 2/2

Project: Corpus Christi
Location: SH44 EB Business
CS: 0373-05-023

Date: 6 April 9
Soil Type(s): 4.5" AC
10" Base (1.5% Lime)
8" Subbase-Salvage (4% Lime)

No. of Blows	Accumulative Penetration mm	Penetration per Blow Set mm	Penetration Per Blow mm	Hammer Blow Factor	DCP Index	CBR %	Depth in
0	0	-	-	-	-	-	0
8	70	70	8.8	1	8.8	26	-2.8
10	115	45	4.5	1	4.5	54	-4.5
10	139	24	2.4	1	2.4	110	-5.5
10	156	17	1.7	1	1.7	161	-6.1
30	187	31	1.0	1	1.0	281	-7.4
20	207	20	1.0	1	1.0	292	-8.1
20	230	23	1.2	1	1.2	250	-9.1
20	245	15	0.8	1	0.8	403	-9.6
20	271	26	1.3	1	1.3	218	-10.7
20	304	33	1.7	1	1.7	167	-12.0
15	346	42	2.8	1	2.8	92	-13.6
6	387	41	6.8	1	6.8	34	-15.2
2	420	33	16.5	1	16.5	13	-16.5
2	490	70	35.0	1	35.0	5	-19.3
1	530	40	40.0	1	40.0	5	-20.9

CORPUS CHRISTI
Depth vs CBR %

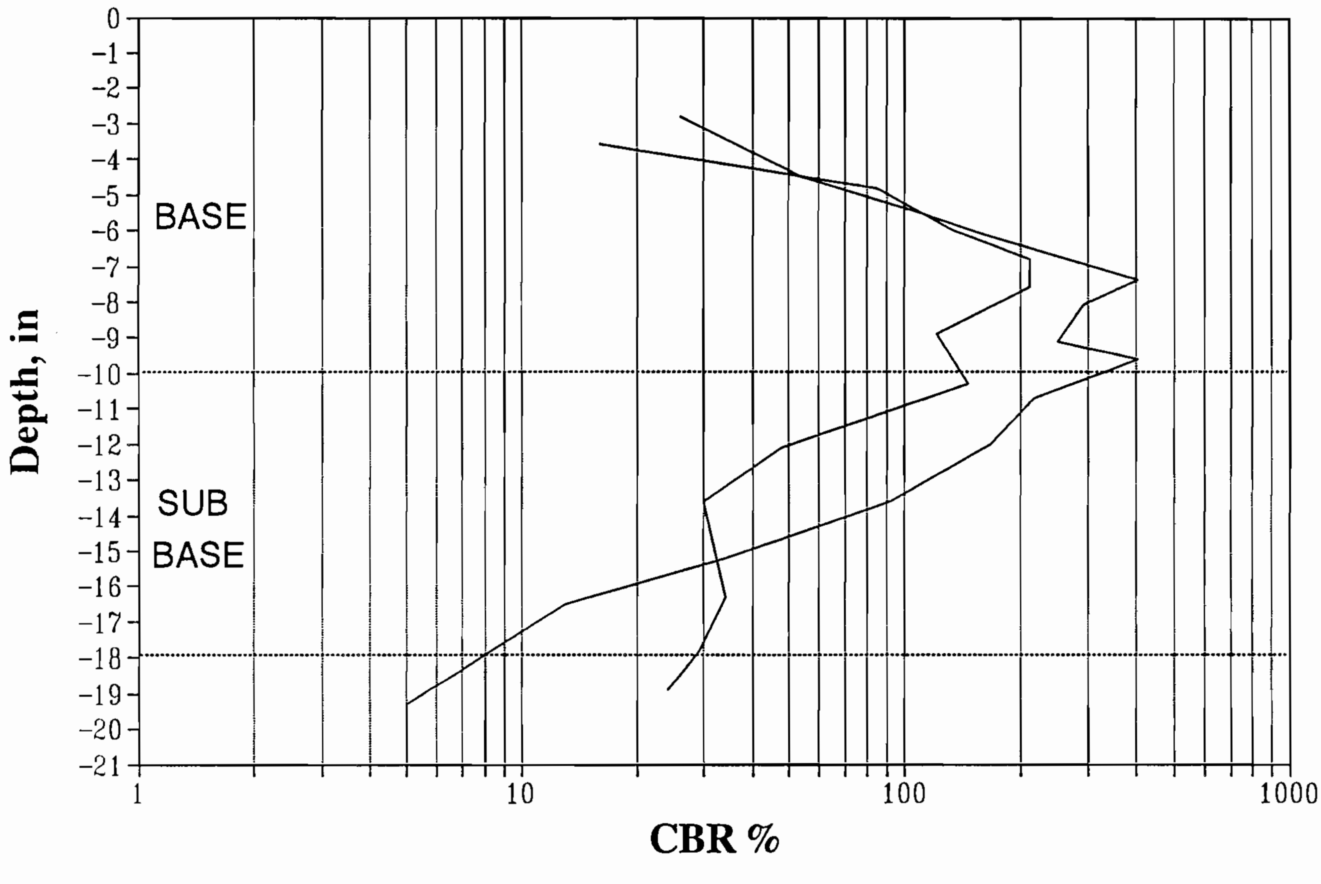

CORPUS CHRISTI

Depth vs Penetration per Blow

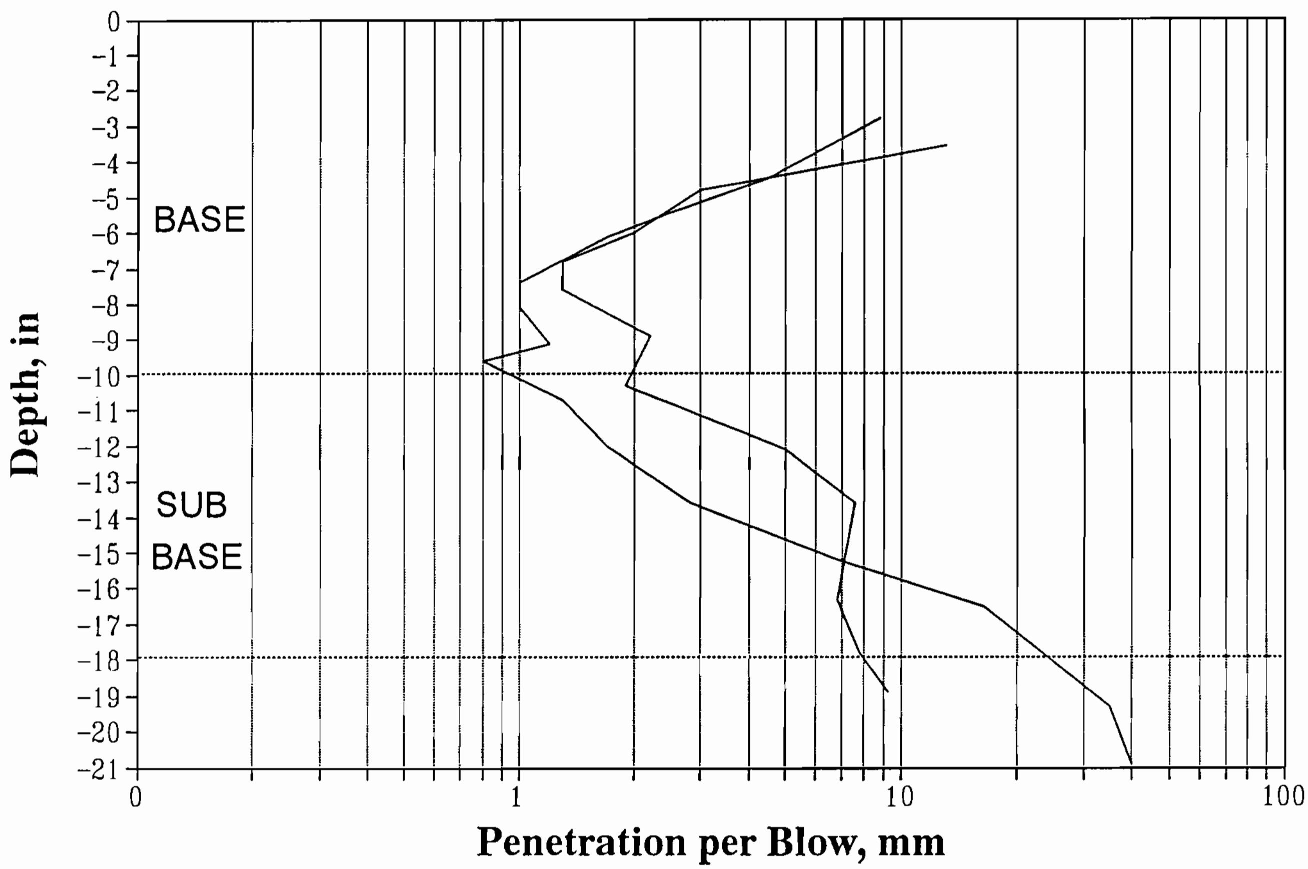

DCP DATA SHEET 1/2

Project: Lufkin
Location: SH-7-CS: 748

Date: 23 March 95
Soil Type(s): 4" AC
14" Flex Base

No. of Blows	Accumulative Penetration mm	Penetration per Blow Set mm	Penetration Per Blow mm	Hammer Blow Factor	DCP Index	CBR %	Depth in
0	0	-	-	-	-	-	0
10	70	70	7.0	1	7.0	33	-2.8
10	117	47	4.7	1	4.7	52	-4.6
10	162	45	4.5	1	4.5	54	-6.4
10	189	27	2.7	1	2.7	96	-7.4
10	220	31	3.1	1	3.1	82	-8.7
10	257	37	3.7	1	3.7	67	-10.1
10	307	50	5.0	1	5.0	48	-12.1
6	352	45	7.5	1	7.5	31	-13.9
5	412	60	12.0	1	12.0	18	-16.2
3	475	63	21.0	1	21.0	10	-18.7
1	492	17	17.0	1	17.0	12	-19.4

DCP DATA SHEET 2/2

Project: Lufkin
Location: SH-7-CS: 748

Date: 23 March 95
Soil Type(s): 4" AC
14" Flex Base

No. of Blows	Accumulative Penetration mm	Penetration per Blow Set mm	Penetration Per Blow mm	Hammer Blow Factor	DCP Index	CBR %	Depth in
0	0	-	-	-	-	-	0
10	69	69	6.9	1	6.9	34	-2.7
10	127	58	5.8	1	5.8	41	-5.0
10	172	45	4.5	1	4.5	54	-6.8
10	215	43	4.3	1	4.3	57	-8.5
10	262	47	4.7	1	4.7	52	-10.3
10	335	73	7.3	1	7.3	32	-13.2
5	397	62	12.4	1	12.4	17	-15.6
3	452	55	18.3	1	18.3	11	-17.8
1	480	28	28.0	1	28.0	7	-18.9

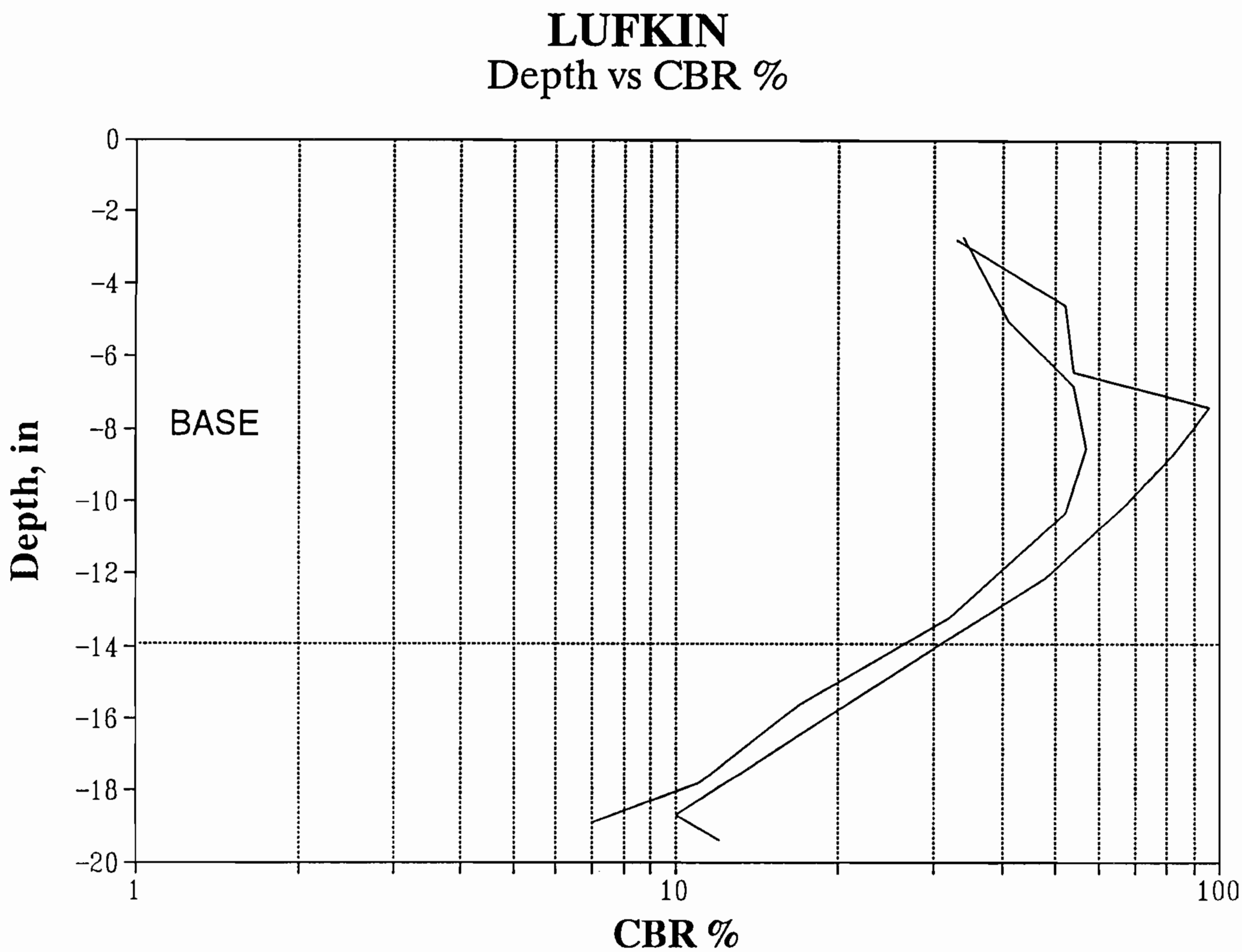
LUFKIN
Depth vs CBR %
Depth, in
BASE
0
-2
-4
-6
-8
-10
-12
-14
-16
-18
-20
1
10
100
CBR %

LUFKIN
Depth vs Penetration per Blow

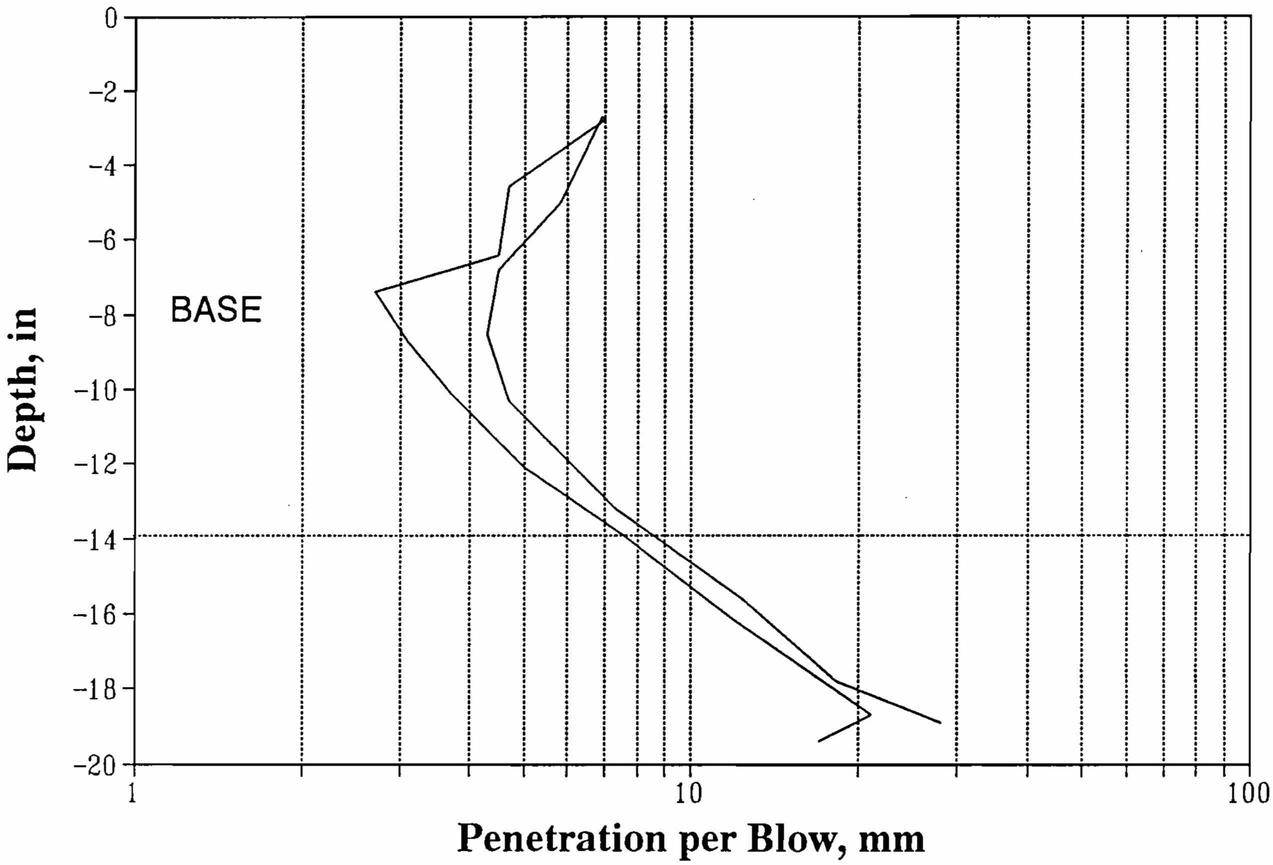

DCP DATA SHEET 1/1

Project: Odessa

Location: FM 1788 EB

CS: 1718-01

Date: 11 Nov. 94

Soil Type(s): 1.5" AC

8" Flex Base

Caliche Subgrade

No. of Blows	Accumulative Penetration mm	Penetration per Blow Set mm	Penetration Per Blow mm	Hammer Blow Factor	DCP Index	CBR %	Depth in
0	0	-	-	-	-	-	0
10	25	25	2.5	1	2.5	105	-1.0
10	35	10	1.0	1	1.0	292	-1.4
10	46	11	1.1	1	1.1	262	-1.8
10	52	6	0.6	1	0.6	517	-2.0
20	73	21	1.1	1	1.1	276	-2.9
40	95	22	0.6	1	0.6	570	-3.7
80	115	20	0.3	1	0.3	1379	-4.5
80	123	8	0.1	1	0.1	3849	-4.8
100	132	9	0.1	1	0.1	4331	-5.2

*Note: Testing was terminated due to high stiffness of the layer

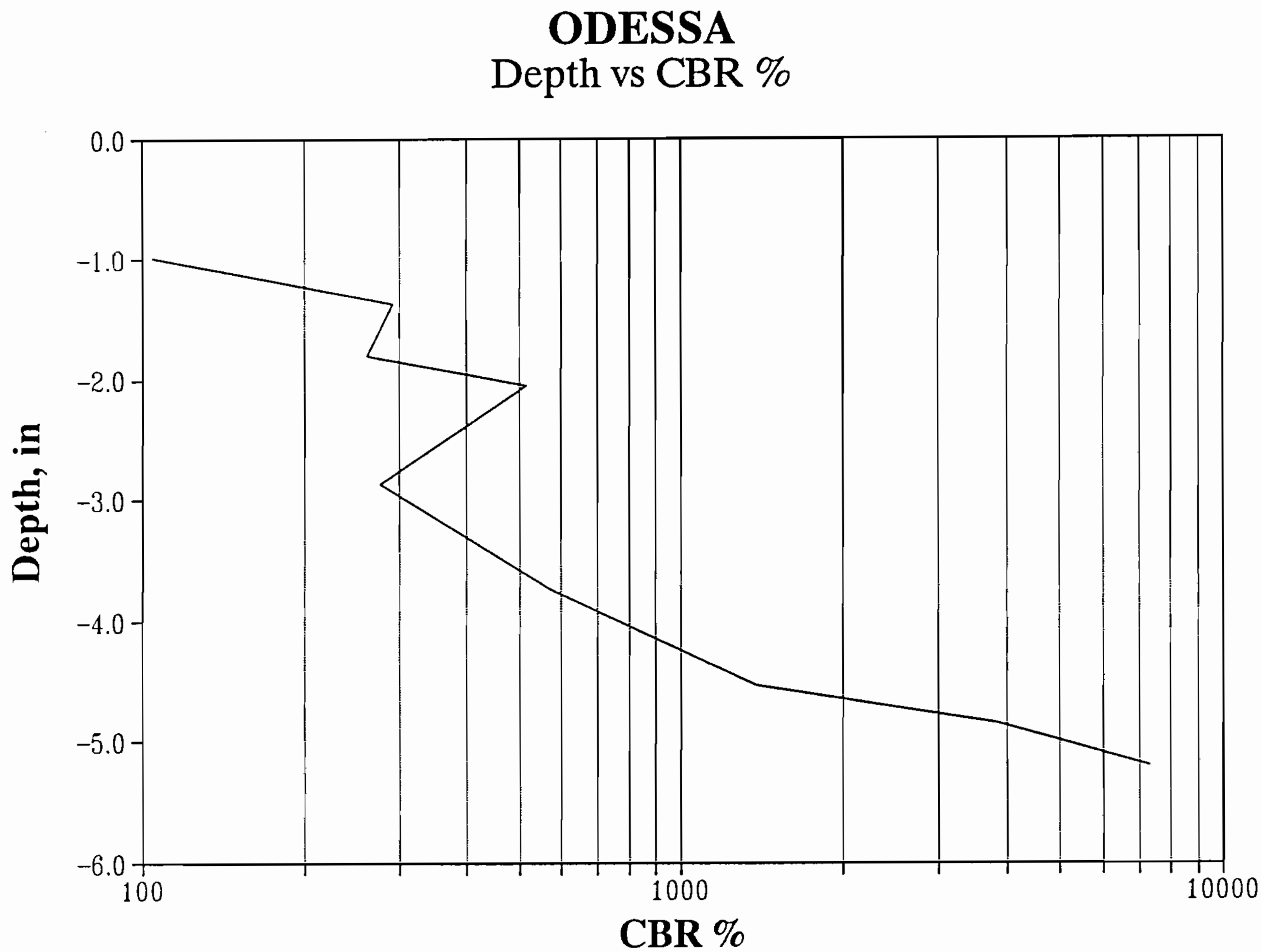
ODESSA
Depth vs CBR %
0.0
-1.0
-2.0
-3.0
-4.0
-5.0
-6.0
Depth, in
100
1000
10000
CBR %

ODESSA

Depth vs Penetration per Blow

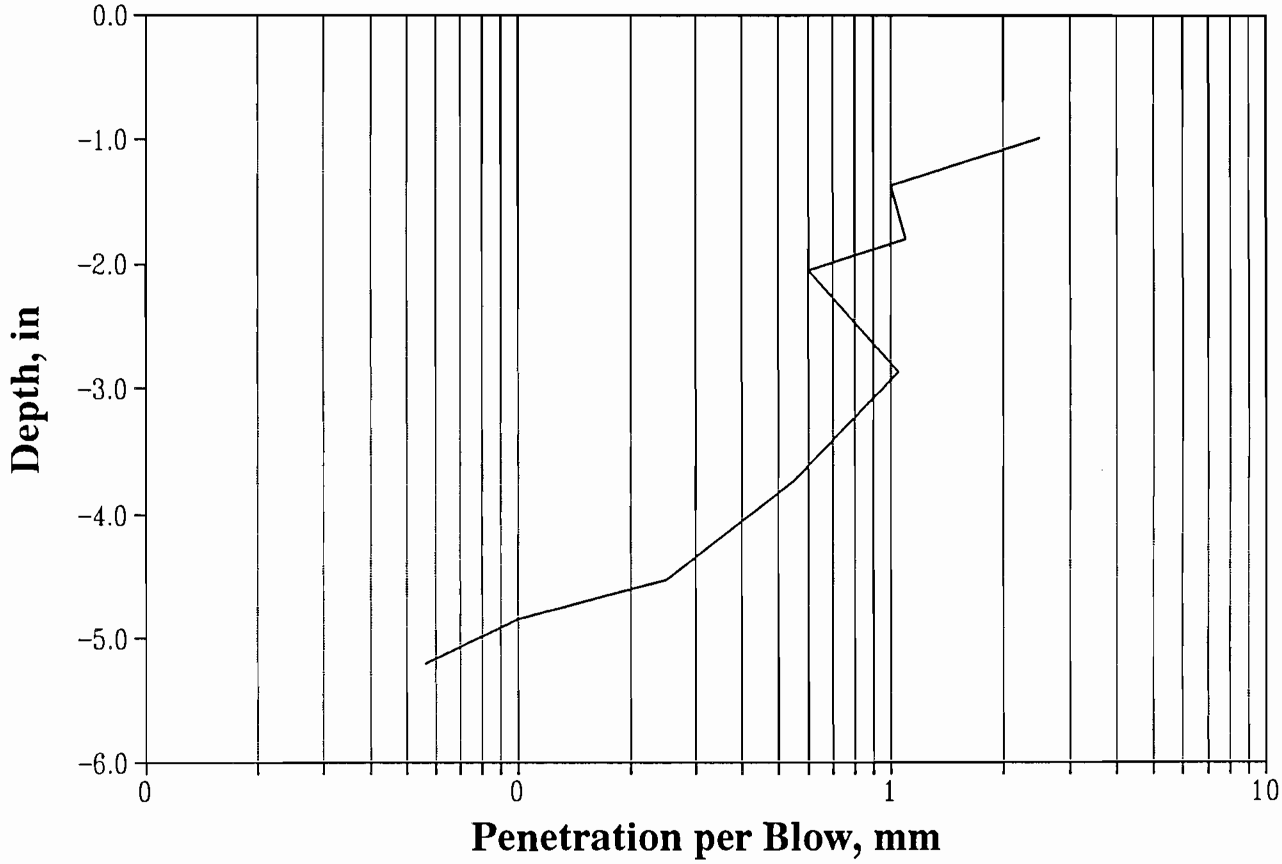

DCP DATA SHEET 1/2

Project: Paris

Location: 2820 FM

Date: 21 March 95

Soil Type(s): 0.5" Surface Treatment
10.5" Base (Sandstone & Salvage)

No. of Blows	Accumulative Penetration mm	Penetration per Blow Set mm	Penetration Per Blow mm	Hammer Blow Factor	DCP Index	CBR %	Depth in
0	0	-	-	-	-	-	0
10	16	16	1.6	1	1.6	172	-0.6
10	48	32	3.2	1	3.2	79	-1.9
10	76	28	2.8	1	2.8	92	-3.0
10	95	19	1.9	1	1.9	142	-3.7
10	124	29	2.9	1	2.9	89	-4.9
10	154	30	3.0	1	3.0	85	-6.1
10	169	15	1.5	1	1.5	185	-6.7
20	197	28	1.4	1	1.4	200	-7.8
10	219	22	2.2	1	2.2	121	-8.6
10	242	23	2.3	1	2.3	115	-9.5
4	271	29	7.3	1	7.3	32	-10.7
2	301	30	15.0	1	15.0	14	-11.9

DCP DATA SHEET 2/2

Project: Paris

Location: 2820 FM

Date: 21 March 95

Soil Type(s): 0.5" Surface Treatment

10.5" Base (Sandstone & Salvage)

No. of Blows	Accumulative Penetration mm	Penetration per Blow Set mm	Penetration Per Blow mm	Hammer Blow Factor	DCP Index	CBR %	Depth in
0	0	-	-	-	-	-	0
10	22	22	2.2	1	2.2	121	0.9
10	43	21	2.1	1	2.1	127	1.7
10	72	29	2.9	1	2.9	89	2.8
10	96	24	2.4	1	2.4	110	3.8
10	122	26	2.6	1	2.6	100	4.8
10	145	23	2.3	1	2.3	115	5.7
10	164	19	1.9	1	1.9	142	6.5
10	175	11	1.1	1	1.1	262	6.9
10	189	14	1.4	1	1.4	200	7.4
20	212	23	1.2	1	1.2	250	8.3
10	247	35	3.5	1	3.5	72	9.7
4	279	32	8.0	1	8.0	28	11.0
2	332	53	26.5	1	26.5	7	13.1

PARIS

Depth vs CBR %

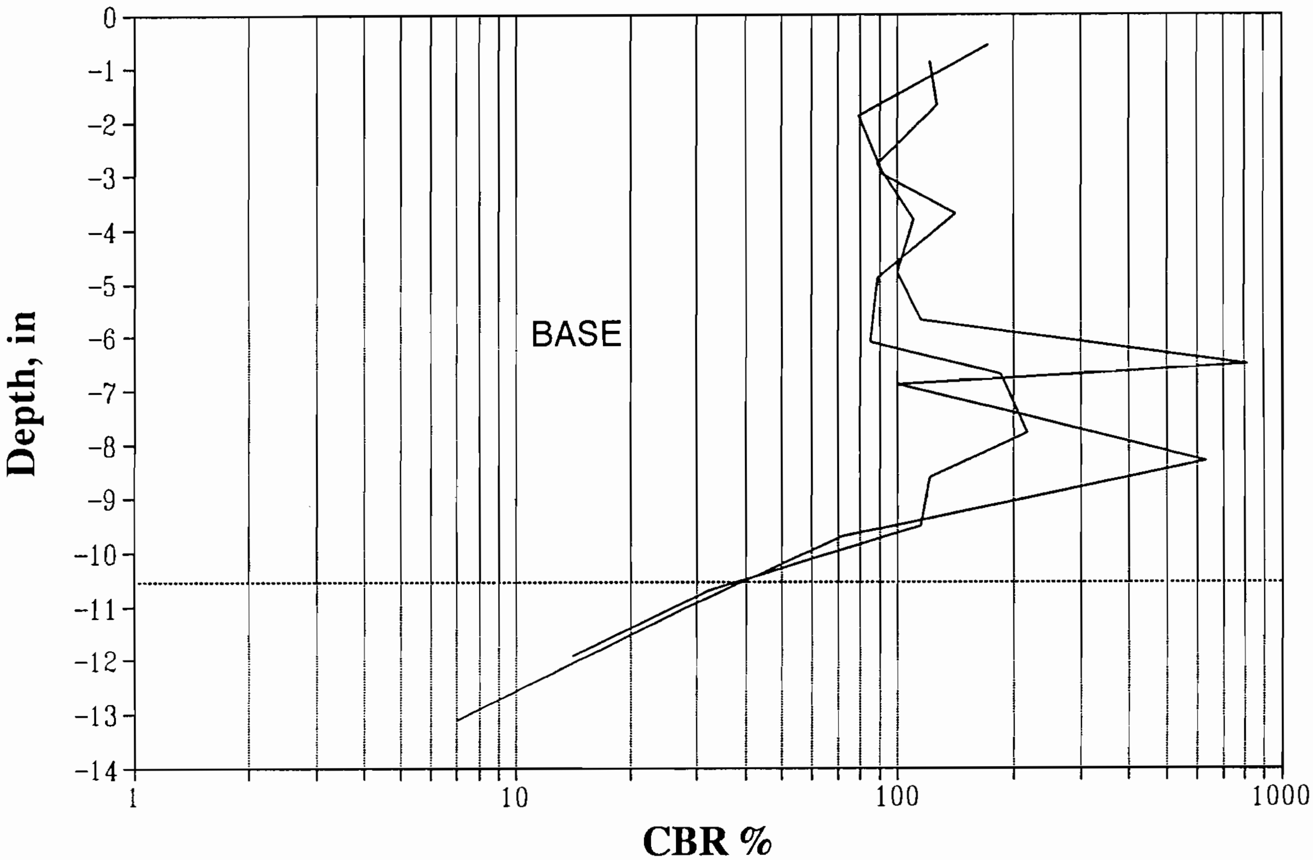

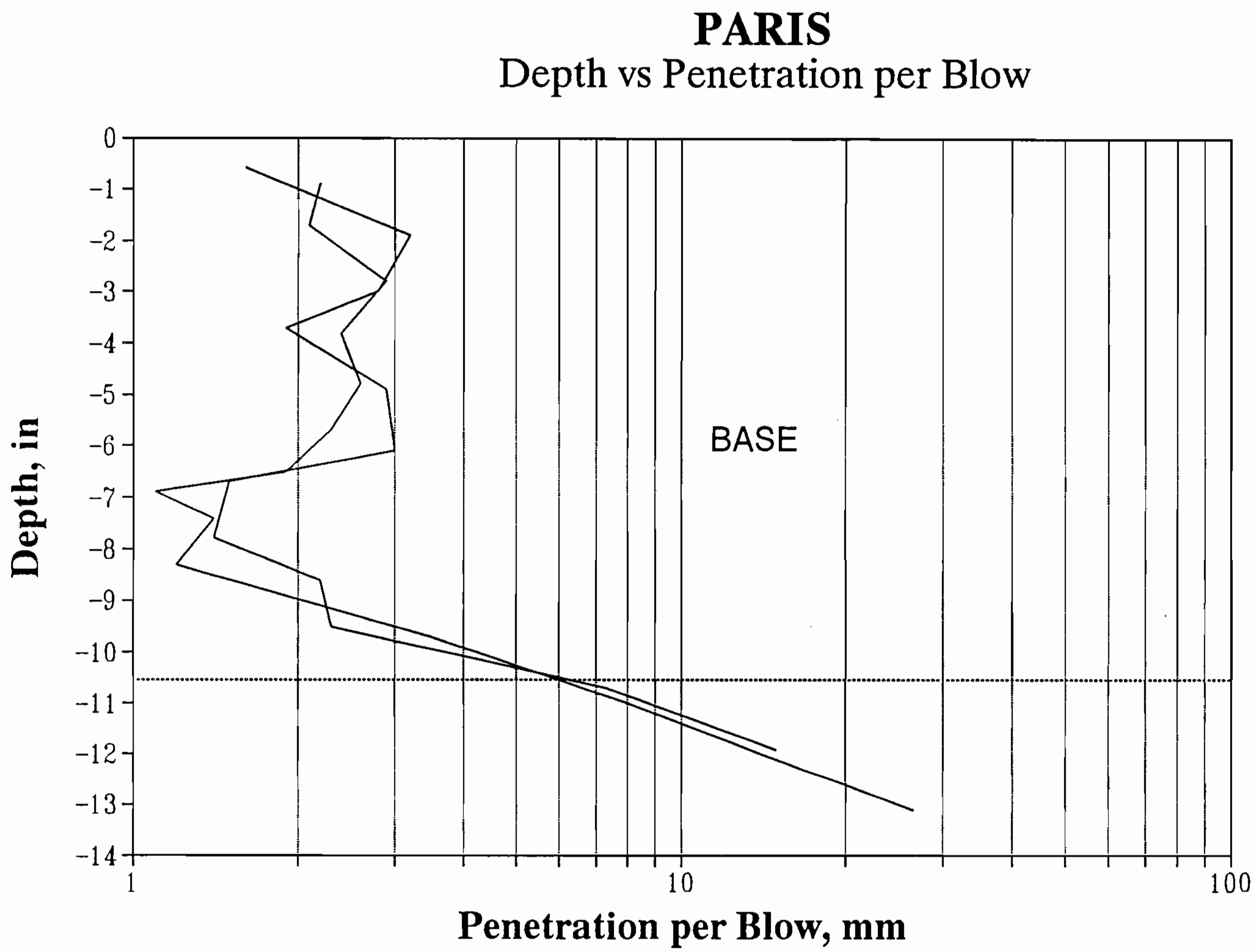
PARIS
Depth vs Penetration per Blow
BASE
Depth, in
Penetration per Blow, mm
0
-1
-2
-3
-4
-5
-6
-7
-8
-9
-10
-11
-12
-13
-14
1
10
100

DCP DATA SHEET 1/1

Project: San Angelo

Location: US 67 -Frontage Road EB CS 1582

Date: 8 Nov. 94

Soil Type(s): 2" AC
12" Base (Crushed Limestone)

No. of Blows	Accumulative Penetration mm	Penetration per Blow Set mm	Penetration Per Blow mm	Hammer Blow Factor	DCP Index	CBR %	Depth in
0	0	-	-	-	-	-	0
16	26	26	1.6	1	1.6	170	-1.0
41	53	27	0.7	1	0.7	466	-2.1
20	70	17	0.9	1	0.9	350	-2.8
20	88	18	0.9	1	0.9	329	-3.5
20	109	21	1.1	1	1.1	276	-4.3
20	130	21	1.1	1	1.1	276	-5.1
20	150	20	1.0	1	1.0	292	-5.9
20	175	25	1.3	1	1.3	227	-6.9
20	200	25	1.3	1	1.3	227	-7.9
20	217	17	0.9	1	0.9	350	-8.5
20	232	15	0.8	1	0.8	403	-9.1
20	290	58	2.9	1	2.9	89	-11.4
6	308	18	3.0	1	3.0	85	-12.1
3	345	37	12.3	1	12.3	18	-13.6
2	377	32	16.0	1	16.0	13	-14.8
2	413	36	18.0	1	18.0	11	-16.3
2	442	29	14.5	1	14.5	15	-17.4
1	455	13	13.0	1	13.0	17	-17.9

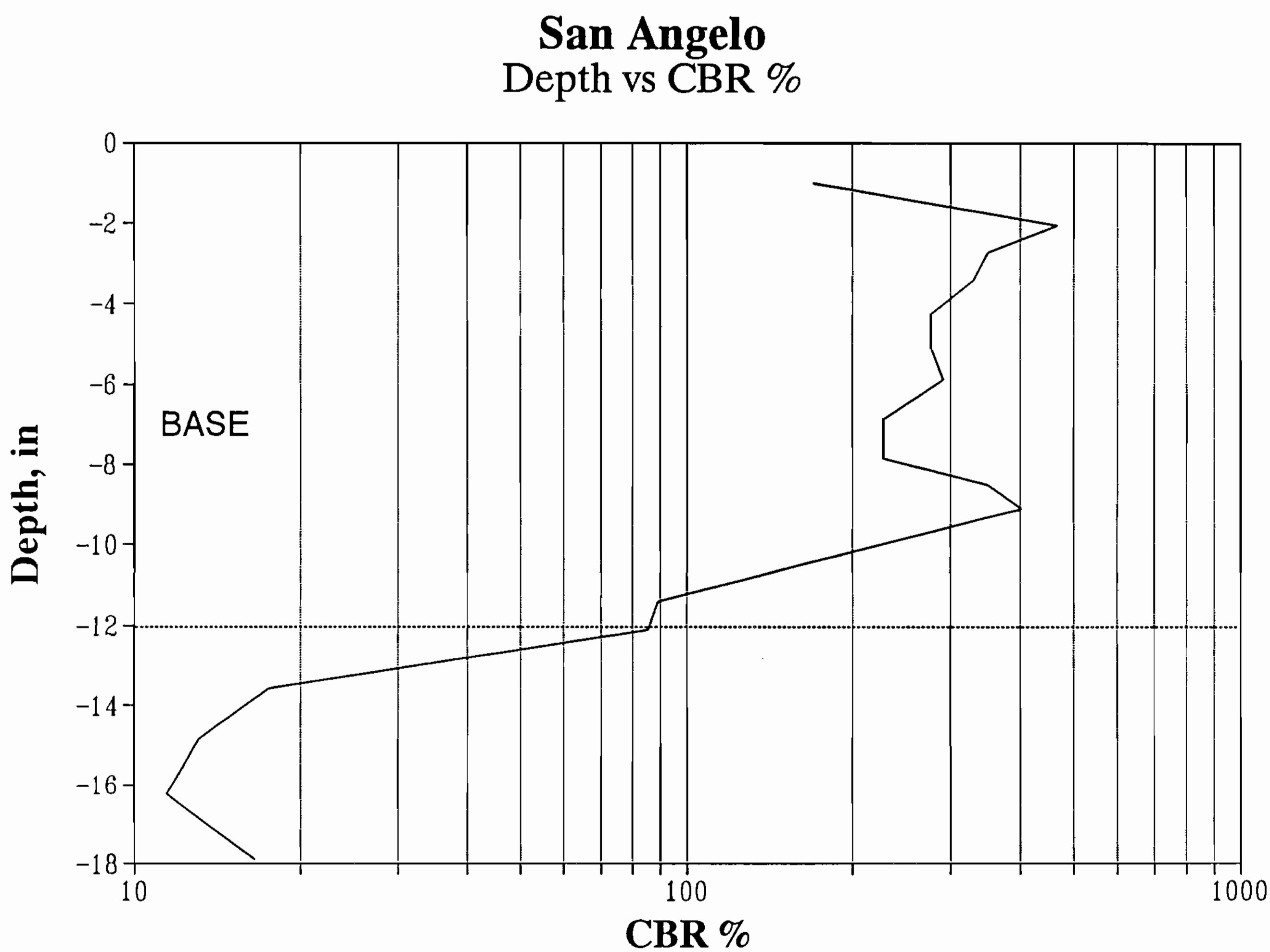

San Angelo
Depth vs CBR %
Depth, in
CBR %
BASE
0
-2
-4
-6
-8
-10
-12
-14
-16
-18
10
100
1000

San Angelo
Depth vs Penetration per Blow

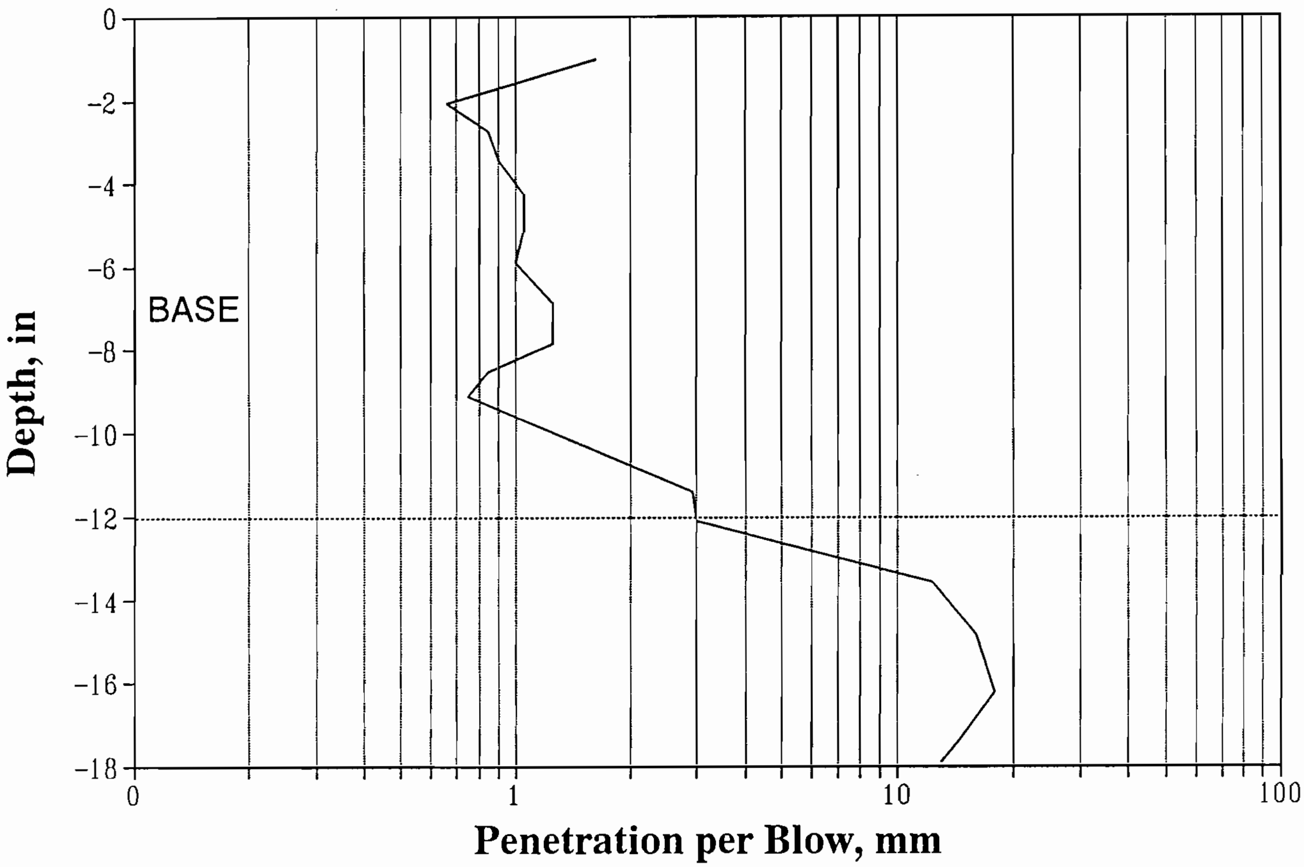

DCP DATA SHEET 1/1

Project: San Antonio
Location: Loop 1604 WB Frontage Road

Date: 3 April 95
Soil Type(s): 2.5" AC
10.5" Flex Base

No. of Blows	Accumulative Penetration mm	Penetration per Blow Set mm	Penetration Per Blow mm	Hammer Blow Factor	DCP Index	CBR %	Depth in
0	0	-	-	-	-	-	0
10	30	30	3.0	1	3.0	85	-1.2
10	53	23	2.3	1	2.3	115	-2.1
20	75	22	1.1	1	1.1	262	-3.0
50	95	20	0.4	1	0.4	815	-3.7
60	115	20	0.3	1	0.3	999	-4.5
60	130	15	0.3	1	0.3	1379	-5.1
80	162	32	0.4	1	0.4	815	-6.4
90	185	23	0.3	1	0.3	1346	-7.3
90	210	25	0.3	1	0.3	1226	-8.3
40	230	20	0.5	1	0.5	635	-9.1
20	250	20	1.0	1	1.0	292	-9.8
20	270	20	1.0	1	1.0	292	-10.6
15	310	40	2.7	1	2.7	97	-12.2
10	335	25	2.5	1	2.5	105	-13.2
10	362	27	2.7	1	2.7	96	-14.3
10	392	30	3.0	1	3.0	85	-15.4
10	410	18	1.8	1	1.8	151	-16.1
15	448	38	2.5	1	2.5	103	-17.6
6	470	22	3.7	1	3.7	68	-18.5
5	495	25	5.0	1	5.0	48	-19.5
2	514	19	9.5	1	9.5	23	-20.2
2	532	18	9.0	1	9.0	25	-20.9

SAN ANTONIO
Depth vs CBR %

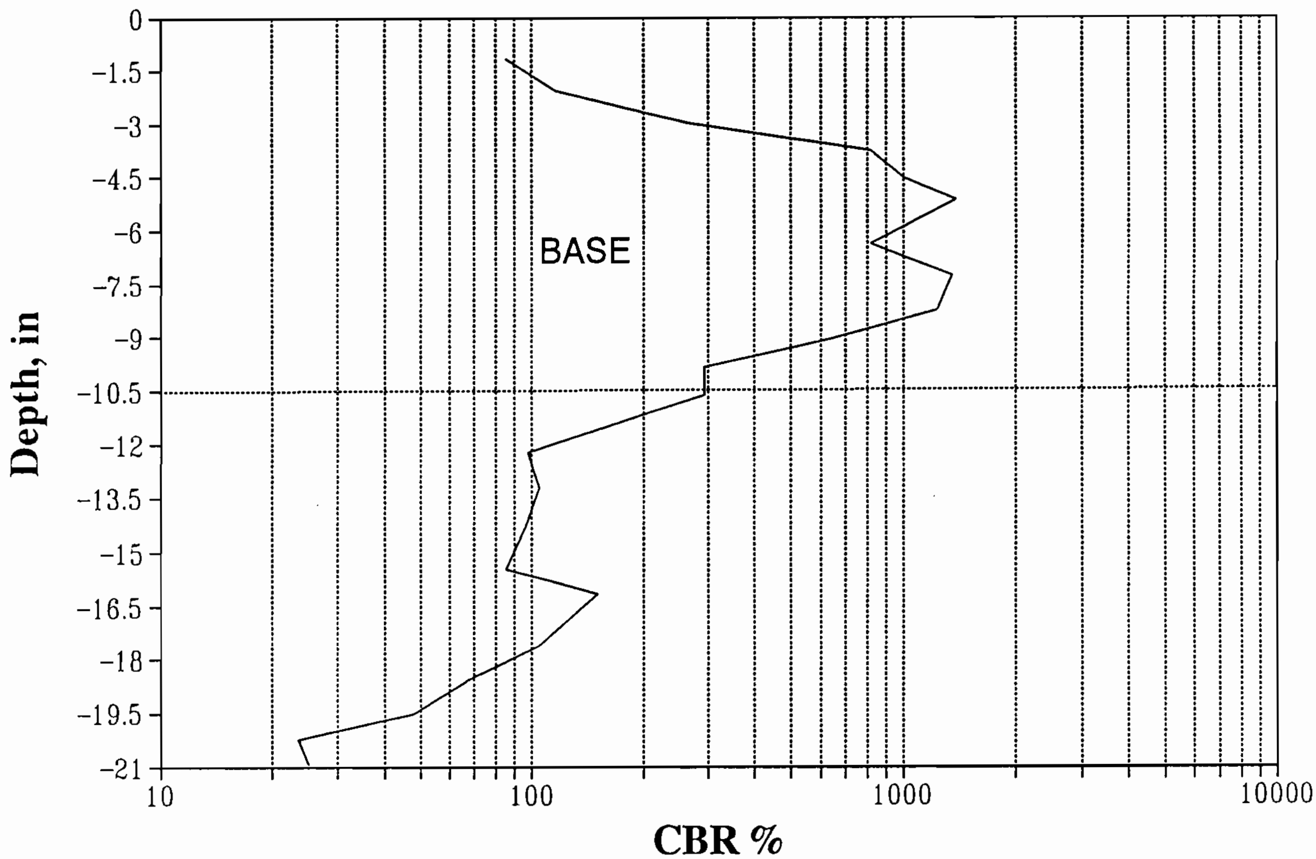

SAN ANTONIO
Depth vs Penetration per Blow

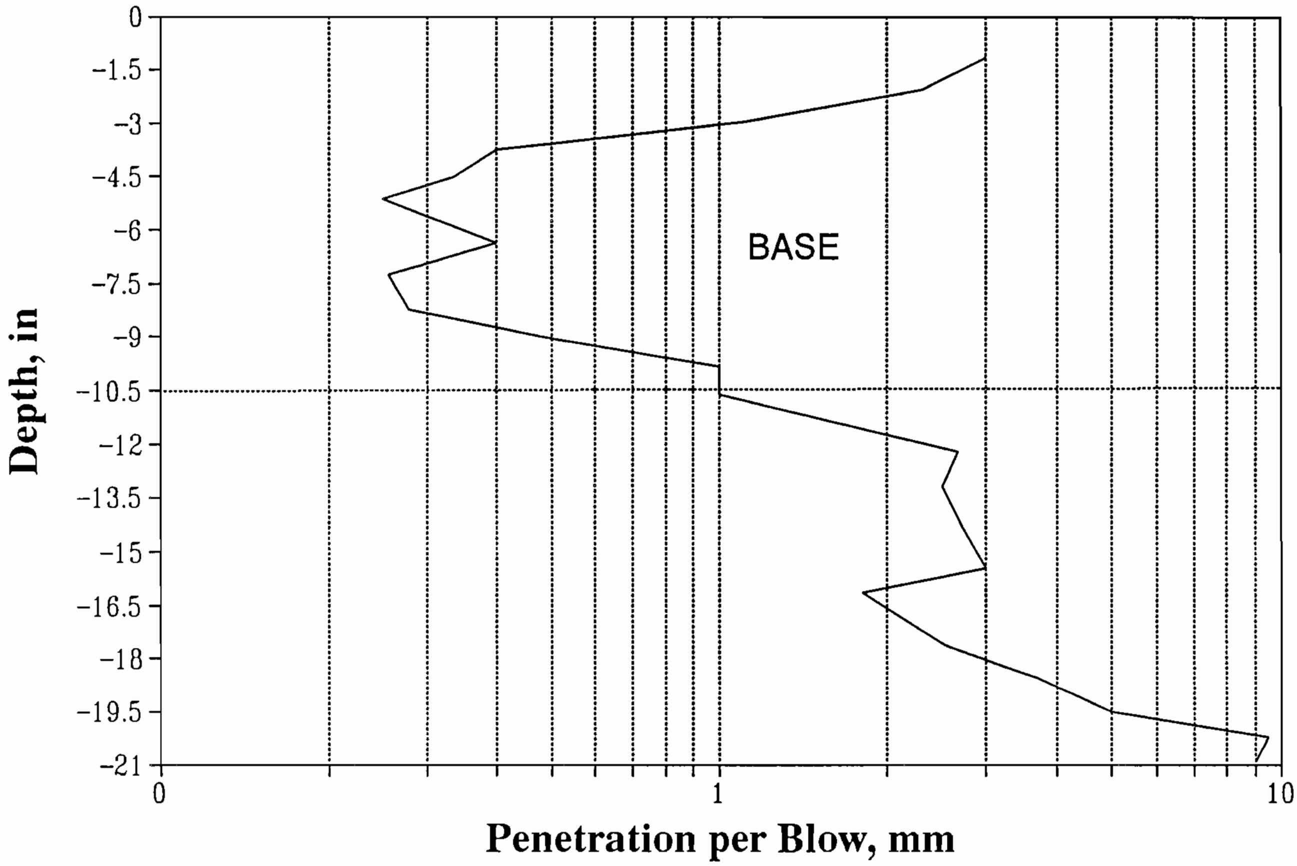

DCP DATA SHEET 1/1

Project: Tyler

Location: SH 110

Date: 21 March 95

Soil Type(s): 3" AC Type D

11" Flex Base (Iron Ore)

No. of Blows	Accumulative Penetration mm	Penetration per Blow Set mm	Penetration Per Blow mm	Hammer Blow Factor	DCP Index	CBR %	Depth in
0	0	-	-	-	-	-	0
10	60	60	6.0	1	6.0	39	-2.4
5	84	24	4.8	1	4.8	50	-3.3
10	108	24	2.4	1	2.4	110	-4.3
15	137	29	1.9	1	1.9	140	-5.4
10	155	18	1.8	1	1.8	151	-6.1
10	185	30	3.0	1	3.0	85	-7.3
10	220	35	3.5	1	3.5	72	-8.7
5	242	22	4.4	1	4.4	56	-9.5
3	263	21	7.0	1	7.0	33	-10.4
3	285	22	7.3	1	7.3	31	-11.2
3	313	28	9.3	1	9.3	24	-12.3
3	337	24	8.0	1	8.0	28	-13.3

DCP DATA SHEET 2/2

Project: Tyler
Location: SH 110

Date: 21 March 95
Soil Type(s): 3" AC
11" Flex Base (Iron Ore)

No. of Blows	Accumulative Penetration mm	Penetration per Blow Set mm	Penetration Per Blow mm	Hammer Blow Factor	DCP Index	CBR %	Depth in
0	0	-	-	-	-	-	0
10	69	69	6.9	1	6.9	34	-2.7
10	113	44	4.4	1	4.4	56	-4.4
10	130	17	1.7	1	1.7	161	-5.1
10	148	18	1.8	1	1.8	151	-5.8
10	164	16	1.6	1	1.6	172	-6.5
10	201	37	3.7	1	3.7	67	-7.9
10	265	64	6.4	1	6.4	37	-10.4
5	305	40	8.0	1	8.0	28	-12.0
5	343	38	7.6	1	7.6	30	-13.5
5	378	35	7.0	1	7.0	33	-14.9
3	405	27	9.0	1	9.0	25	-15.9

TYLER
Depth vs CBR %

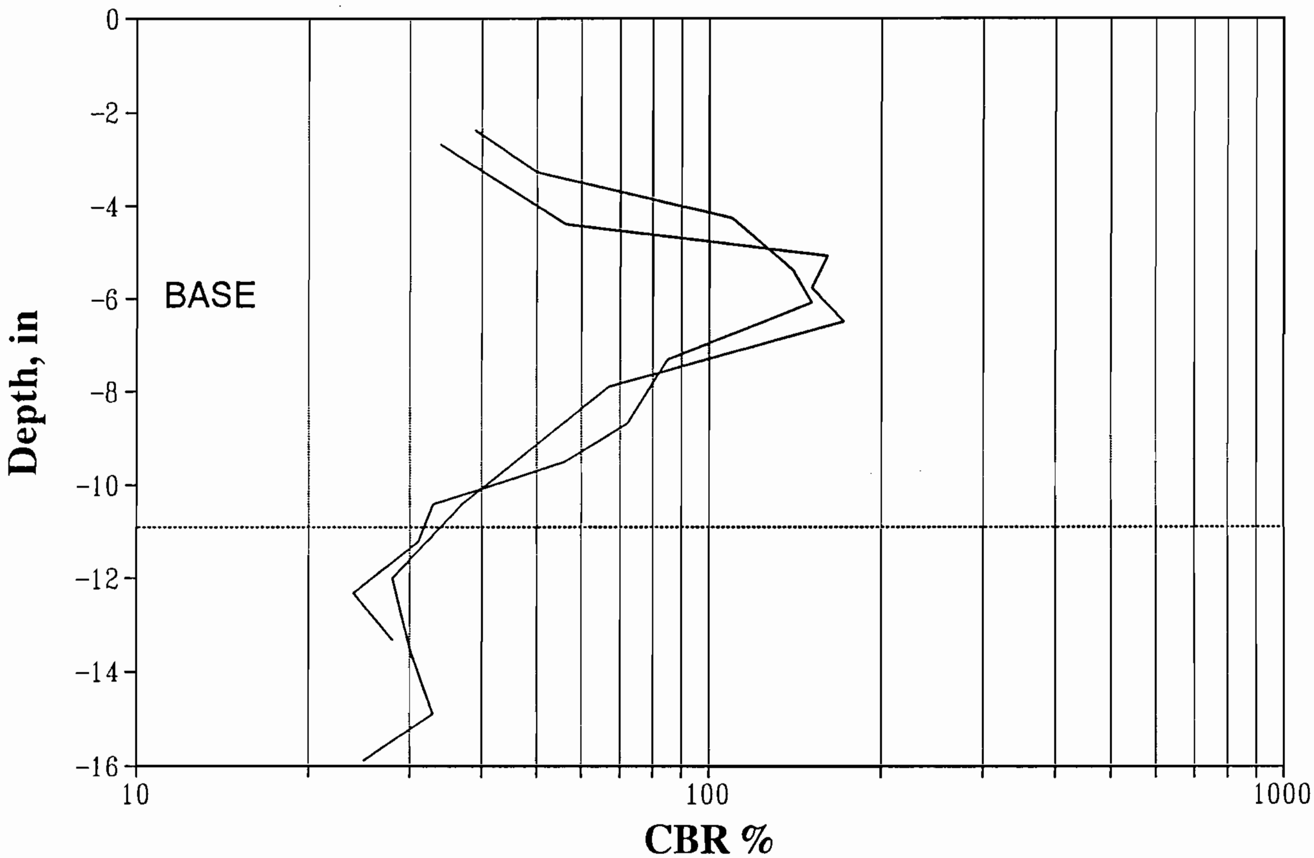

TYLER
Depth vs Penetration per Blow

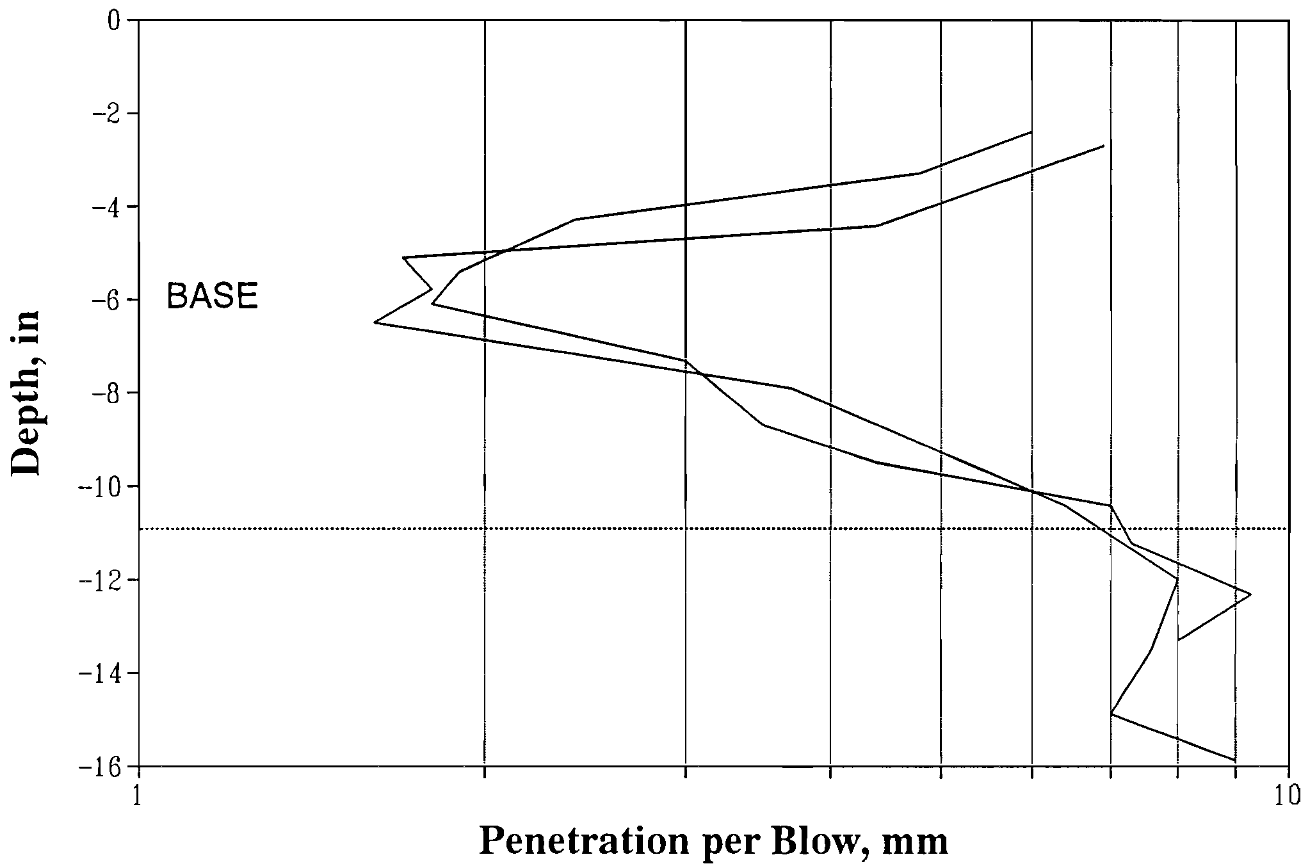

Appendix C

Results from Resilient Modulus Tests of In-Service Materials

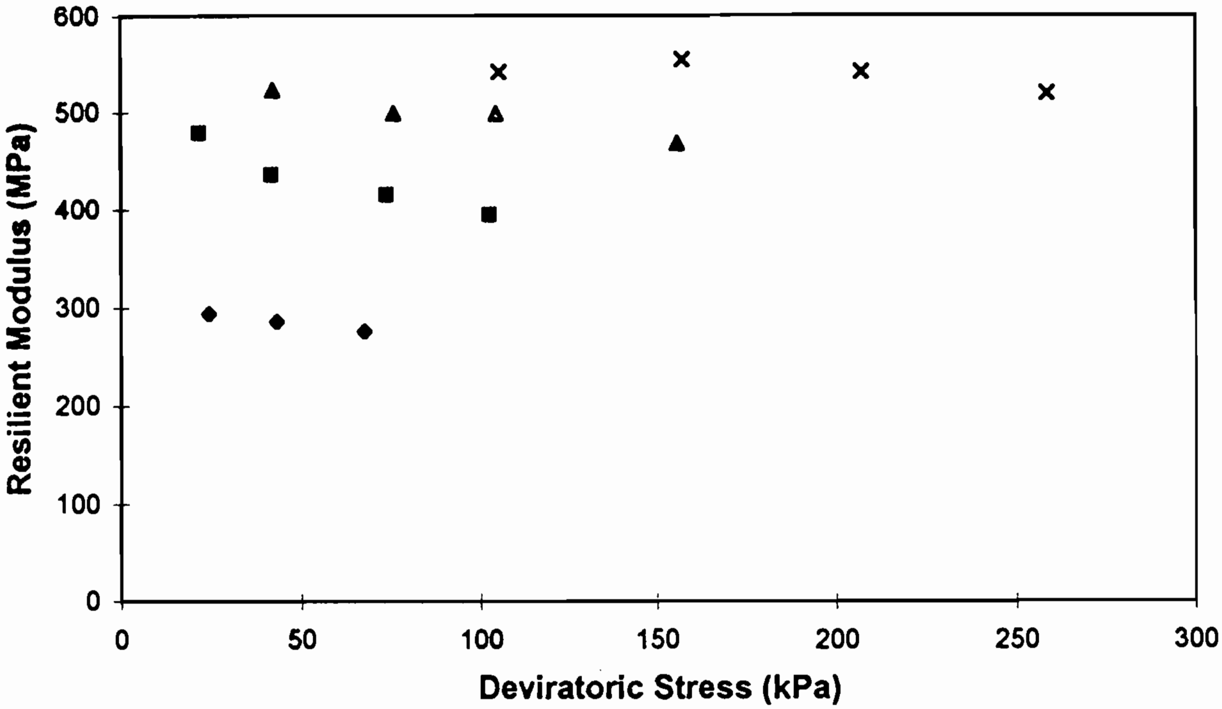

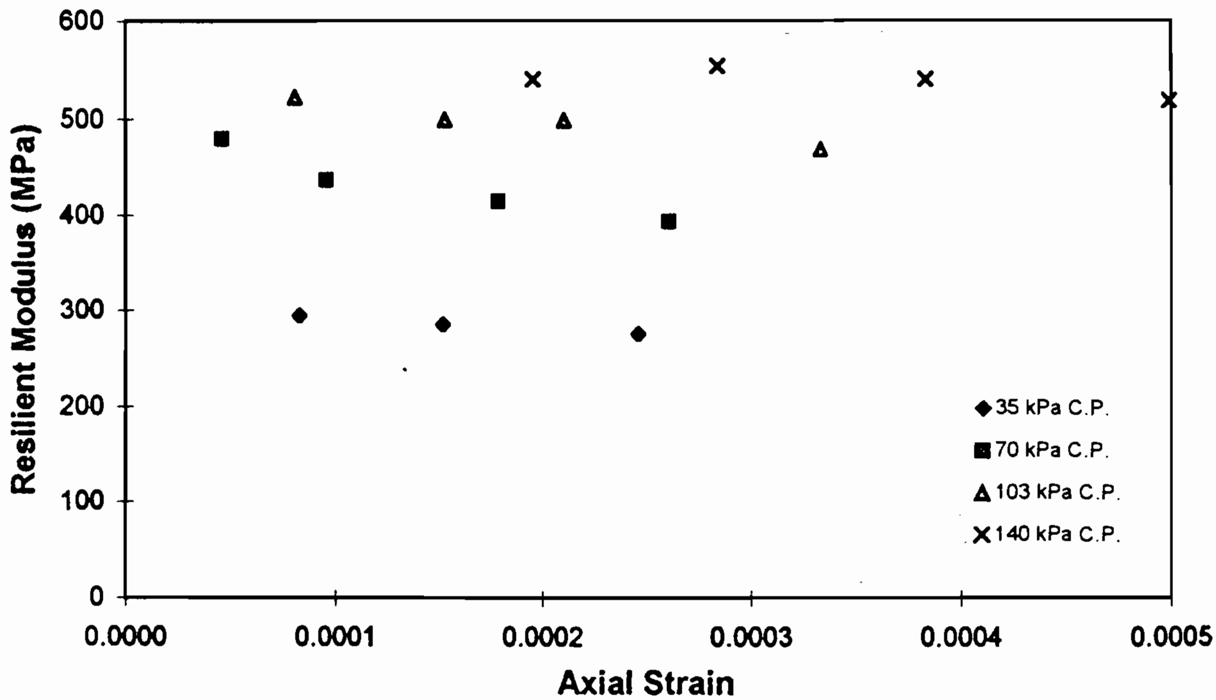

Resilient Modulus Tests Results from Brownwood District

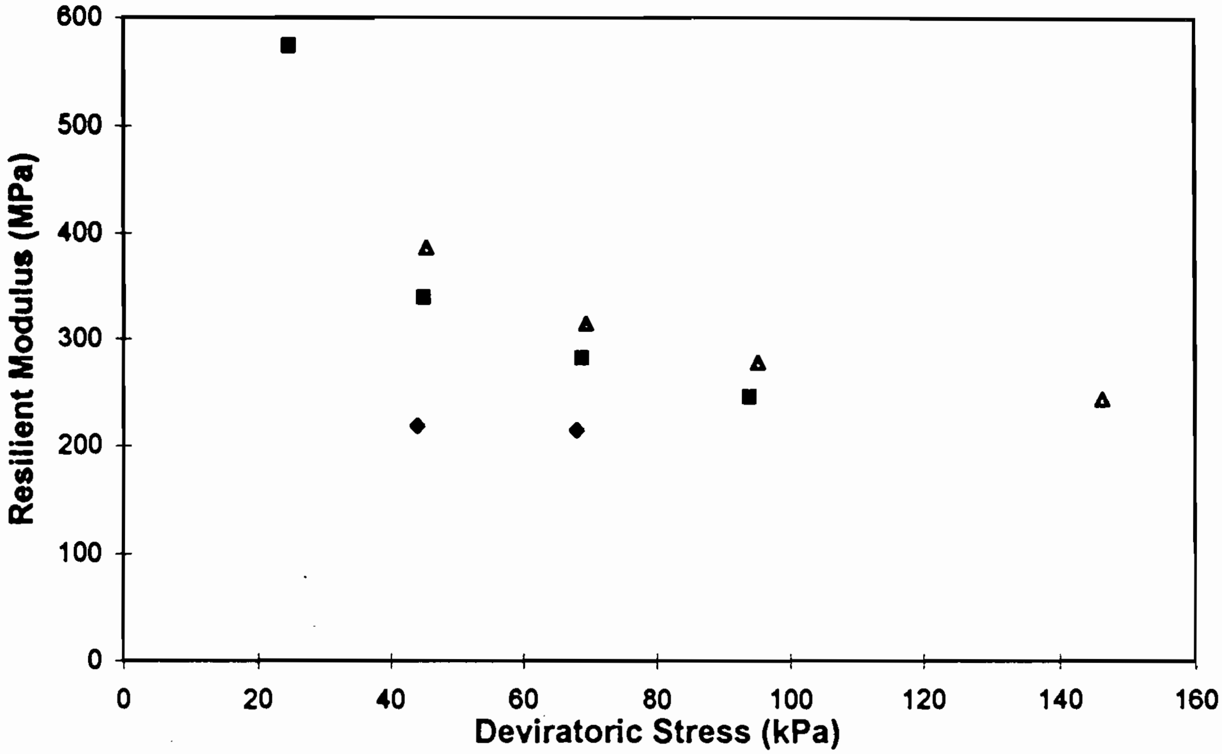

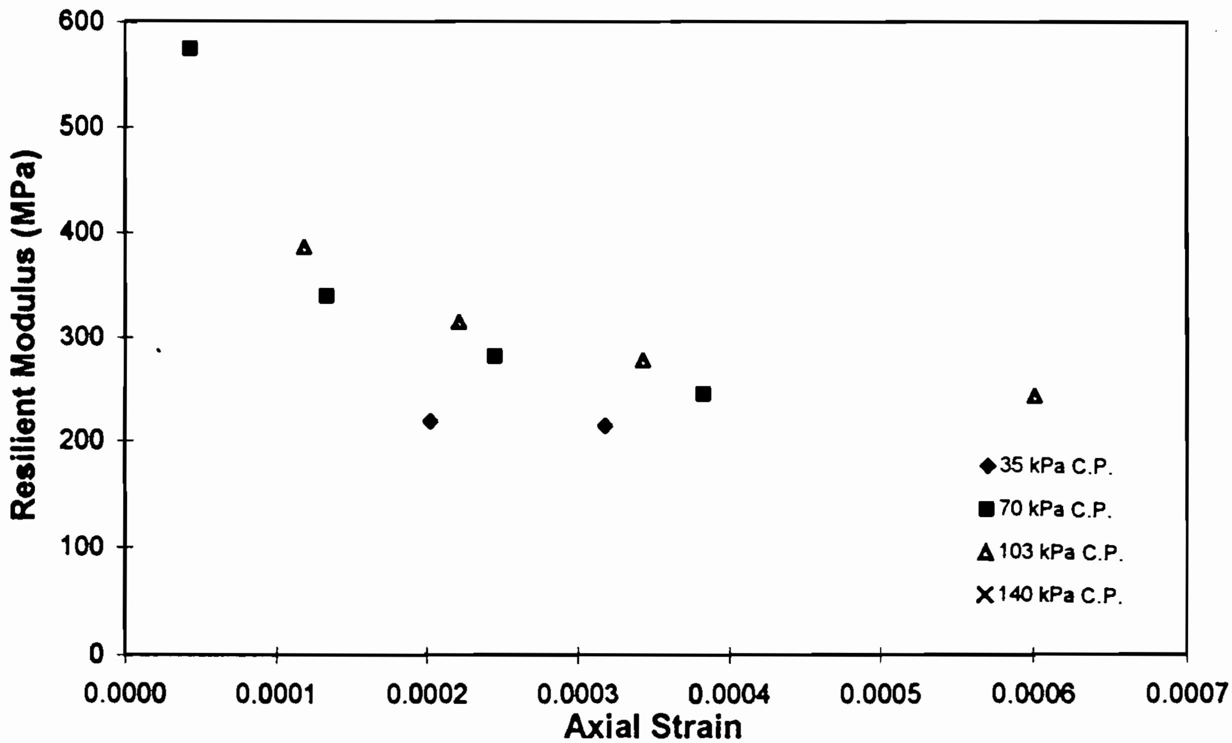

Resilient Modulus Tests Results from Childress District

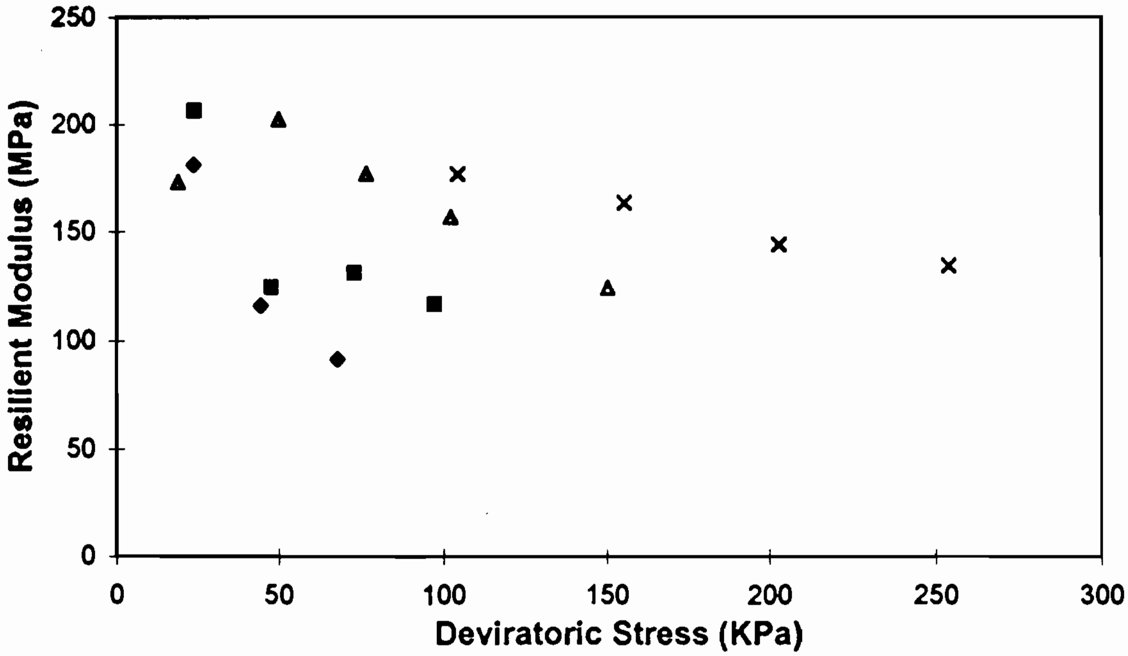

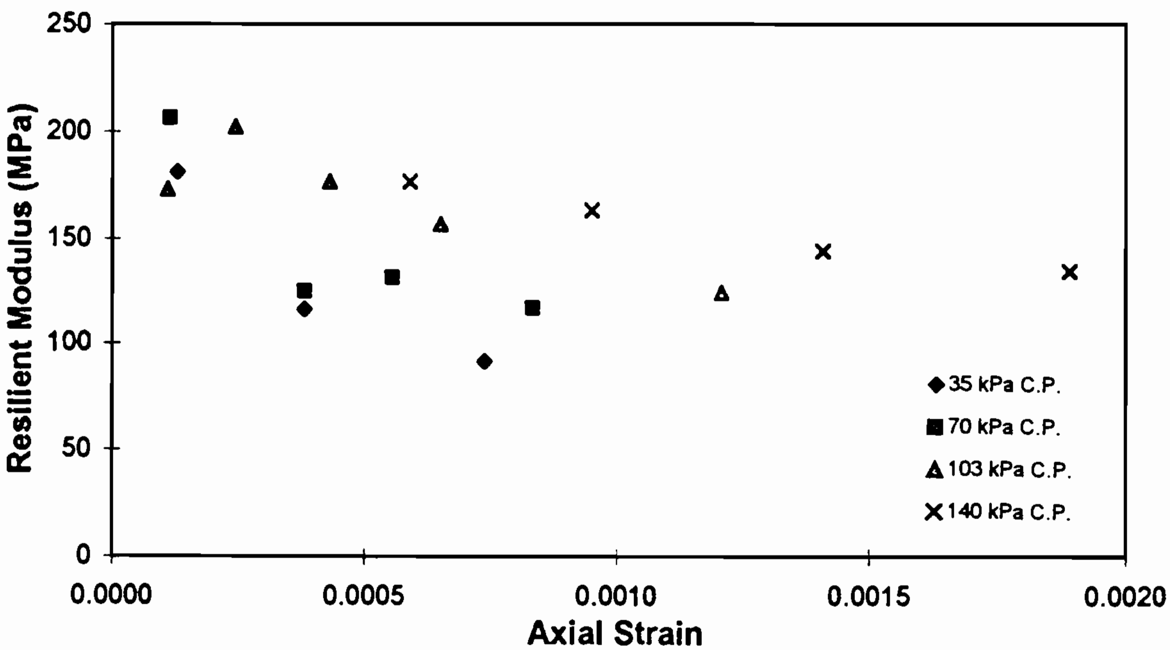

Resilient Modulus Tests Results from Corpus Christi District

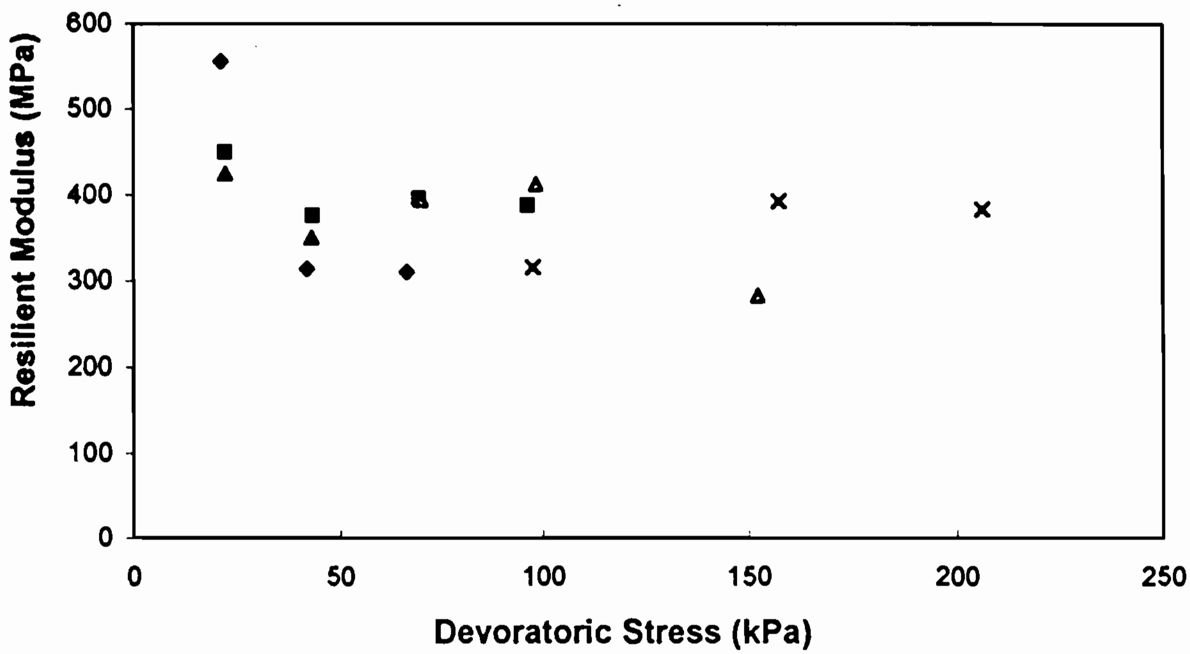

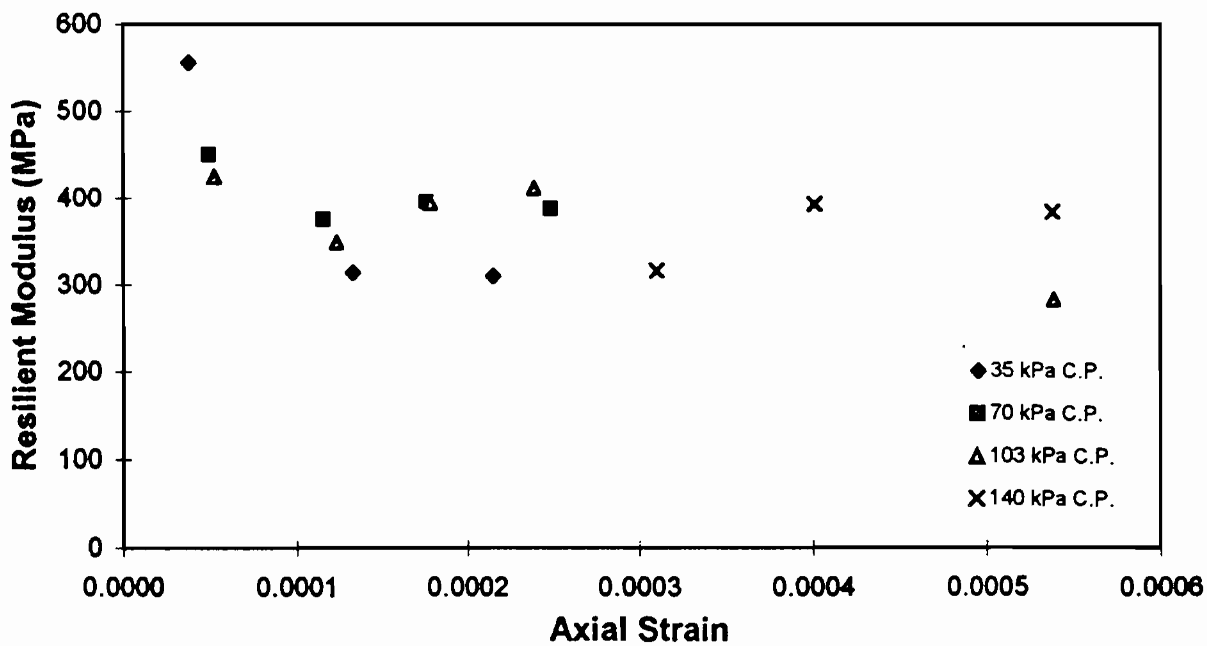

Resilient Modulus Tests Results from El Paso District

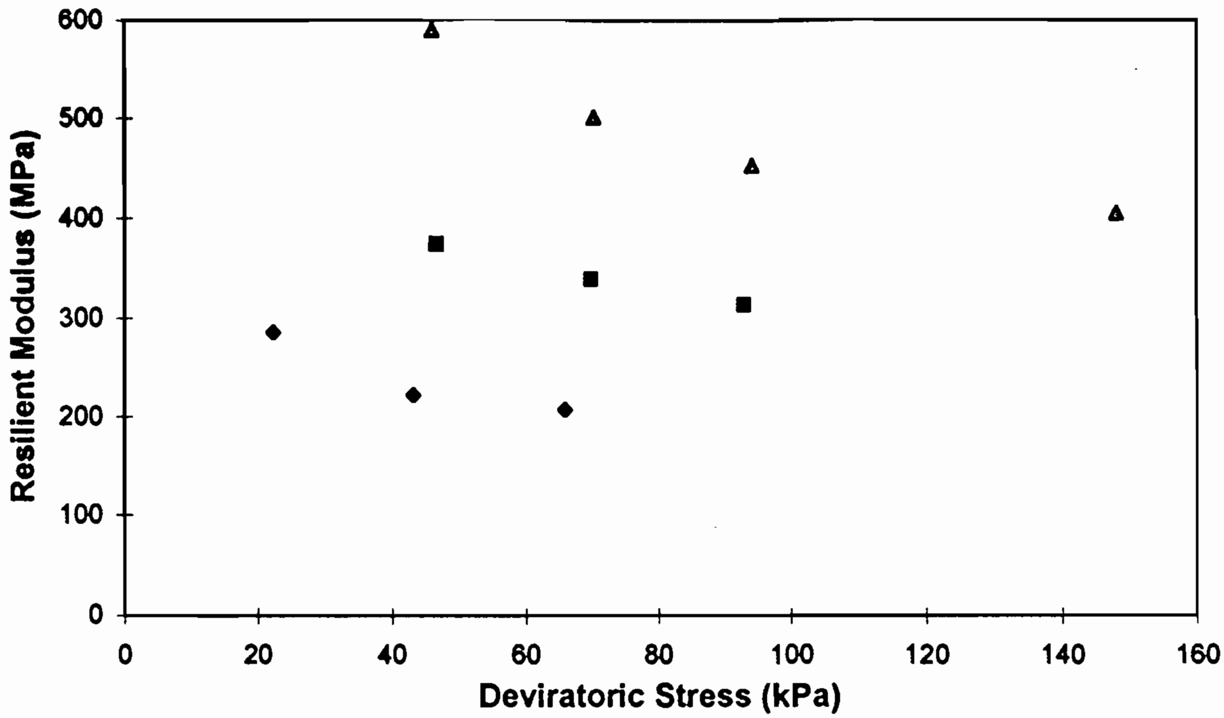

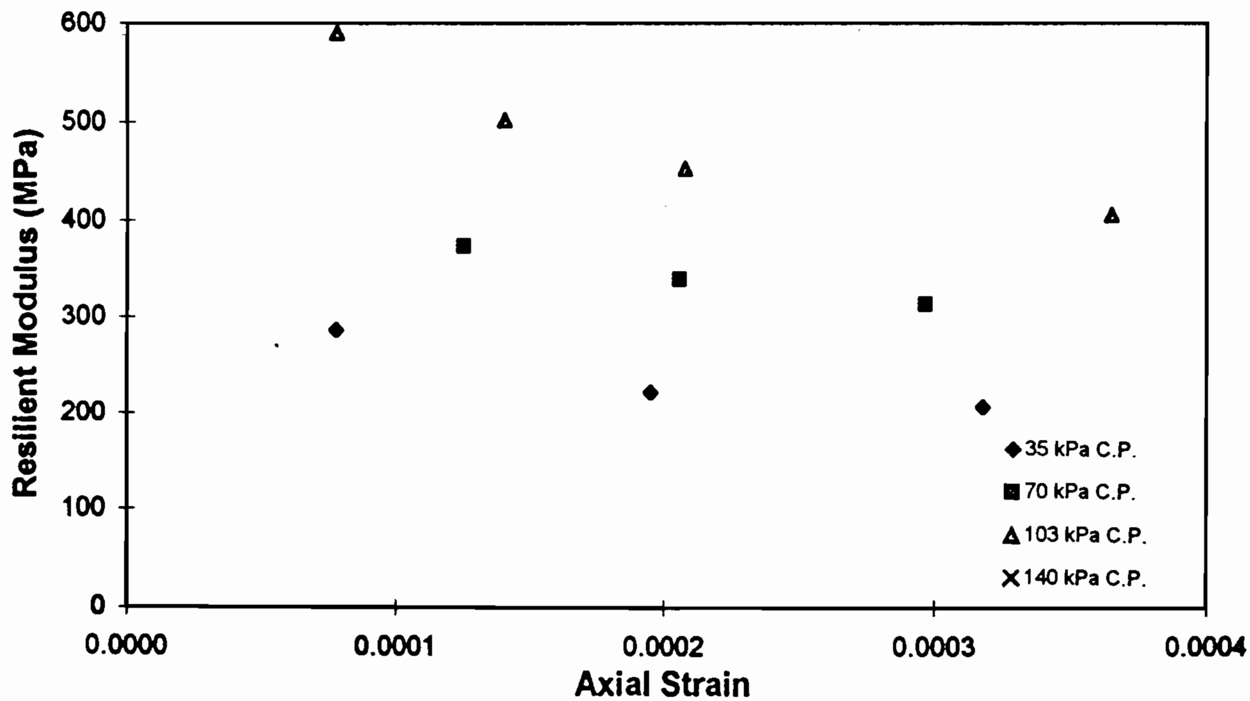

Resilient Modulus Tests Results from Lufkin District

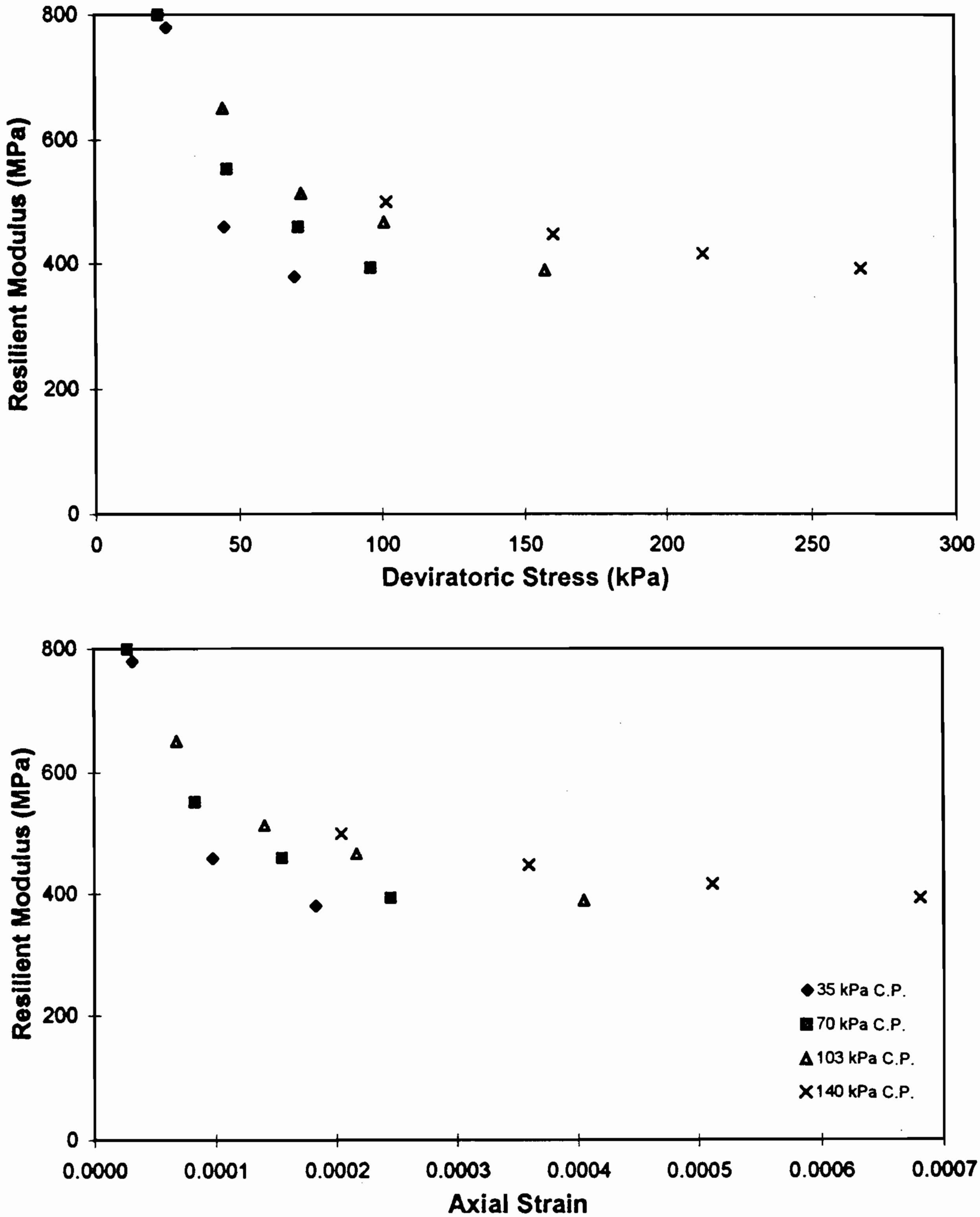

Resilient Modulus Tests Results from Odessa District

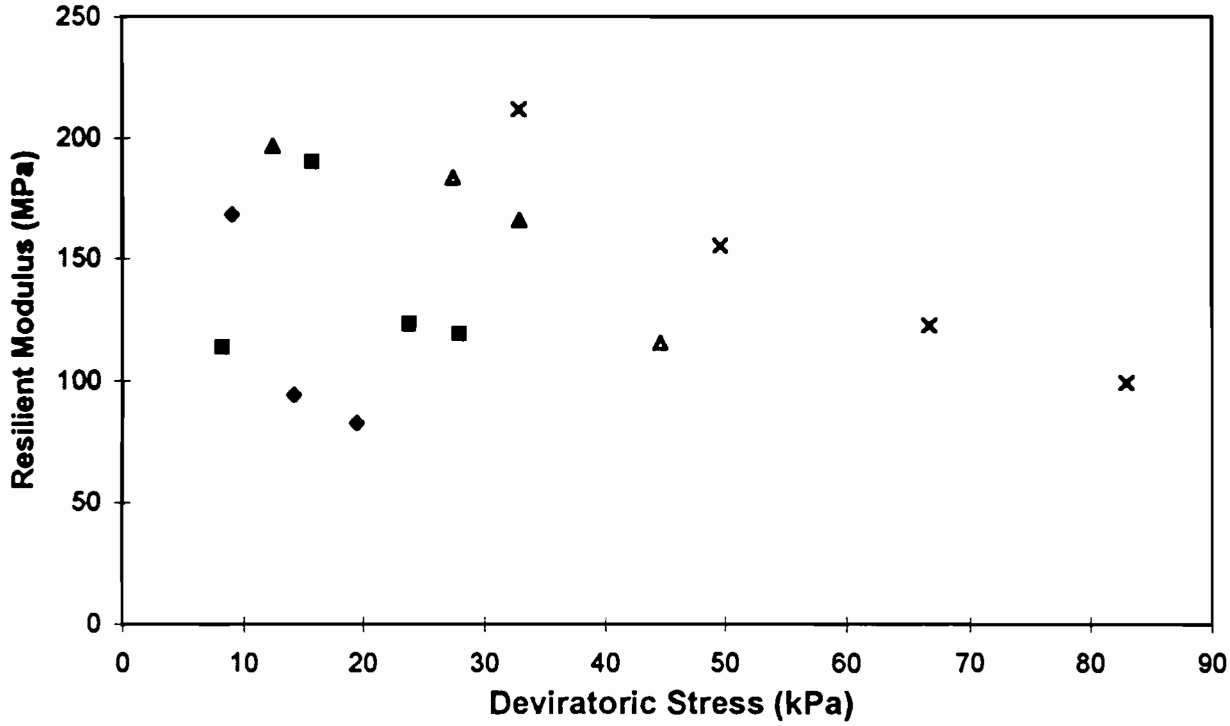

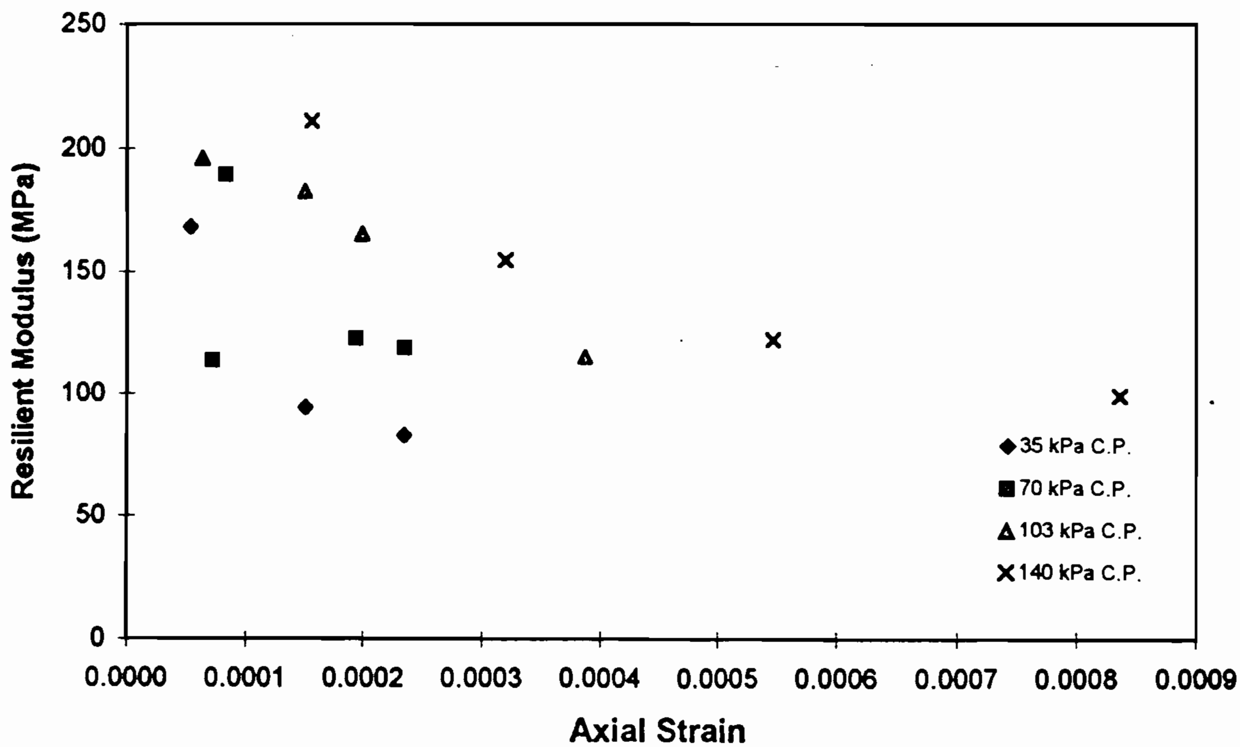

Resilient Modulus Tests Results from Paris District

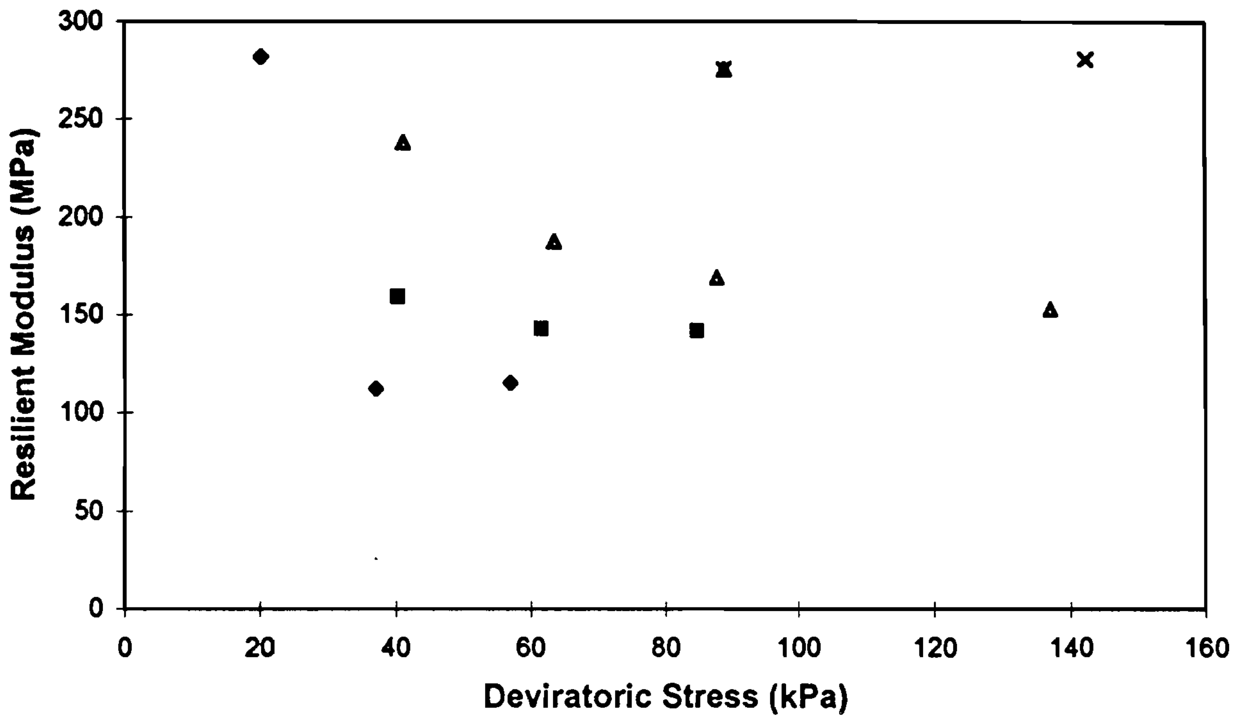

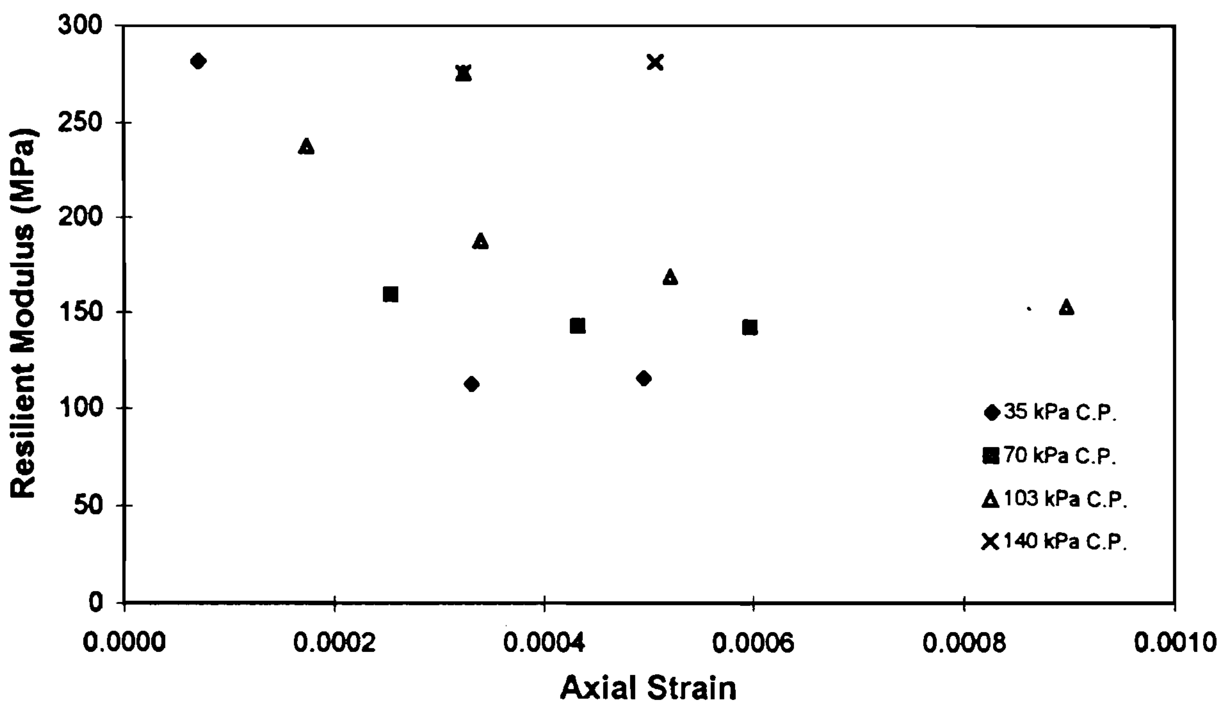

Resilient Modulus Tests Results from San Angelo District

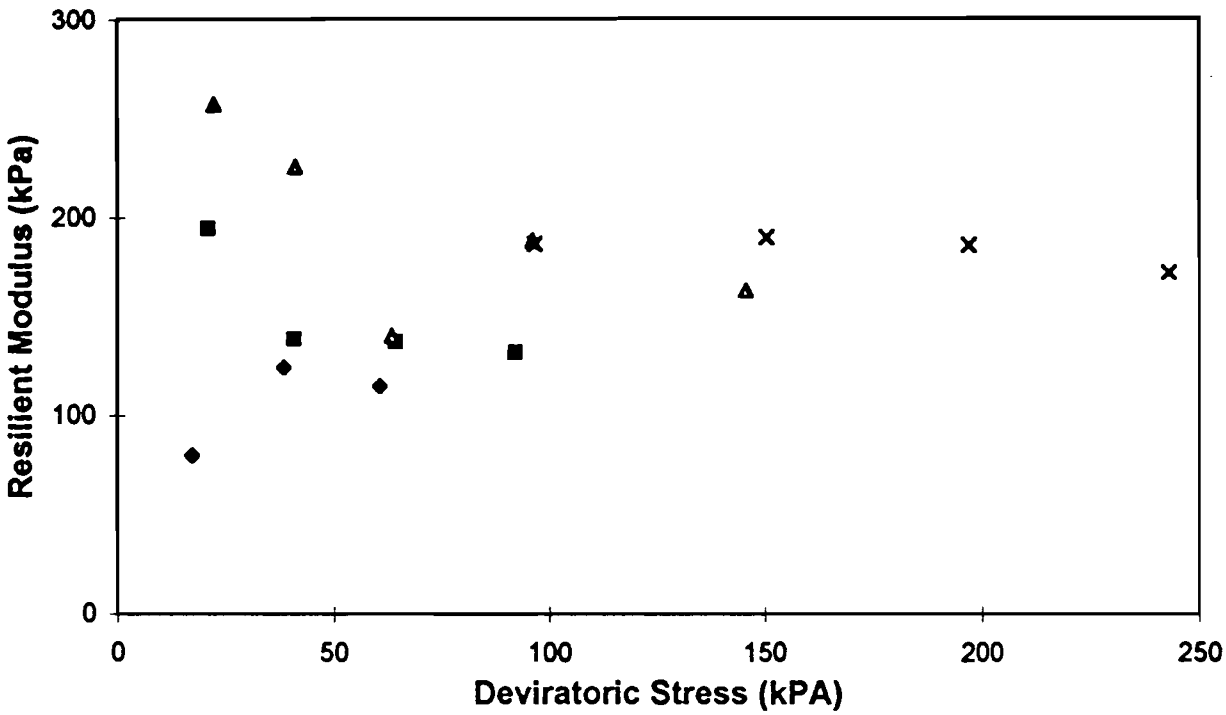

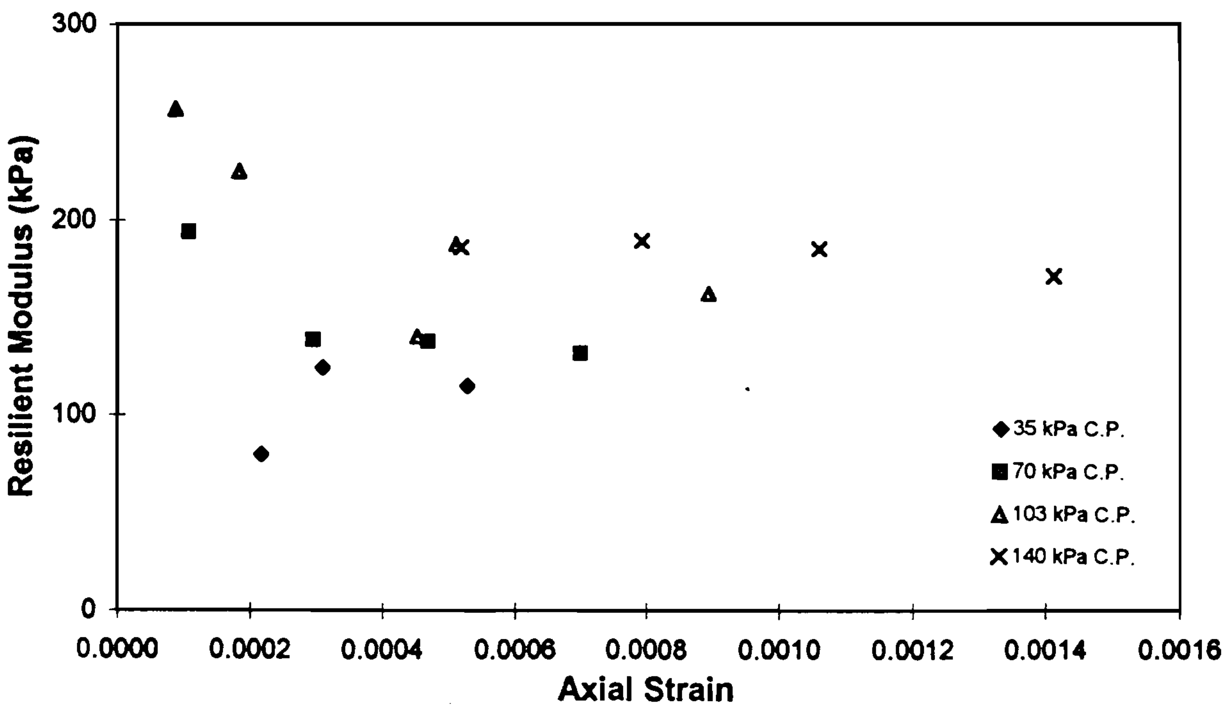

Resilient Modulus Tests Results from San Antonio District

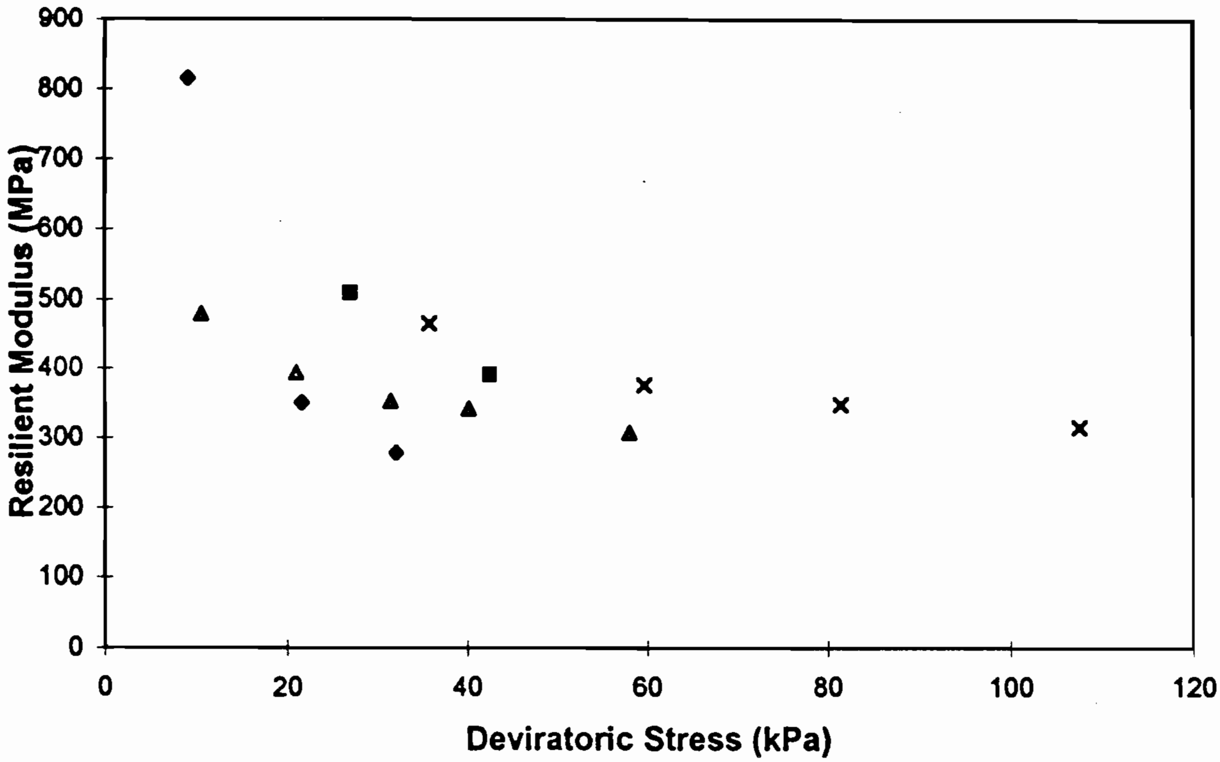

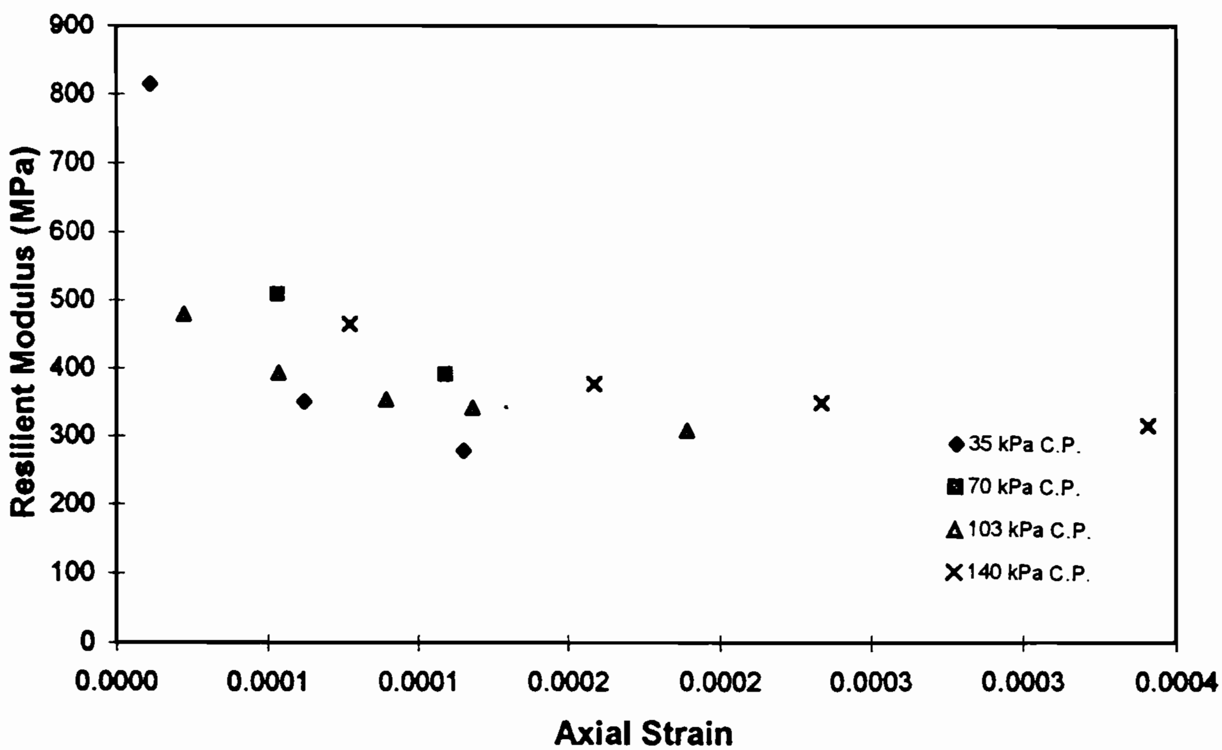

Resilient Modulus Tests Results from Tyler District

Appendix D

Dispersion Curves from SASW Tests

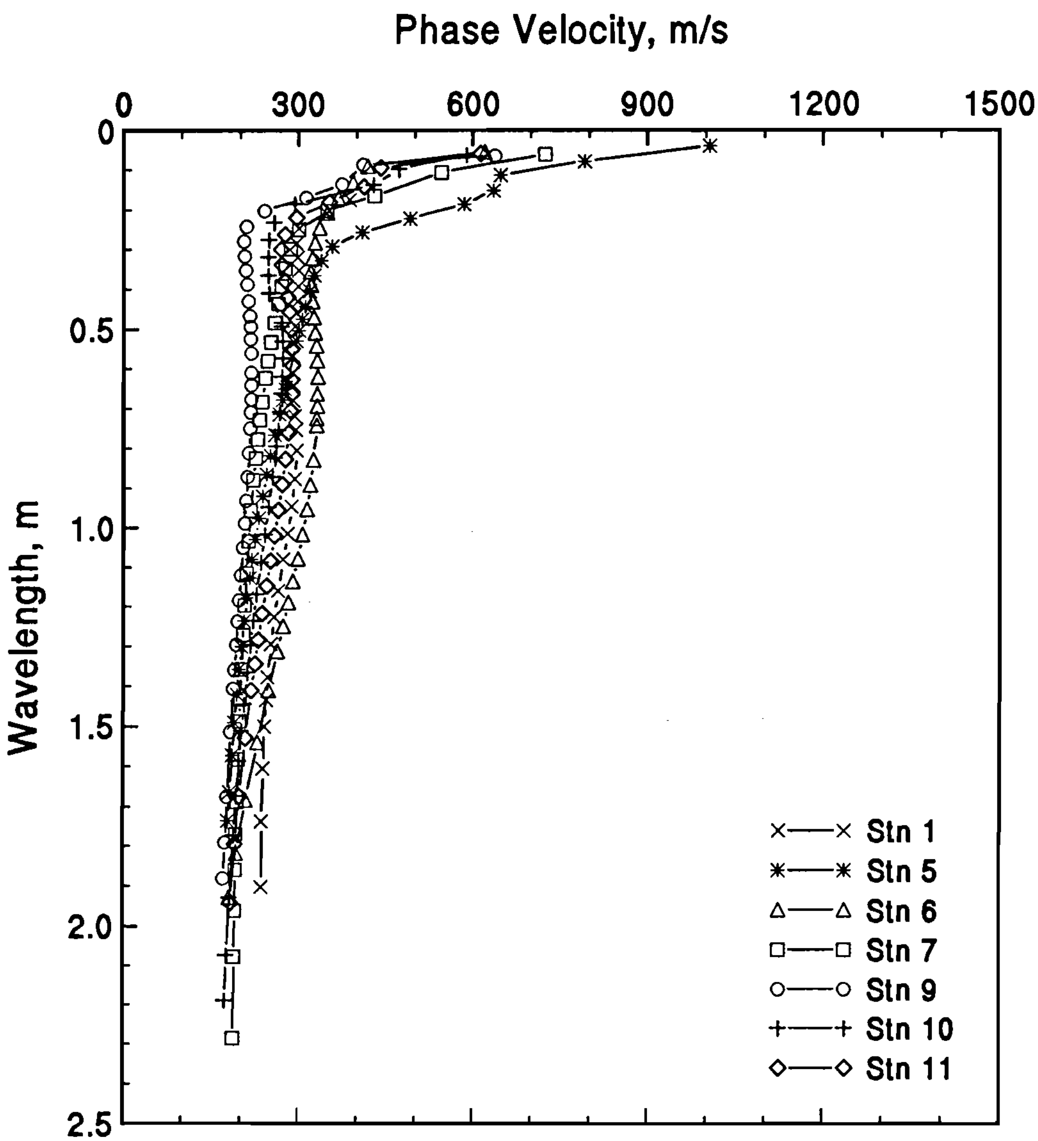

Brownwood Site

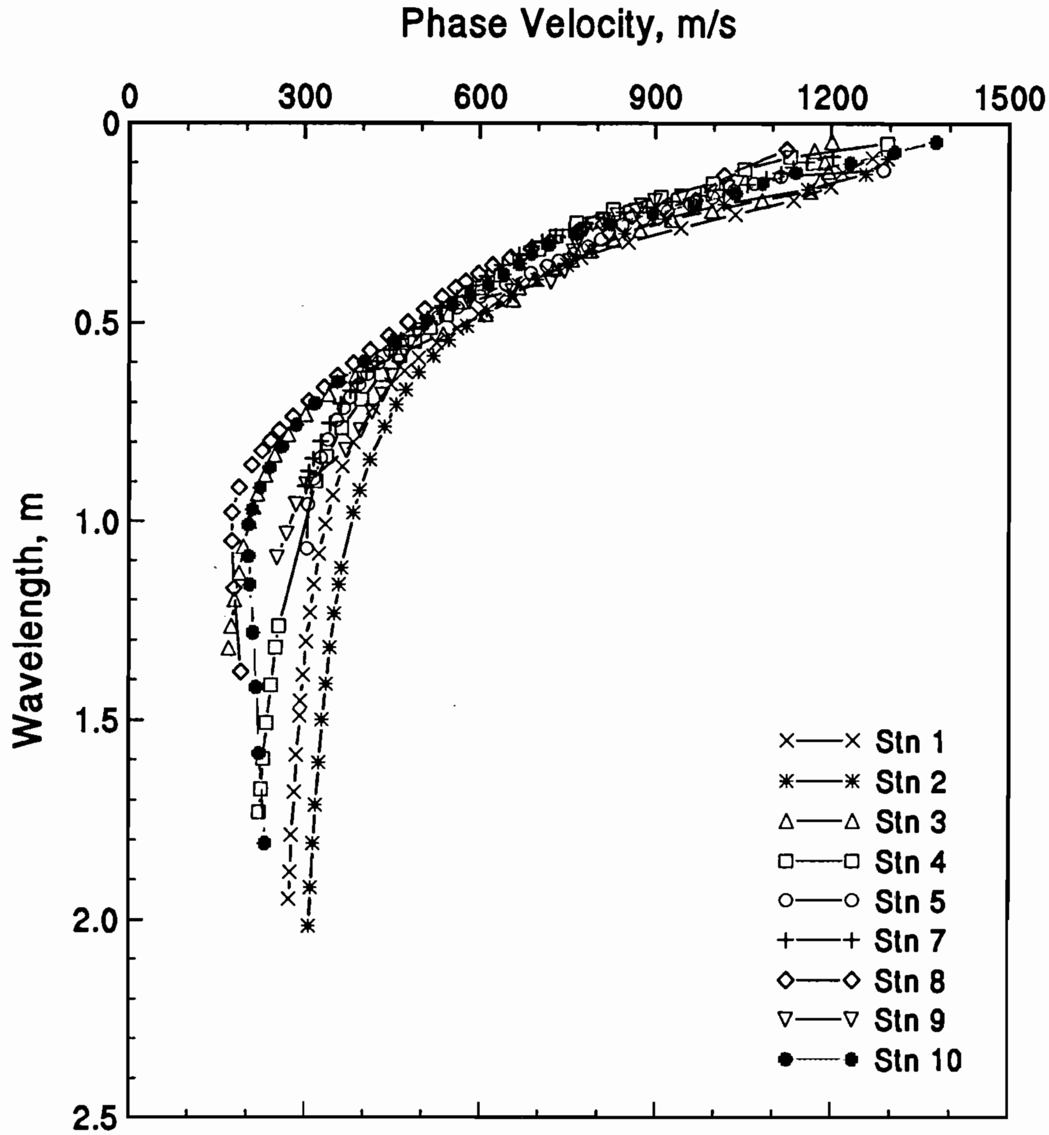

Childress Site

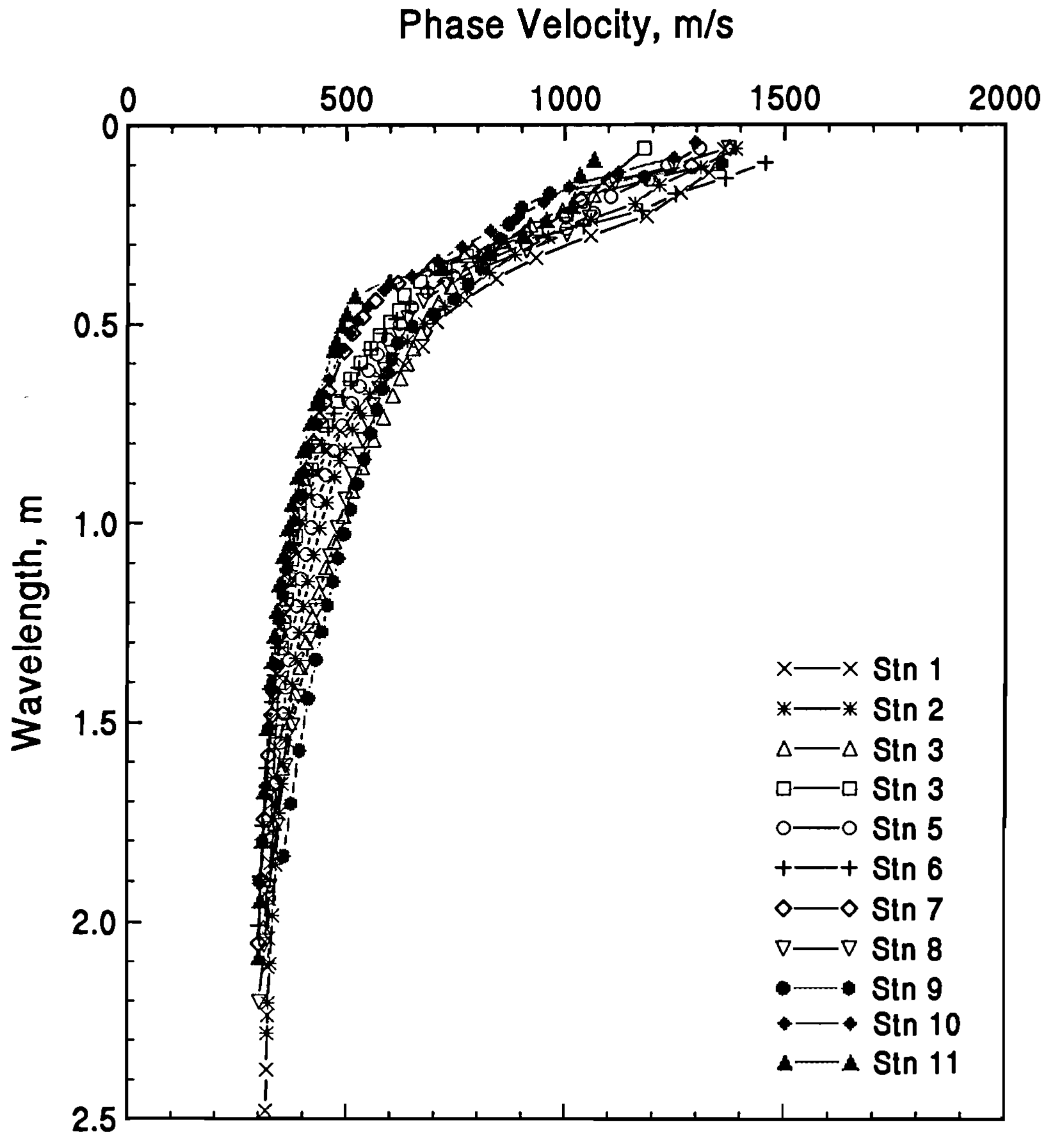

Corpus Christi Site

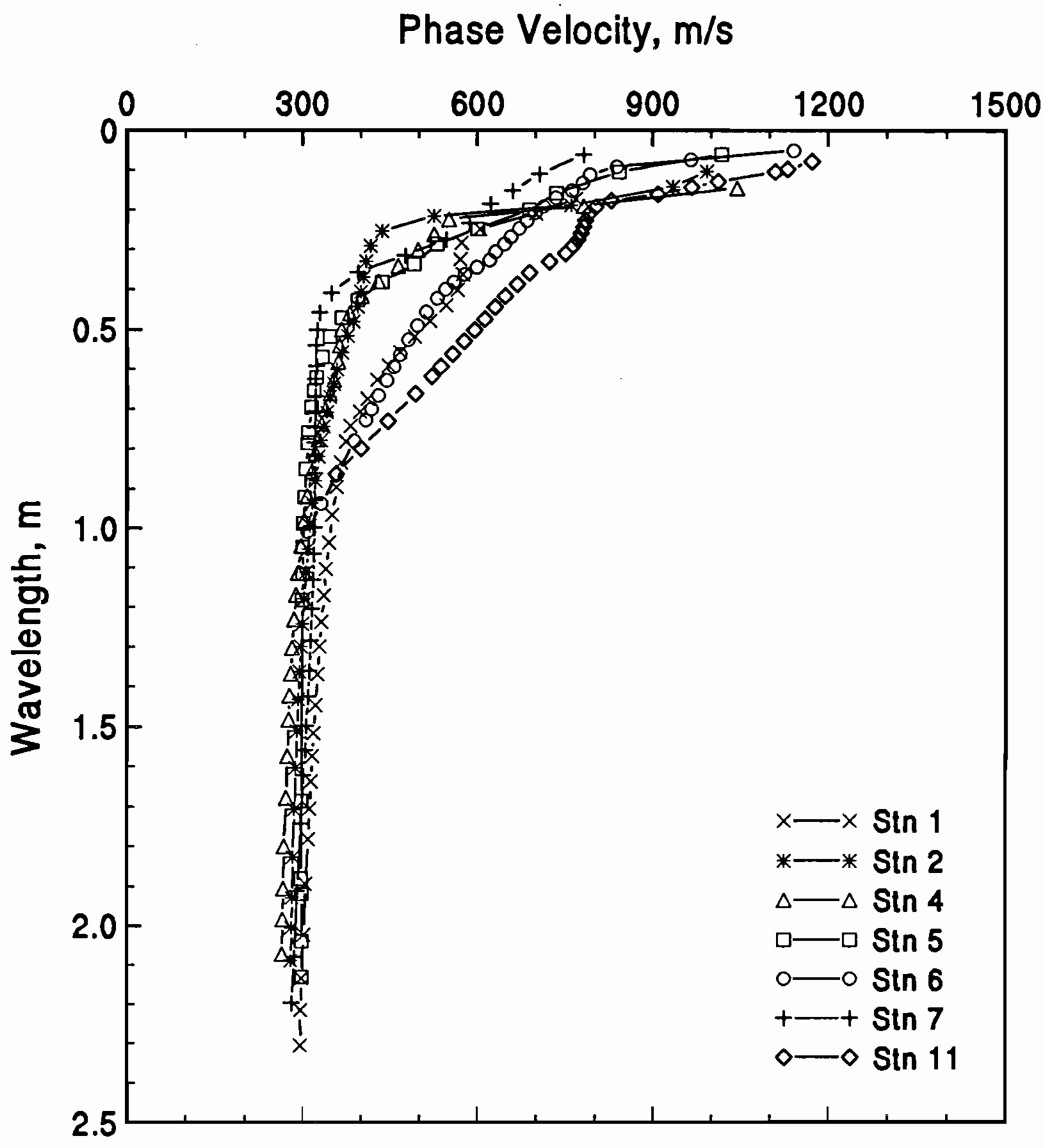
Phase Velocity, m/s
0
300
600
900
1200
1500
Wavelength, m
0
0.5
1.0
1.5
2.0
2.5
Stn 1
Stn 2
Stn 4
Stn 5
Stn 6
Stn 7
Stn 11

El Paso Site

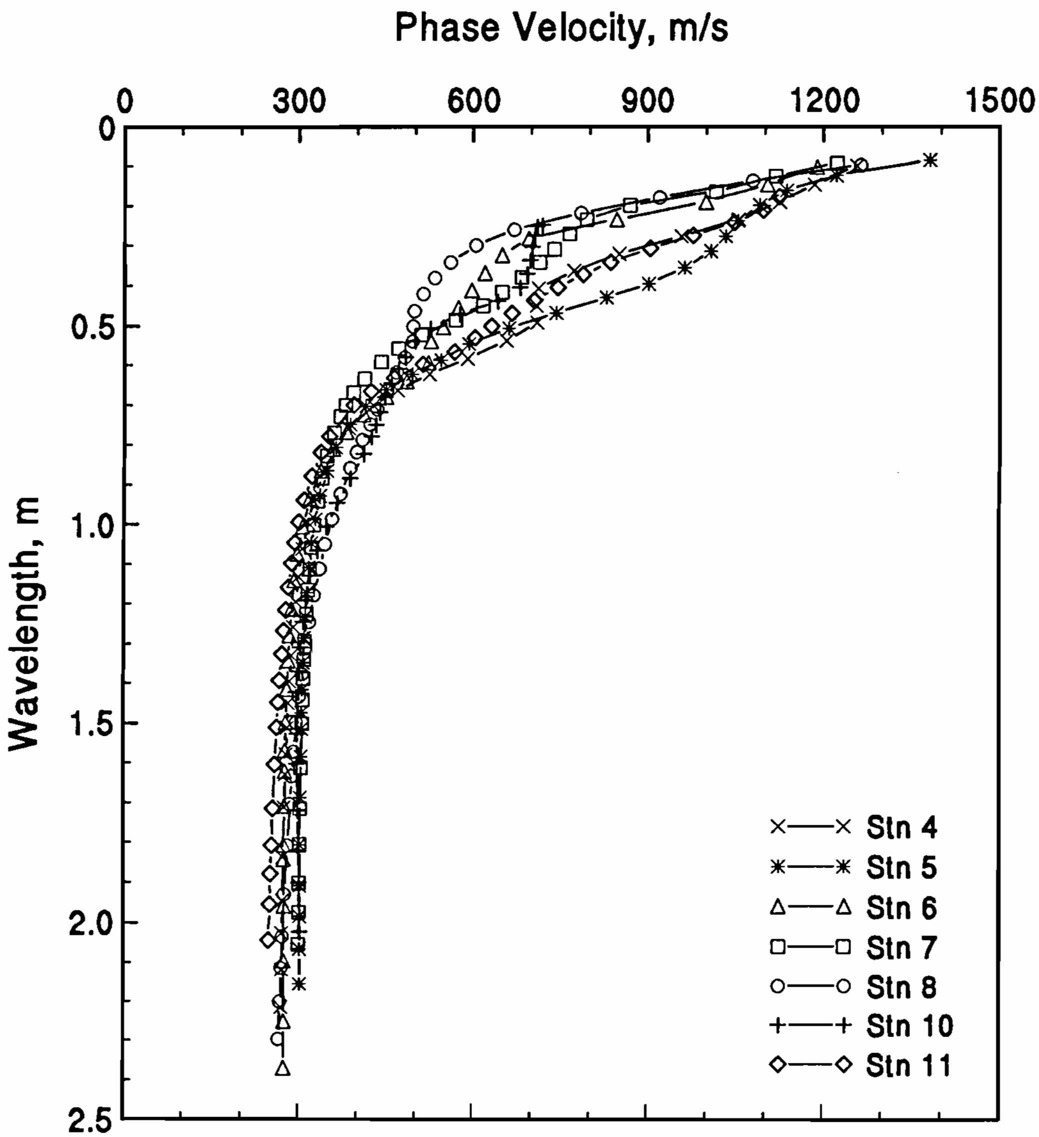

Phase Velocity, m/s
0
300
600
900
1200
1500
Wavelength, m
0
0.5
1.0
1.5
2.0
2.5
Stn 4
Stn 5
Stn 6
Stn 7
Stn 8
Stn 10
Stn 11

Lufkin Site

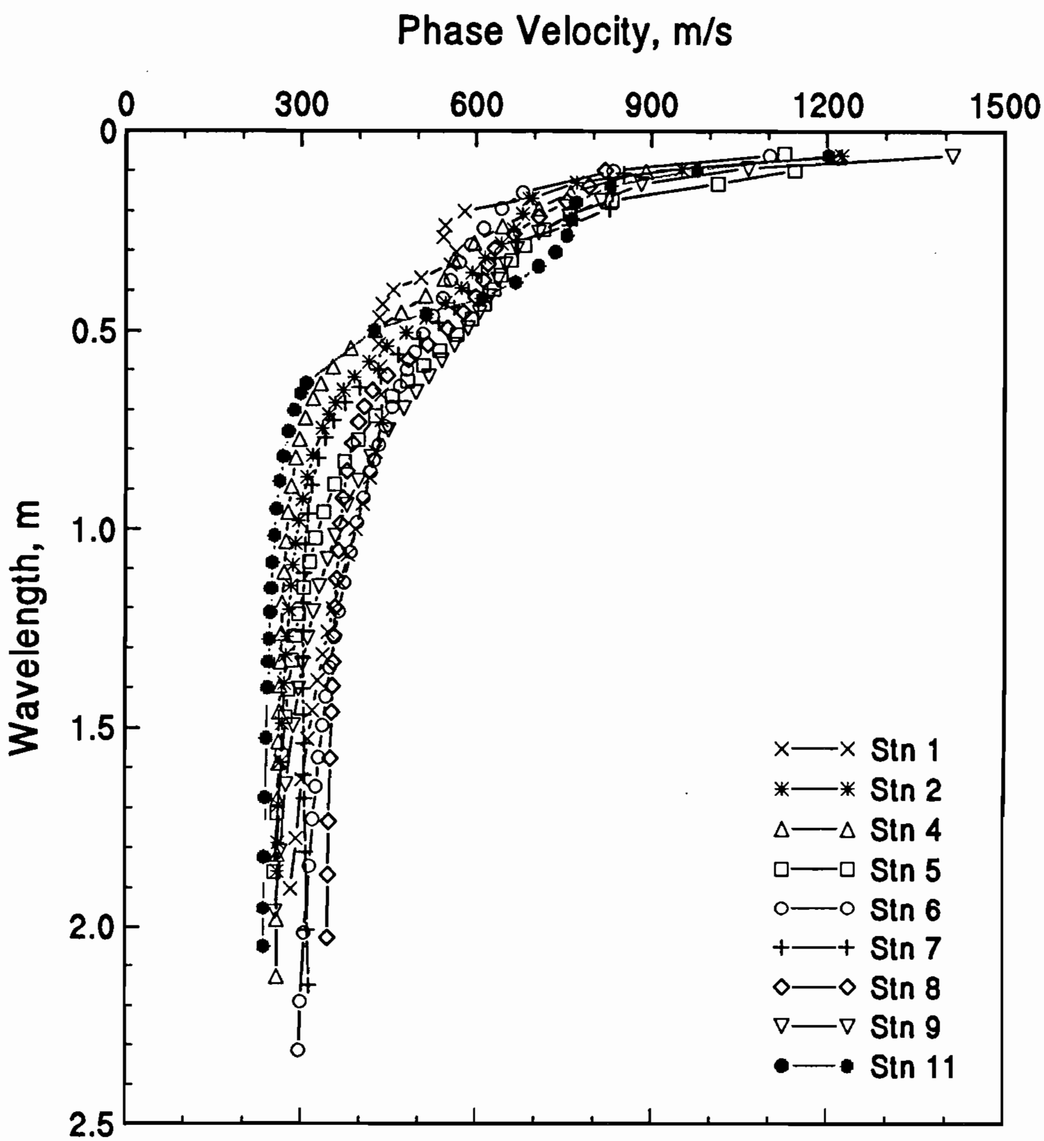

Phase Velocity, m/s
0
300
600
900
1200
1500
0
0.5
1.0
1.5
2.0
2.5
Wavelength, m
Stn 1
Stn 2
Stn 4
Stn 5
Stn 6
Stn 7
Stn 8
Stn 9
Stn 11

Odessa Site

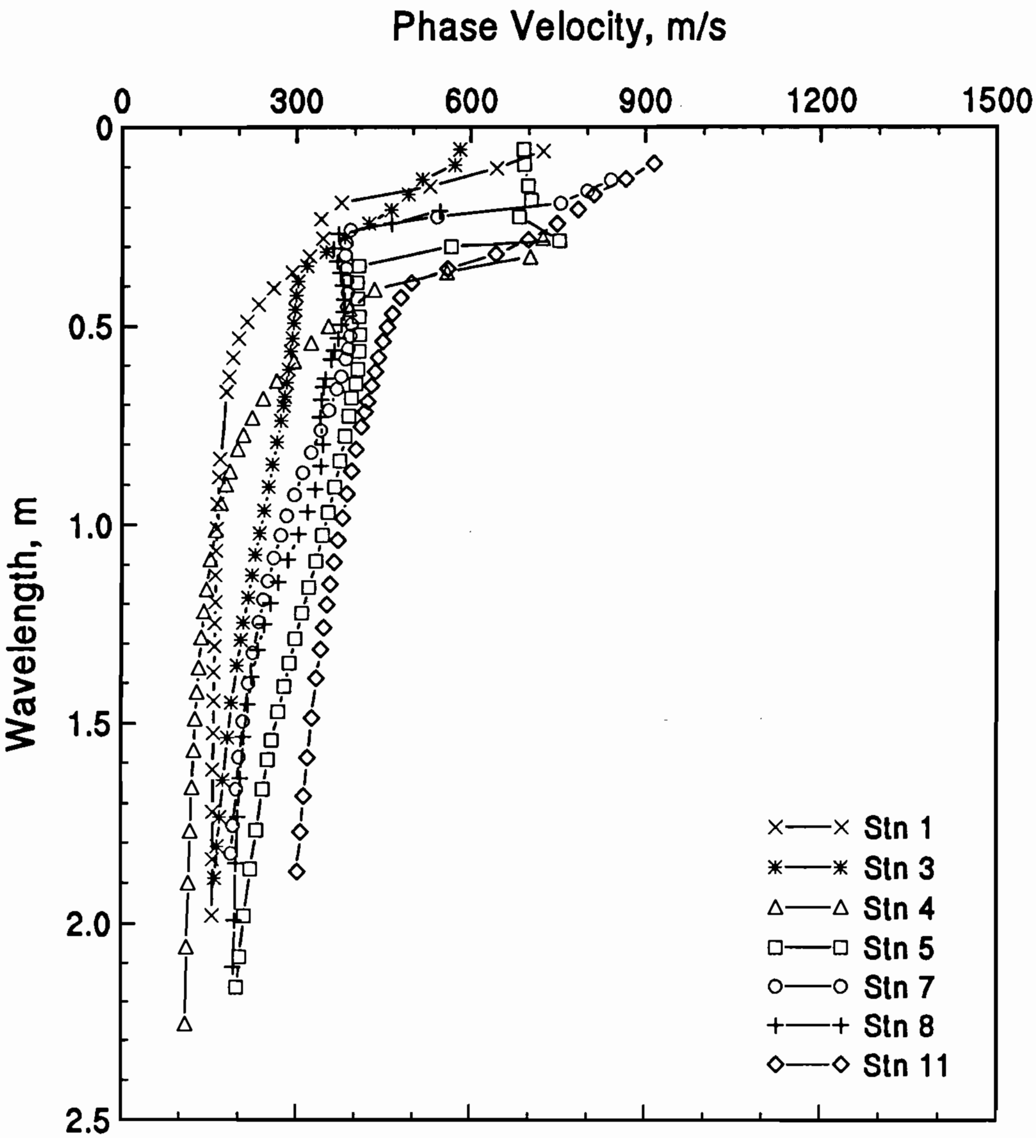

Phase Velocity, m/s
0
300
600
900
1200
1500
Wavelength, m
0
0.5
1.0
1.5
2.0
2.5
Stn 1
Stn 3
Stn 4
Stn 5
Stn 7
Stn 8
Stn 11

Paris Site

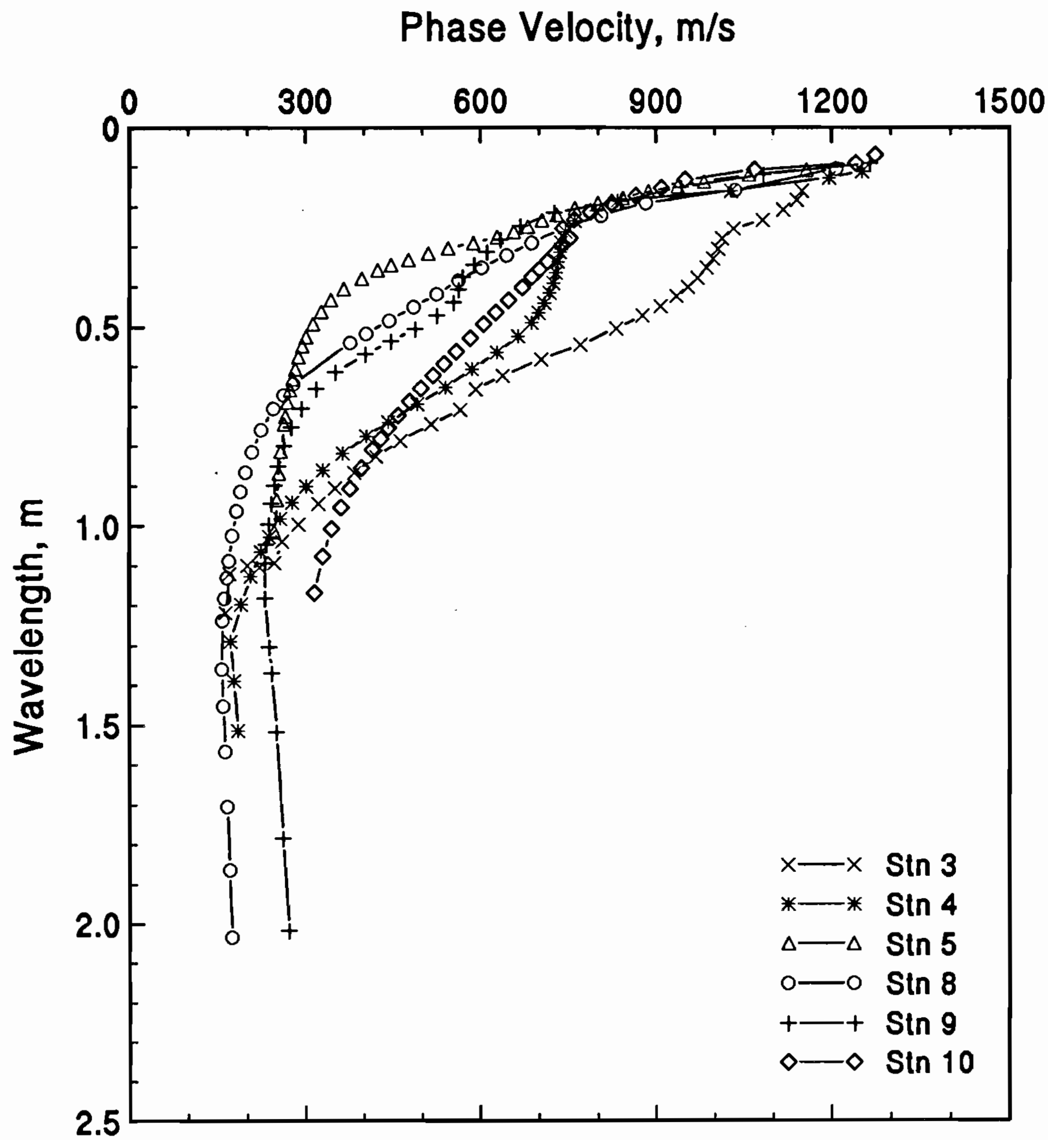

San Angelo Site

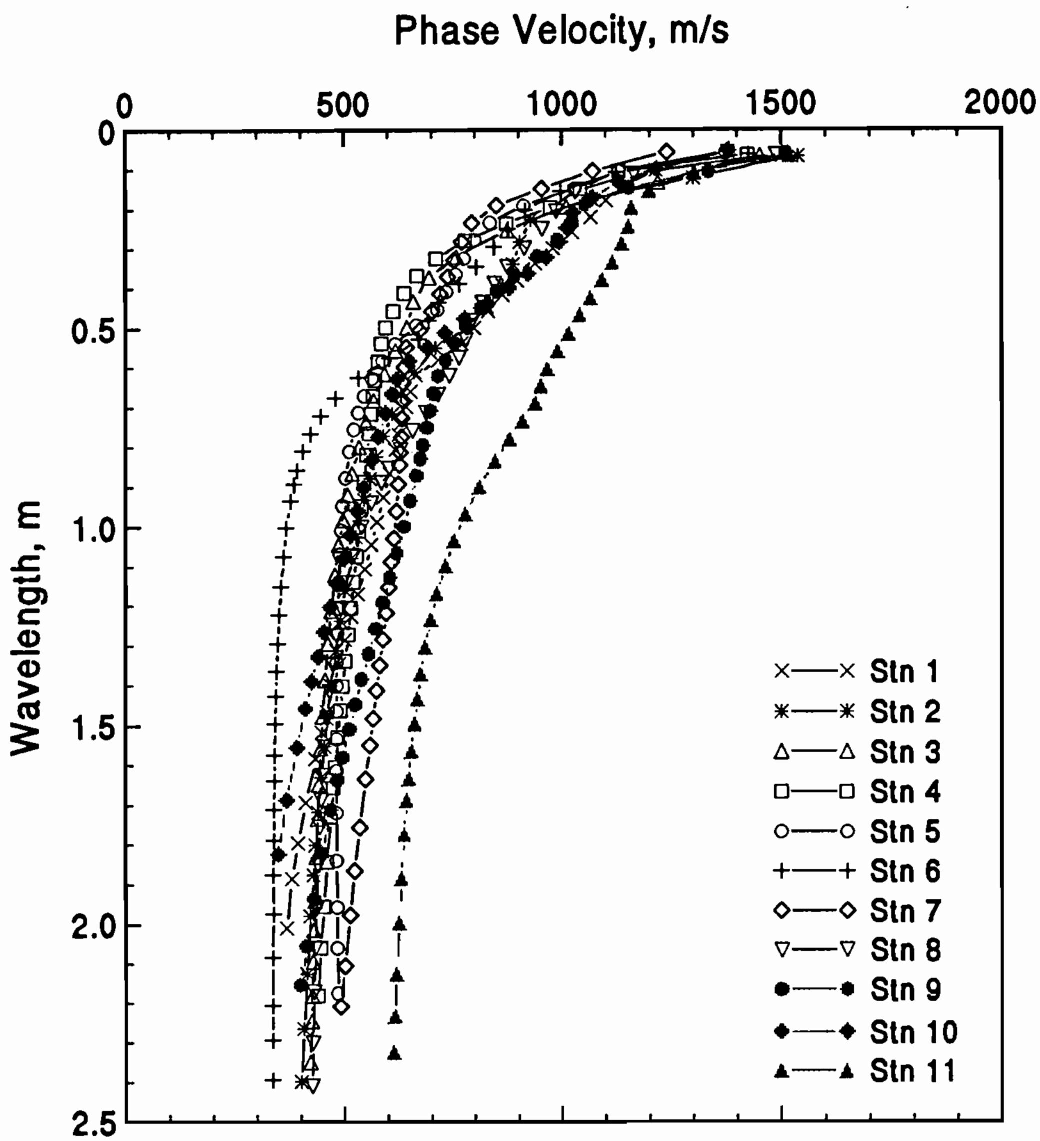

San Antonio Site

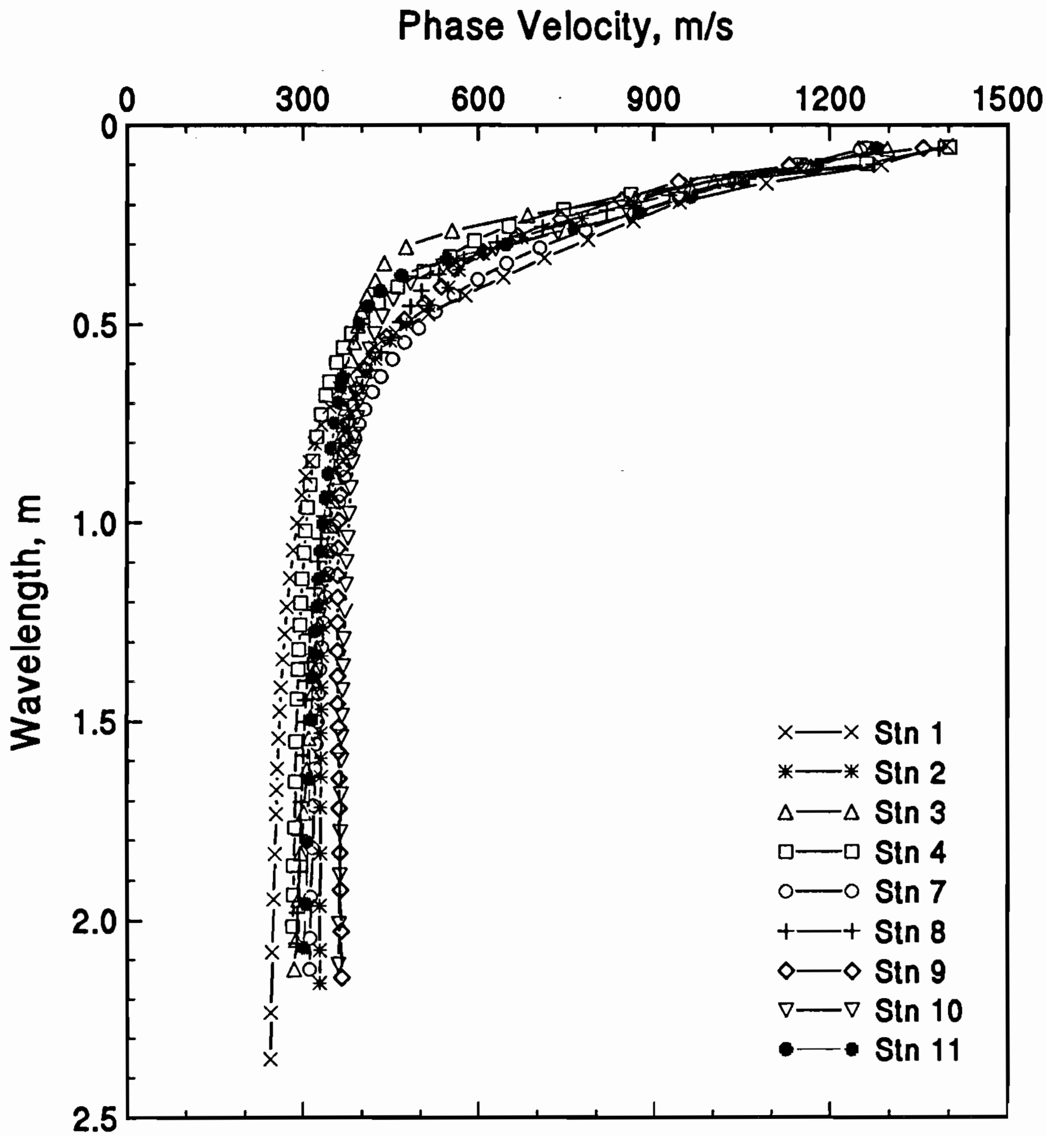
Phase Velocity, m/s
0
300
600
900
1200
1500
0
0.5
1.0
1.5
2.0
2.5
Wavelength, m
Stn 1
Stn 2
Stn 3
Stn 4
Stn 7
Stn 8
Stn 9
Stn 10
Stn 11

Tyler Site

Appendix E

Modulus Profiles from SASW Tests

BROWNWOOD

Station	AC-VS MPa	Base-VS MPa	Sub-VS MPa	AC-E MPa	Base-E MPa	Sub-E MPa	AC-H mm	Base-H mm
1	1288	340	202	9708	687	242	24	282
2	1346	349	213	10602	723	269	15	292
3	1392	320	254	11339	608	383	15	229
4	1341	253	206	10524	380	252	12	278
5	1357	272	233	10776	439	322	12	270
6	1285	287	247	9663	489	362	13	296
Mean	1335	304	226	10435	555	305	15	275
Std.Dev.	41.5	38.7	22.0	647.2	139.1	59.5	4.5	24.2
C.V.(%)	3.11	12.75	9.74	6.20	25.09	19.49	29.90	8.81

CORPUS CRISTI

Station	AC-VS MPa	Base-VS MPa	Sub-VS MPa	AC-E MPa	Base-E MPa	Sub-E MPa	AC-H mm	Base-H mm
1	1483	348	337	12870	719	675	97	203
2	1505	350	339	13255	728	683	97	133
3	1502	469	367	13202	1307	800	83	196
4	1428	388	353	11933	894	740	94	191
5	1435	386	333	12051	885	659	95	197
5.9	1477	404	328	12766	970	639	76	275
6	1519	377	320	13503	844	608	95	225
6.1	1469	397	322	12628	936	616	83	245
7	1490	371	344	12992	818	703	77	225
8	1432	402	372	12000	960	822	107	259
9	1480	450	355	12818	1203	749	99	220
10	1454	396	345	12372	931	707	73	213
11	1403	371	322	11519	818	616	91	195
Mean	1467	393	341	12608	924	694	90	214
Std.Dev.	34.7	34.7	16.9	594.0	168.2	69.1	10.4	35.6
C.V.(%)	2.37	8.82	4.94	4.71	18.20	9.97	11.53	16.64

CHILDRESS

Station	AC-VS MPa	Base-VS MPa	Sub-VS MPa	AC-E MPa	Base-E MPa	Sub-E MPa	AC-H mm	Base-H mm
1	1590	387	175	14794	890	182	57	192
2	1405	342	168	11552	695	168	65	168
3	1345	262	163	10586	408	158	68	158
4	1464	339	225	12543	683	301	63	220
5	1505	280	259	13255	466	398	65	217
6	1492	238	177	13027	336	186	51	192
7	1551	338	199	14078	679	235	64	234
8	1755	411	388	18024	1003	894	49	192
9	1588	402	287	14757	960	489	71	206
Mean	1522	333	227	13624	680	335	61	198
Std.Dev.	119.2	62.0	74.3	2162.3	241.1	238.9	7.5	24.5
C.V.(%)	7.83	18.61	32.74	15.87	35.47	71.41	12.24	12.41

SAN ANGELO

Station	AC-VS MPa	Base-VS MPa	Sub-VS MPa	AC-E MPa	Base-E MPa	Sub-E MPa	AC-H mm	Base-H mm
1	1477	266	185	12766.3	420	203	79	133
2	1491	444	303	13009.5	1171	545	52	176
3	1505	253	232	13254.9	380	320	58	192
4	1496	380	189	13096.9	858	212	52	177
5	1322	302	235	10227.4	542	328	57	146
6	1511	461	191	13360.8	1262	217	53	216
Mean	1467	351	223	12619	772	304	59	173
Std.Dev.	72.0	90.4	45.3	1189.7	384.0	130.6	10.4	30.2
C.V.(%)	4.91	25.74	20.35	9.43	49.72	42.93	17.72	17.43

EL PASO

Station	AC-VS MPa	Base-VS MPa	Sub-VS MPa	AC-E MPa	Base-E MPa	Sub-E MPa	AC-H mm	Base-H mm
1	1291	362	335	9753	778	667	66	272
2	1294	330	298	9799	647	527	52	256
3	1324	318	297	10258	601	524	53	216
4	1186	306	300	8231	556	535	59	241
5	1232	310	300	8882	571	535	62	290
6	1210	325	287	8568	627	489	74	265
7	1333	445	283	10398	1176	476	75	202
Mean	1267	342	300	9413	708	536	63	249
Std.Dev.	57.7	48.9	16.8	850.7	219.0	62.0	9.2	31.3
C.V.(%)	4.55	14.28	5.60	9.04	30.93	11.57	14.66	12.58

PARIS

Station	AC-VS MPa	Base-VS MPa	Sub-VS MPa	AC-E MPa	Base-E MPa	Sub-E MPa	AC-H mm	Base-H mm
1	1190	208	181	8287	257	195	25	272
2	1201	348	173	8441	719	178	18	222
3	1216	279	147	8653	462	128	20	244
4	1155	315	203	7807	589	245	20	250
5	1275	386	194	9513	885	224	19	237
6	1225	345	165	8782	707	162	24	267
7	1272	407	345	9468	984	707	45	303
Mean	1219	327	201	8707	658	263	24	256
Std.Dev.	43.3	67.4	66.1	618.6	247.6	199.7	9.4	26.7
C.V.(%)	3.55	20.62	32.84	7.10	37.64	76.08	38.61	10.42

LUFKIN

Station	AC-VS MPa	Base-VS MPa	Sub-VS MPa	AC-E MPa	Base-E MPa	Sub-E MPa	AC-H mm	Base-H mm
1	1465	292	237	12560	506	334	94	294
2	1449	273	260	12287	443	402	86	317
3	1358	301	280	10792	538	466	90	259
4	1351	298	238	10681	527	336	87	367
5	1345	308	233	10586	563	322	102	312
6	1386	291	283	11242	503	476	89	195
7	1310	303	292	10043	545	506	98	291
8	1441	255	226	12152	386	303	103	303
Mean	1388	290	256	11293	502	393	94	292
Std.Dev.	56.9	17.7	26.0	927.4	59.2	80.0	6.7	49.7
C.V.(%)	4.10	6.11	10.15	8.21	11.81	20.35	7.15	17.00

SAN ANTONIO

Station	AC-VS MPa	Base-VS MPa	Sub-VS MPa	AC-E MPa	Base-E MPa	Sub-E MPa	AC-H mm	Base-H mm
1	1644	562	393	15816	1876	917	65	272
2	1635	608	338	15644	2196	679	59	245
3	1607	552	398	15112	1810	941	63	253
4	1514	536	425	13414	1707	1073	65	270
5	1530	564	400	13699	1889	950	60	246
5.9	1511	415	296	13361	1023	520	69	245
6.1	1504	417	363	13237	1033	783	64	267
7	1516	651	474	13449	2517	1335	60	248
8	1583	582	483	14664	2012	1386	72	259
9	1622	687	477	15396	2803	1352	69	248
10	1605	650	351	15075	2510	732	67	231
11	1655	712	573	16029	3011	1950	70	292
Mean	1577	578	414	14575	2032	1051	65	256
Std.Dev.	58.2	93.7	76.8	1073.0	622.4	396.1	4.3	16.5
C.V.(%)	3.69	16.22	18.54	7.36	30.63	37.67	6.54	6.42

ODESSA

Station	AC-VS MPa	Base-VS MPa	Sub-VS MPa	AC-E MPa	Base-E MPa	Sub-E MPa	AC-H mm	Base-H mm
1	1337	433	309	10461	1114	567	37	223
2	1438	574	294	12101	1957	513	38	148
3	1453	503	267	12355	1503	423	39	146
4	1381	584	262	11161	2026	408	31	142
5	1313	595	335	10089	2103	667	40	165
6	1474	590	284	12714	2068	479	34	166
7	1335	529	370	10430	1662	813	36	203
8	1409	656	304	11618	2556	549	39	174
9	1350	635	321	10665	2395	612	42	164
10	1410	653	263	11634	2533	411	43	126
Mean	1390	575.2	300.9	11322.8	1992	544	38	166
Std.Dev.	55.3	70.3	34.7	901.5	461	129	4	29
C.V.(%)	3.98	12.21	11.54	7.96	23	24	10	18

TYLER

Station	AC-VS MPa	Base-VS MPa	Sub-VS MPa	AC-E MPa	Base-E MPa	Sub-E MPa	AC-H mm	Base-H mm
1	1533	386	255	13753	885	386	66	268
2	1414	347	304	11700	715	549	61	197
3	1402	342	248	11503	695	365	64	233
4	1455	350	269	12389	728	430	66	205
5	1680	725	406	16517	3122	979	75	237
6	1629	739	392	15529	3244	913	71	257
6.1	1607	790	365	15112	3707	791	80	268
7	1470	395	286	12646	927	486	66	276
8	1413	382	236	11684	867	331	64	267
9	1472	363	333	12680	783	659	58	256
10	1468	360	346	12611	770	711	56	270
11	1482	331	321	12853	651	612	55	262
Mean	1502	459	313	13248	1424	601	65	250
Std.Dev.	91.0	177.8	56.7	1637.4	1176.0	215.7	7.5	26.2
C.V.(%)	6.06	38.71	18.10	12.36	82.56	35.89	11.44	10.48

Appendix F

Deflections from FWD Tests

BROWNWOOD

Station	Load	Measured Deflection (microns):						
	(KN)	R1	R2	R3	R4	R5	R6	R7
1	47	463.8	227.3	122.2	77.2	54.4	40.6	32.5
2	47	439.9	205.7	124.2	82.3	57.7	46.7	35.3
3	45	484.4	246.9	133.9	89.7	66.0	53.6	42.2
4	44	427.5	184.2	113.8	78.2	59.7	50.5	36.3
5	46	453.4	178.8	101.1	70.1	53.3	41.7	34.5
6	45	369.3	168.9	100.1	68.8	51.1	40.6	33.5
7	46	526.0	239.3	133.9	83.3	56.4	50.5	35.3
8	44	567.4	265.4	135.9	80.3	56.4	48.8	39.4
9	43	638.0	315.2	157.0	93.7	68.3	56.6	44.2
10	43	645.2	302.3	154.9	99.8	68.3	54.6	43.2
11	44	542.5	256.8	128.5	80.3	55.4	44.7	34.5
Mean:		505.2	235.5	127.8	82.0	58.9	48.0	37.3
Std.Dev.		91.1	51.1	19.5	9.7	6.2	5.4	4.0
Var Coeff(%):		18.0	21.7	15.2	11.8	10.5	11.3	10.8

CORPUS CRISTI

Station	Load	Measured Deflection (microns):						
	(KN)	R1	R2	R3	R4	R5	R6	R7
1	39	426.7	249.4	149.4	108.0	85.1	67.3	54.6
2	40	333.0	194.8	121.9	87.6	69.1	53.8	41.9
3	41	234.7	153.7	115.6	90.4	73.7	59.2	49.3
4	40	389.4	194.8	115.6	86.1	68.8	55.1	46.7
5	40	287.5	164.3	115.6	93.5	76.7	61.5	50.0
6	39	421.4	237.2	168.1	128.0	101.3	78.5	62.0
7	39	479.8	303.3	186.7	127.8	99.8	75.9	59.4
8	39	465.8	264.7	179.3	134.9	103.6	80.8	62.5
9	39	403.6	259.8	187.7	140.5	108.0	82.3	64.3
10	40	317.8	210.6	145.5	106.4	81.0	65.8	52.1
11	39	292.1	173.5	113.8	83.8	68.3	56.4	48.3
12	39	395.7	241.8	146.8	99.3	76.7	59.9	50.5
13	43	475.7	311.4	183.4	119.6	89.4	69.3	56.9
Mean:		378.7	227.6	148.3	108.2	84.8	66.5	53.8
Std.Dev.		79.0	50.5	30.0	20.1	14.2	10.2	6.9
Var Coeff(%):		20.9	22.2	20.2	18.5	16.8	15.3	12.7

EL PASO

Station	Load	Measured Deflection (microns):						
	(KN)	R1	R2	R3	R4	R5	R6	R7
1	41	349.0	164.1	78.2	52.1	39.6	31.8	23.1
2	40	446.5	202.7	89.9	58.9	46.0	34.3	23.9
3	41	278.4	128.5	65.8	48.3	39.4	33.3	24.1
4	40	358.1	165.9	70.4	48.0	37.8	30.0	22.1
5	40	288.8	133.4	63.0	42.9	33.8	30.7	20.8
6	40	379.7	153.9	74.7	52.1	40.9	34.0	22.9
7	40	490.7	224.3	94.5	63.5	49.5	41.1	27.7
8	40	419.4	190.0	80.8	54.4	45.0	35.3	25.7
9	40	411.5	184.4	86.4	57.4	45.7	32.5	22.1
10	40	503.7	258.3	108.7	64.5	49.0	40.9	29.2
11	40	349.8	169.4	78.5	52.3	40.9	33.3	22.4
12	40	439.7	197.6	88.9	58.2	44.2	33.8	25.7
13	40	279.1	123.7	65.8	48.8	40.9	33.8	27.2
14	40	381.8	151.9	67.8	46.7	37.6	31.0	24.4
15	40	289.8	133.1	63.8	41.9	34.5	29.7	22.6
16	41	569.7	276.1	115.6	71.1	54.1	40.4	28.2
17	39	558.0	273.8	115.8	69.6	51.1	39.6	27.7
Mean:		377.7	172.0	78.5	52.6	41.7	33.8	24.1
Std.Dev.		93.05	49.38	17.49	8.69	5.80	3.81	2.55
Var Coeff(%):		19.67	22.14	16.86	12.99	11.54	10.1	9.83

PARIS

Station	Load	Measured Deflection (microns):						
	(KN)	R1	R2	R3	R4	R5	R6	R7
1	40	1081.0	581.7	274.8	169.9	119.4	83.8	79.2
2	29	540.0	323.9	189.0	124.2	90.4	68.6	54.6
3	40	714.2	374.9	208.8	135.4	97.8	75.4	58.4
4	40	959.9	413.0	180.3	111.8	84.1	65.3	47.5
5	42	715.5	310.4	155.4	114.3	88.4	68.6	55.1
Mean:		802.1	400.8	201.7	131.1	96.0	72.3	59.0
Std.Dev.		216.0	109.1	45.2	23.6	14.0	7.4	12.0
Var Coeff(%):		26.9	27.2	22.4	18.0	14.6	10.2	20.4

LUFKIN

Station	Load (KN)	Measured Deflection (microns):						
		R1	R2	R3	R4	R5	R6	R7
1	42	485.9	281.2	133.4	81.0	58.4	47.0	38.6
2	42	477.3	289.3	146.3	82.8	56.9	43.2	38.6
3	41	472.9	285.5	149.4	83.8	55.6	45.0	35.3
4	41	477.3	295.7	150.1	84.6	56.6	43.4	32.5
5	41	438.4	267.5	133.6	71.9	44.5	33.8	23.9
6	40	642.6	385.1	185.2	109.7	77.0	62.0	47.5
7	40	685.0	430.0	247.9	153.4	100.1	74.2	57.7
8	40	677.9	431.0	248.4	154.7	100.8	76.7	59.7
9	41	405.1	248.4	140.7	91.7	64.3	47.5	36.6
10	40	400.8	248.2	141.2	91.4	64.5	48.3	35.6
11	39	693.9	392.4	200.4	118.1	80.3	59.7	45.0
12	40	545.6	300.0	161.8	101.1	70.4	51.8	38.1
13	39	644.4	413.3	216.9	123.2	79.5	58.9	43.7
Mean:		542.0	328.2	173.5	103.6	69.9	53.1	40.9
Std.Dev.		111.3	70.4	42.2	26.9	17.0	12.4	9.9
Var Coeff(%):		20.51	21.43	24.24	26.01	24.45	23.6	24

SAN ANTONIO

Station	Load (KN)	Measured Deflection (microns):						
		R1	R2	R3	R4	R5	R6	R7
1	40	193.0	114.8	78.0	55.6	41.4	31.5	23.1
2	40	144.3	68.6	39.4	24.1	18.3	13.2	9.9
3	41	175.0	67.8	34.8	23.1	18.0	14.2	11.9
4	40	155.2	57.7	26.9	18.3	15.7	12.4	10.2
5	40	181.1	86.1	53.1	38.6	30.2	22.9	16.8
6	40	195.8	148.6	109.0	58.4	42.4	31.5	24.4
7	40	179.3	65.0	30.7	21.1	17.3	13.7	11.2
8	40	131.8	49.8	31.5	21.8	17.0	12.7	9.9
9	40	112.3	64.8	40.4	27.4	20.3	14.5	9.9
10	40	138.7	74.4	47.2	30.0	20.6	14.0	9.4
Mean:		160.5	79.8	49.0	31.8	24.1	18.0	13.7
Std.Dev.		28.3	30.1	25.7	14.4	10.2	7.7	5.7
Var Coeff(%):		17.6	37.7	52.5	45.5	42.3	42.6	41.8

ODESSA

Station	Load (KN)	Measured Deflection (microns):						
		R1	R2	R3	R4	R5	R6	R7
1	42	195.1	101.6	59.9	36.8	27.9	21.6	17.5
2	41	275.1	145.8	75.2	47.2	34.3	26.4	22.9
3	40	326.4	147.3	69.3	42.9	33.5	24.6	23.9
4	41	353.3	152.4	66.0	42.2	32.0	26.2	22.4
5	40	277.9	129.5	68.3	46.0	38.6	29.2	22.9
6	40	274.8	124.7	59.2	38.6	30.7	26.4	18.8
7	41	248.2	113.8	55.9	39.9	29.5	22.6	18.3
8	39	231.1	114.0	55.9	33.0	26.4	20.3	16.8
9	40	206.0	105.2	56.9	35.3	23.6	18.8	15.0
10	40	262.6	146.6	66.8	39.9	27.7	22.6	19.6
Mean:		265.2	128.0	63.2	40.1	30.5	23.9	19.8
Std.Dev.		49.1	19.0	6.7	4.5	4.4	3.2	3.0
Var Coeff(%):		18.5	14.9	10.6	11.3	14.3	13.5	15.3

Tyler

Station	Load (KN)	Measured Deflection (microns):						
		R1	R2	R3	R4	R5	R6	R7
1	41	299.5	157.2	66.3	35.3	23.6	17.0	13.5
2	38	295.4	141.5	58.9	33.3	22.6	16.0	13.5
3	38	303.5	138.2	56.9	32.3	21.6	17.0	13.5
4	38	394.5	176.0	62.0	35.3	24.4	18.0	15.5
5	39	437.1	215.9	80.0	43.7	29.5	21.3	17.8
6	39	398.5	190.8	71.6	37.3	23.6	18.0	14.5
7	38	362.2	150.9	42.2	21.8	18.5	15.0	12.4
8	39	318.3	135.1	42.2	26.9	22.6	19.1	16.5
9	38	404.9	208.5	84.1	48.8	34.3	25.7	20.8
Mean:		357.1	168.1	62.7	35.1	24.6	23.9	15.2
Std.Dev.		54.0	30.8	14.8	8.1	4.7	3.2	2.7
Var Coeff(%):		15.1	18.3	23.5	23.0	18.9	13.5	17.5

Appendix G

Modulus Profiles from FWD Tests

BROWNWOOD

Station	Calculated Moduli Values (ksi):					Absolute Dpth to Bedrock
	SURF(E1)	BASE(E2)	SUBB(E3)	SUBG(E4)	ERR/Sens	
1	2069	561	0	150	2.01	300
2	2069	633	0	144	4.02	299.47
3	2069	556	0	125	4.95	300
4	2069	616	0	146	9.31	300
5	2069	525	0	173	8.66	300
6	2069	738	0	167	6.99	300
7	2069	462	0	137	3.79	224.72
8	2069	387	0	130	5.47	176.36
9	2069	347	0	109	5.8	197.46
10	2069	337	0	108	3.33	253.32
11	2069	412	0	134	4.18	265.71
Mean:	2069	507	0	139	5.32	275.1
Std.Dev.	0.0	134.8	0.0	21.5	2.25	78.47
Var Coeff(%):	0.0	26.6	0.0	15.5	42.27	28.52

CORPUS CRISTI

Station	Calculated Moduli Values (ksi):					Absolute Dpth to Bedrock
	SURF(E1)	BASE(E2)	SUBB(E3)	SUBG(E4)	ERR/Sens	
1	2110	221	696	70	3.02	188.14
2	2386	350	696	90	2.7	130.82
3	2158	1381	696	84	3.11	248.38
4	1379	305	696	92	5.56	300
5	1379	910	696	85	5.62	164.87
6	1379	363	696	60	2.41	160.75
7	2758	154	696	57	1.67	300
8	1379	272	696	57	1.22	140.31
9	2379	323	690	52	0.81	153.45
10	2758	447	695	70	2.17	155.69
11	2124	526	696	90	4.31	300
12	2758	203	690	74	2.04	300
13	2758	138	690	61	3.01	222.48
Mean:	2131	430	694	72	2.9	193.55
Std.Dev.	572	349	3	14	1.5	57.4
Var Coeff(%):	26.9	81.1	0.4	20.0	51.7	29.66

EL PASO

Station	Calculated Moduli Values (ksi):					Absolute Dpth to Bedrock
	SURF(E1)	BASE(E2)	SUBB(E3)	SUBG(E4)	ERR/Sens	
1	2069	380	379	166	7.14	300
2	2069	240	309	143	7.01	173.33
3	2069	474	909	174	9.47	300
4	2069	339	355	179	9.45	121.65
5	2069	456	545	196	9.87	300
6	2069	247	867	161	7.43	300
7	2069	194	337	130	8.93	115.77
8	2069	246	383	150	9.95	123.18
9	2069	266	387	147	6.33	300
10	2069	195	276	120	8.47	114.68
11	2069	383	354	161	8.64	292.37
12	2069	243	316	145	6.38	200.24
13	2069	436	1254	169	9.4	300
14	2069	234	716	175	8.69	185.99
15	2069	451	530	195	9.97	300
16	2069	159	276	114	6.21	110.88
17	2069	154	276	112	6.1	118.26
Mean:	2069	300	499	155	8.2	193.04
Std.Dev.	0.00	109.66	279.51	25.88	1.44	101.42
Var Coeff(%):	0	36.5	56.1	16.7	17.49	52.54

PARIS

Station	Calculated Moduli Values (ksi):					Absolute Dpth to
	SURF(E1)	BASE(E2)	SUBB(E3)	SUBG(E4)	ERR/Sens	Bedrock
1	2482	222	0	59	5.85	300
2	2482	743.97	0.00	88.26	4.40	300.00
3	2482	413.01	0.00	77.91	4.33	300.00
4	2482	201.33	0.00	84.12	6.16	140.19
5	2482	344.06	0.00	99.29	11.02	300.00
Mean:	2482	384.88	0.00	81.64	6.35	268.04
Std.Dev.	0.0	218.87	0.00	15.05	2.74	71.47
Var Coeff(%):	0.0	56.87	0.00	18.43	43.10	26.66

LUFKIN

Station	Calculated Moduli Values (ksi):					Absolute Dpth to Bedrock
	SURF(E1)	BASE(E2)	SUBB(E3)	SUBG(E4)	ERR/Sens	
1	2772	201	0	106	6.4	254.96
2	3978	168	0	104	3.54	143.56
3	3999	171	0	102	3.92	136.97
4	4433	154	0	103	3.35	139.82
5	5171	141	0	124	2.73	112.17
6	2455	132	0	76	5.6	196.5
7	2827	136	0	57	1.56	189.65
8	2951	137	0	56	1.96	188.83
9	3461	291	0	94	2.35	300
10	3565	293	0	93	2.59	266.43
11	1875	130	0	70	2.48	187.83
12	1744	211	0	83	2.51	260.18
13	3827	100	0	70	2.35	144.89
Mean:	3310	174	0	88	3.18	179.14
Std.Dev.	993	60	0	21	1.41	54.39
Var Coeff(%):	30	34.5	0	23.9	44.41	30.36

SAN ANTONIO

Station	Calculated Moduli Values (ksi):					Absolute Dpth to Bedrock
	SURF(E1)	BASE(E2)	SUBB(E3)	SUBG(E4)	ERR/Sens	
1	2489	2366	696	40	11.47	266
2	2489	2346	696	109	4.48	36
3	2489	1265	696	126	5.05	36
4	2489	1506	696	161	6.34	36
5	2489	2101	696	66	10.06	265.16
6	2489	2154	690	32	7.87	111.99
7	2489	1160	696	140	7.84	36
8	2489	2621	696	150	6.06	36
9	2489	2758	696	117	5.25	48
10	2489	2758	696	90	7.13	48
Mean:	2489	2104	696	103	7.15	50.76
Std.Dev.	0.0	596.8	2.2	45.0	2.2	25.15
Var Coeff(%):	0.0	28.4	0.3	43.5	31.3	49.55

ODESSA

Station	Calculated Moduli Values (ksi):					Absolute Dpth to Bedrock
	SURF(E1)	BASE(E2)	SUBB(E3)	SUBG(E4)	ERR/Sens	
1	2482	1034	0	292	11.47	236.53
2	2482	1034	0	208	4.48	300
3	2482	652	0	219	5.05	259.33
4	2482	556	0	229	6.34	122.27
5	2482	955	0	217	10.06	300
6	2482	832	0	250	7.87	300
7	2482	1022	0	270	7.84	300
8	2482	1034	0	274	6.06	166.77
9	2482	1034	0	286	5.25	193.76
10	2482	985	0	224	7.13	182.98
Mean:	2482	914	0	247	7.15	224.02
Std.Dev.	0.0	176.3	0.0	31.2	2.2	66.0
Var Coeff(%):	0.0	19.3	0.0	12.7	31.3	29.5

Tyler

Station	Calculated Moduli Values (ksi):					Absolute Dpth to Bedrock
	SURF(E1)	BASE(E2)	SUBB(E3)	SUBG(E4)	ERR/Sens	
1	4137	522	0	132	11.47	236.53
2	3579	476	0	138	4.48	300
3	2951	448	0	142	5.05	259.33
4	2758	301	0	125	6.34	122.27
5	2758	296	0	100	10.06	300
6	2758	322	0	115	7.87	300
7	2758	268	0	183	7.84	300
8	2758	380	0	175	6.06	166.77
9	3399	339	0	93	5.25	193.76
Mean:	3096	372	0	134	5.25	72.09
Std.Dev.	500.1	89.8	0.0	30.6	2.4	21.67
Var Coeff(%):	16.2	24.1	0.0	22.9	45.2	30.1